

**Biotransformation of *trans*-1,1,1,3-tetrafluoropropene,
2,3,3,3-tetrafluoropropene
and 1,2,3,3,3-pentafluoropropene**

Dissertation zur Erlangung des
naturwissenschaftlichen Doktorgrades der
Bayerischen Julius-Maximilians-Universität Würzburg

vorgelegt von
Paul Xaver Schuster
aus
Greifenberg

Würzburg 2009

Eingereicht am: 04.11.2009

bei der Fakultät für Biologie der Bayerische Julius-Maximilians-Universität Würzburg

1. Gutachter: Prof. Dr. Wolfgang Dekant

2. Gutachter: Prof. Dr. Roland Benz

der Dissertation

1. Prüfer: Prof. Dr. Wolfgang Dekant

2. Prüfer: Prof. Dr. Roland Benz

3. Prüfer:.....

des öffentlichen Promotionskolloquiums

Datum des öffentlichen Promotionskolloquiums:.....

Doktorurkunde ausgehändigt am:.....

Contents

	page	
1	Introduction	1
1.1	Environmental characteristics and metabolic susceptibility of chlorofluorocarbons and their replacements	1
1.2	Catabolism of glutathione S-conjugates	3
1.3	Bioactivation of haloalkenes	5
1.3.1	Cytochrome P450-dependent bioactivation	5
1.3.2	Glutathione-dependent bioactivation	7
1.4	Toxicity testing results with 2,3,3,3-tetrafluoropropene (HFO-1234yf) and <i>trans</i> -1,1,1,3-tetrafluoropropene (HFO-1234ze)	9
1.4.1	Toxicity testing of HFO-1234yf in rats and mice	10
1.4.2	Developmental toxicity testing of HFO-1234yf with rabbits	10
1.4.3	Toxicity testing of HFO-1234ze in rats and mice	11
1.4.4	Toxicity testing of HFO-1225yeZ	12
1.5	Task and scope	13
2	Materials and methods	15
2.1	Chemicals	15
2.2	Chemical syntheses	15
2.2.1	Metabolites of HFO-1234ze	15
2.2.1.1	<i>S</i> -(3,3,3-Trifluoro- <i>trans</i> -propenyl)- <i>L</i> -cysteine	15
2.2.1.2	<i>N</i> -Acetyl- <i>S</i> -(3,3,3-trifluoro- <i>trans</i> -propenyl)- <i>L</i> -cysteine	16
2.2.1.3	<i>S</i> -(3,3,3-Trifluoro- <i>trans</i> -propenyl)mercaptolactic acid	16
2.2.2	Metabolites of HFO-1234yf	17
2.2.2.1	<i>S</i> -(3,3,3-Trifluoro-2-hydroxypropanyl)- <i>L</i> -cysteine	17
2.2.2.2	<i>S</i> -(3,3,3-Trifluoro-2-hydroxypropanyl)mercaptolactic acid	18
2.2.2.3	<i>N</i> -Acetyl- <i>S</i> -(3,3,3-trifluoro-2-hydroxypropanyl)- <i>L</i> -cysteine	18
2.2.2.4	<i>S</i> -(3,3,3-Trifluoro-2-hydroxypropanyl)glutathione	19
2.2.2.5	<i>S</i> -(3,3,3-Trifluoro-2-oxopropanyl)glutathione	19
2.2.2.6	3,3,3-Trifluoro-1,2-dihydroxypropane	19

2.3	Animals	20
2.4	Pretreatment of animals to induce CYP450 2E1	20
2.5	Oral gavage of metabolites of HFO-1234yf and HFO-1234ze to rats	20
2.6	Procedure of inhalation exposures	21
2.7	Enzymatic reactions <i>in vitro</i>	21
2.8	Instrumental analyses	23
2.8.1	¹⁹ F-NMR spectroscopy	23
2.8.2	Mass spectrometry, coupled with LC or GC	25
2.8.3	Fluoride selective electrode	25
2.9	Qualitative analysis of metabolites by mass spectrometry	25
2.9.1	Qualitative analysis of metabolites by GC/MS	26
2.9.1.1	3,3,3-Trifluoroacetone	26
2.9.1.2	3,3,3-Trifluoro-2-propanol	26
2.9.1.3	3,3,3-Trifluoroacetic acid	26
2.9.1.4	3,3,3-Trifluoro-1,2-dihydroxypropane	27
2.9.2	Qualitative analysis of metabolites by LC/MS-MS	27
2.9.2.1	3,3,3-Trifluorolactic acid	27
2.9.2.2	Glutathione S-conjugates and derivatives of cysteine S-conjugates	28
2.10	Quantitation of metabolites	29
2.10.1	Quantitation by GC/MS	29
2.10.1.1	HFO-1234yf, HFO-1234ze, HFO-1225yeZ and JDH	29
2.10.1.2	3,3,3-Trifluoropropionic acid	30
2.10.2	Quantitations by LC/MS	30
2.10.3	Quantitation of inorganic fluoride	32

3 Results 33

3.1	Biotransformation of HFO-1234ze in rats and mice	33
3.1.1	Inhalation exposures	33
3.1.2	Qualitative analyses of urine samples by ¹⁹ F-NMR	34
3.1.2.1	¹ H-decoupled ¹⁹ F-NMR spectra	34
3.1.2.2	¹ H-coupled ¹⁹ F-NMR spectra	35
3.1.2.3	Identification of metabolites of HFO-1234ze by ¹⁹ F-NMR	37
3.1.2.4	Oral gavage of 3,3,3-trifluoro-1-propanol to a rat	38
3.1.2.5	Conjugation of 3,3,3-trifluoropropanal with urea	39

3.1.3	Qualitative analyses of urine samples by mass spectrometry	40
3.1.3.1	Identification of urinary metabolites of HFO-1234ze by LC/MS	41
3.1.3.2	Identification of urinary metabolites of HFO-1234ze by GC/MS	43
3.1.4	Quantitation of urinary metabolites of HFO-1234ze	44
3.1.5	Qualitative analyses of metabolites of HFO-1234ze in incubations with liver protein	46
3.1.5.1	Identification of metabolites by ¹⁹ F-NMR	46
3.1.5.2	Identification of metabolites by LC/MS	47
3.1.5.3	Analysis by a fluoride selective electrode	48
3.2	Biotransformation of HFO-1234yf in rabbits, rats and mice	49
3.2.1	Inhalation exposures	49
3.2.2	Qualitative analyses of urine samples by ¹⁹ F-NMR	50
3.2.2.1	¹ H-decoupled ¹⁹ F-NMR spectra	50
3.2.2.2	¹ H-coupled ¹⁹ F-NMR spectra	50
3.2.2.3	Identification of metabolites of HFO-1234yf by ¹⁹ F-NMR	53
3.2.2.4	Oral gavage of 3,3,3-trifluoro-1,2-dihydroxypropane to a rat	55
3.2.2.5	Oral gavage of 3,3,3-trifluorolactic acid to a rat	56
3.2.2.6	Oral gavage of 3,3,3-trifluoropyruvic acid to a rat	57
3.2.3	Qualitative analyses of urine samples by mass spectrometry	58
3.2.3.1	Identification of urinary metabolites of HFO-1234yf by LC/MS	58
3.2.3.2	Identification of urinary metabolites of HFO-1234yf by GC/MS	60
3.2.4	Quantitation of urinary metabolites of HFO-1234yf	62
3.2.5	Qualitative analyses of metabolites in incubations with liver protein	64
3.2.5.1	Identification of metabolites of HFO-1234yf by ¹⁹ F-NMR	64
3.2.5.2	Identification of metabolites of S-(3,3,3-trifluoro-2-oxo- propanyl)glutathione by ¹⁹ F-NMR	67
3.2.5.3	Identification of metabolites of HFO-1234yf by LC/MS and GC/MS	68
3.2.6	Quantitation of inorganic fluoride in incubations of HFO-1234yf with liver protein	70
3.3	Comparative biotransformation of pure 1,2,3,3,3-pentafluoropropene	

	(HFO-1225yeZ) and a mixture of HFO-1225yeZ and HFO-1234yf (JDH)	72
3.3.1	Inhalation exposure	72
3.3.2	Qualitative analyses of urine samples by ¹⁹ F-NMR	73
3.3.3	Semi-quantitative analysis of urinary metabolites by ¹⁹ F-NMR	76
4	Discussion	78
4.1	Biotransformation of HFO-1234ze in rats and mice	78
4.2	Assessment of the toxicity potential of HFO-1234ze	81
4.3	Biotransformation of HFO-1234yf in rabbits, rats and mice	83
4.4	Assessment of the toxicity potential of HFO-1234yf	87
4.5	Biotransformation of pure HFO-1225yeZ and JDH, a mixture containing equal volumes of HFO-1225yeZ and HFO-1234yf	89
5	Summary	90
6	Zusammenfassung	94
7	References	98

List of abbreviations

b.w.	body weight
CFC	chlorofluorocarbon
CYP450	cytochrome P450
δ	NMR chemical shift
d	doublet
dd	doublet of doublet
DCVC	<i>S</i> -(1,2-dichlorovinyl)- <i>L</i> -cysteine
DFA	difluoroacetic acid
EDTA	ethylenediaminetetraacetic acid
EPI	enhanced product ion
FID	flame ionization detector
FMO	flavin monooxygenase
G-6-P	glucose-6-phosphate
GC/MS	gas chromatograph coupled to a mass spectrometer
Glu	glutamic acid
Gly	glycine
GS ⁻	thiolate ion of glutathione
GSH	glutathione
GSSH	glutathione disulfide
GST	glutathione <i>S</i> -transferase
GSTO1-1	glutathione <i>S</i> -transferase omega-class 1
GWP	global warming potential
HCFC	hydrofluorofluorocarbon
HFC	hydrofluorocarbon
HFO	hydrofluoroolefin
HFO-1234ze	<i>trans</i> -1,1,1,3-tetrafluoropropene
HFO-1234yf	2,3,3,3-tetrafluoropropene
HFO-1225yeZ	1,2,3,3,3-pentafluoropropene
HPLC	high performance liquid chromatography
IDA	information dependent acquisition
J _{HF}	fluorine-proton coupling constant
JDH	gas mixture of HFO-1225yeZ and HFO-1234yf (1/1; v/v)

LC ₅₀	lethal dose showing 50% lethality in a defined group
LC/MS	liquid chromatograph coupled to a mass spectrometer
m	multiplet
MRM	multiple reaction monitoring
NADPH	β-nicotinamide adenine dinucleotide 2'-phosphate
NL	neutral loss
NMR	nuclear magnetic resonance spectroscopy
NOAEL	no observed adverse effect level
ODP	ozone depletion potential
ppm	parts per million
s	singlet
S9	subcellular fraction
SD	standard deviation
SIM	single ion monitoring
t	triplet
t _{1/2}	half lifetime

1 Introduction

1.1 Environmental characteristics and metabolic susceptibility of chlorofluorocarbons and their replacements

Chlorofluorocarbons (CFCs) were developed in the early 1930s and have been used in a variety of industrial, commercial, and household applications as flame retardants, fire extinguishants, refrigerants, propellants and electronic cleaning solvents. Most of these fully halogenated CFCs along with other chlorine- and bromine-containing compounds are non-flammable, non-reactive with other chemical compounds and non-toxic, thus rendering them safe to use in customer applications. However, CFCs are known for their adverse environmental effects such as ozone depletion and global warming. Due to their stable thermodynamic properties, gaseous CFCs do not decompose in the atmosphere but reach the stratosphere where chlorine and bromine atoms are liberated from the parent compounds by the action of ultraviolet light. A single chlorine atom is able to react with 100,000 ozone molecules in a variety of catalytic cycles, thus efficiently destroying the stratospheric UVB-light protection shield [1]. Beside their ozone depletion potential, CFCs are potent greenhouse gases. Solar radiation passes through the atmosphere, is absorbed at the earth's surface and readily emitted as infrared radiation which is largely absorbed by CFCs and thus contributes to global warming [2-4]. The non-reactivity of fully saturated CFCs gives rise to their accumulation in the atmosphere, thus enforcing the process of global warming. However, several other non-CFC chemicals are also known to be potent greenhouse gases, i.e. methane and CO₂, considerably contributing to the greenhouse effect [5-7]. In order to relieve environmental damages, a phase-out of CFCs is mandated by international agreements [8].

Hydrochlorofluorocarbons (HCFCs) were developed as the first generation of CFC-replacements. Due to the insertion of C-H bonds, these compounds are structurally less stable and thus, more susceptible to breakdown reactions with atmospheric hydroxyl radicals [9]. The lower atmospheric lifetime of HCFCs makes for reduced global warming and ozone depletion potential as compared to CFCs. However, human exposure to HCFCs may result in toxicity, as C-H moieties are susceptible to CYP450-mediated oxidation and biotransformation may yield electrophilic intermediates covalently binding to tissue nucleophiles. This bioactivation has

Table 1: Environmental characteristics of selected examples of chlorofluorocarbons (CFC), hydrochlorofluorocarbons (HCFC), hydrofluorocarbons (HFC) and hydrofluoroolefins (HFO). ODP: Ozone Depletion Potential; GWP: Global Warming Potential.

Compound	Lifetime [years]	ODP	GWP at 100 years, rel. to CO ₂
CFC-114 Dichlorotetrafluoroethane	300	1	9300
CFC-12 Dichlorodifluoromethane	100	1	8500
HCFC-22 Monochlorodifluoromethane	12	0.05	1780
HCFC-141b Dichlorofluoroethane	9	0.12	630
HFC-245fa 1,1,1,3,3-Pentafluoropropane	8	0	1020
HFC-152a 1, 1-Difluoroethane	2	0	140
HFO-1234yf 2,3,3,3-Tetrafluoropropene	11 days	0	4
HFO-1234ze <i>trans</i> -1,1,1,3-Tetrafluoropropene	18 days	0	6

been delineated for many HCFCs, e.g. 1,1-dichloro-2,2,2-trifluoroethane which undergoes a CYP450 2E1-catalyzed oxidation to give trifluoroacetyl chloride, a reactive intermediate which alkylates proteins and other tissue nucleophiles [10].

Fluorohydrocarbons (HFCs) are the second generation of CFC-replacements, developed to further reduce environmental impact. The ozone layer is not affected by these non-chlorinated compounds, and for commercial development those HFCs are favored which possess only a low global warming potential and a short atmospheric lifetime (Table 1). Again, intensive studies to assess risks of human exposures to HFCs are required, since C–H bonds are targets of CYP450 oxidations and alkylating intermediates may be formed during biotransformation. A new generation of HFCs are hydrofluoroolefins (HFOs) which possess excellent environmental characteristics regarding atmospheric lifetime and global warming potential (Table 1). The presence

of C–C double bonds facilitate the atmospheric breakdown and explain the short lifetimes of only a few days. However, biotransformation of HFOs is more complex than that of HFCs and reactive electrophilic intermediates may be additionally formed by epoxidation and processing of glutathione S-conjugates which are formed by direct reaction of glutathione with the parent compound.

1.2 Catabolism of glutathione S-conjugates

Glutathione conjugation is the predominant mechanism of formation of excretable metabolites derivative of HFOs and is mainly carried out in the liver. Due to their electron withdrawing halogen substituents, partially positively charged carbon atoms are highly susceptible to the nucleophilic attack of the thiolate ion of glutathione, catalyzed by glutathione S-transferase. Thereby, HFOs may undergo addition and/or addition-elimination reactions with the tripeptide, yielding alkyl and/or allyl glutathione S-conjugates. Additionally, epoxidation of the C–C double bond of HFOs during phase I metabolism may yield electrophilic intermediates which are efficiently detoxicated by glutathione conjugation. Glutathione S-conjugates predominantly undergo processing by enzymes of the mercapturic acid pathway which has been shown to be an interorgan process, with the liver as the major site for glutathione conjugation. Processing of glutathione S-conjugates is initialized by γ -glutamyltransferase catalyzed hydrolysis to cysteinylglycine S-conjugates, followed by aminopeptidase M and cysteinylglycine dipeptidase mediated formation of cysteine S-conjugates [11, 12] (Figure 1). However, due to large species differences in activity and distribution of the involved enzymes, processing of glutathione S-conjugates to cysteine S-conjugates is not restricted to the liver, but also takes place in the small intestine or the kidney [13]. Cysteine S-conjugates formed in the kidney or gut appear to be transported back to the liver for acetylation [14], although the acetylation reaction can also occur in the kidney. Efficiency of catalysis by *N*-acetyltransferase has been found to correlate with the lipophilicity of the substituent on the sulfur atom of the cysteine S-conjugate [15]. Apart from metabolism to *N*-acetyl-*L*-cysteine S-conjugates, cysteine S-conjugates can follow

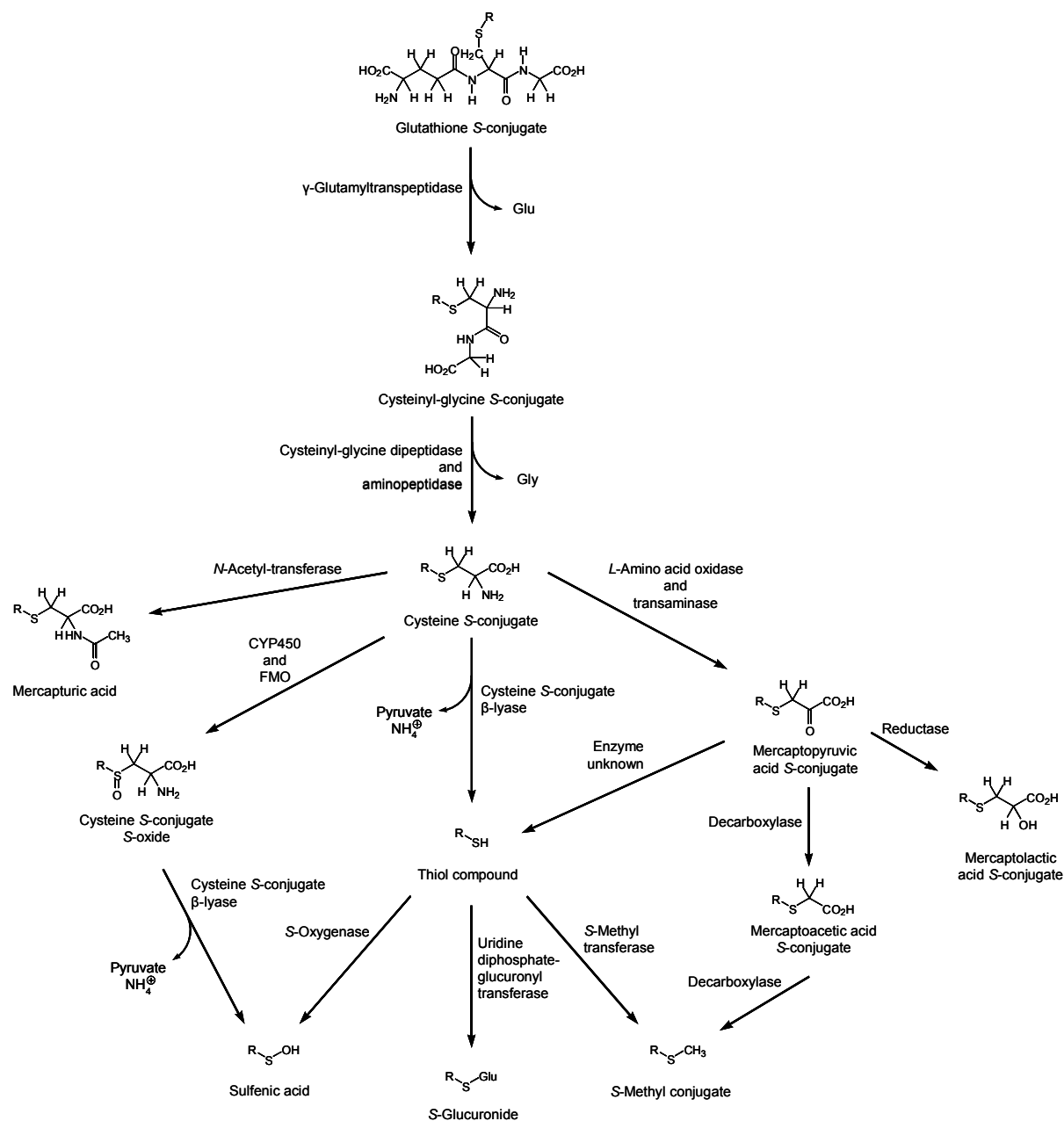


Figure 1: Possible routes of catabolism of glutathione S-conjugates.

various metabolic routes, such as transamination or oxidative deamination to mercaptopyruvic acid S-conjugates, oxidation to cysteine S-conjugates S-oxides and β -elimination to thiol-compounds [16] (Figure 1). The mercaptopyruvic acid S-conjugates are generally excreted in low concentrations because rapid further metabolism occurs. Mercaptopyruvic acid S-conjugates may undergo reduction to the corresponding mercaptolactic acid S-conjugates, decarboxylation to mercaptoacetic acid S-conjugates or β -elimination to the corresponding thiol-compounds. β -

Elimination of cysteine S-conjugates and cysteine S-conjugate S-oxides catalyzed by β -lyase is paralleled by the release of pyruvate and ammonia and results in the formation of thiol-compounds and sulfenic acids which may be electrophilic intermediates formed from halogenated compounds and thus be toxicologically relevant [17]. In a manner similar to that of hydroxy compounds, thiols may further form S-glucuronides which are excreted with urine. Sulfoxidation of cysteine S-conjugates and related metabolites such as mercapturic acids and mercaptolactic acids is flavoprotein- or cytochrome P450-dependent and S-oxides were found in urines from humans and animals exposed to different compounds, including allyl halides [18-20]. S-Methyl conjugates may be formed by decarboxylation of mercaptoacetic acid S-conjugates or S-methyl transfer to the thiol compounds.

1.3 Bioactivation of haloalkenes

Several halogenated alkenes are nephrotoxic, hepatotoxic and mutagen in rodents and thus have been intensively studied to elucidate the ways of bioactivation [21-24]. Mechanisms of the organ-specific toxicity of these compounds are associated with both cytochrome P450-mediated oxidations in biotransformation phase I and glutathione conjugation in phase II. Haloalkenes are highly susceptible to biotransformation reactions and thus to bioactivation due to their reactive C=C double bond.

1.3.1 Cytochrome P450-dependent bioactivation

The CYP450 system plays a major role in bioactivation of haloalkanes, haloalkenes and halobenzenes [25, 26]. In general, low molecular haloolefins are substrates of CYP450 enzymes and may be bioactivated to electrophilic epoxides, vicinal haloaldehydes and acyl halides [27, 28]. These intermediates may further react with nucleophilic sites of cellular macromolecules such as proteins, phospholipids and DNA, or may inhibit CYP450 activity by heme alkylation [29]. Haloalkene-induced toxicity and carcinogenicity by electrophilic acyl halides has been observed in the biotransformation of several halogenated alkenes, such as tetrachloro-, trichloro- and

1,1-dichloroethylene. As delineated for tetrachloroethene (Figure 2), the CYP450-mediated oxidation of the parent compound may yield several electrophilic intermediates [30-32]. The initially formed epoxide of tetrachloroethene, as well as its derivatives acetyl and oxalyl chloride have been shown to covalently bind to liver proteins and microsomal macromolecules, thus contributing to the hepatotoxic effects after exposure of rats to the parent compound [33, 34]. However, these hepatotoxic effects were not severe, due to the generally low extent of biotransformation of tetrachloroethylene.

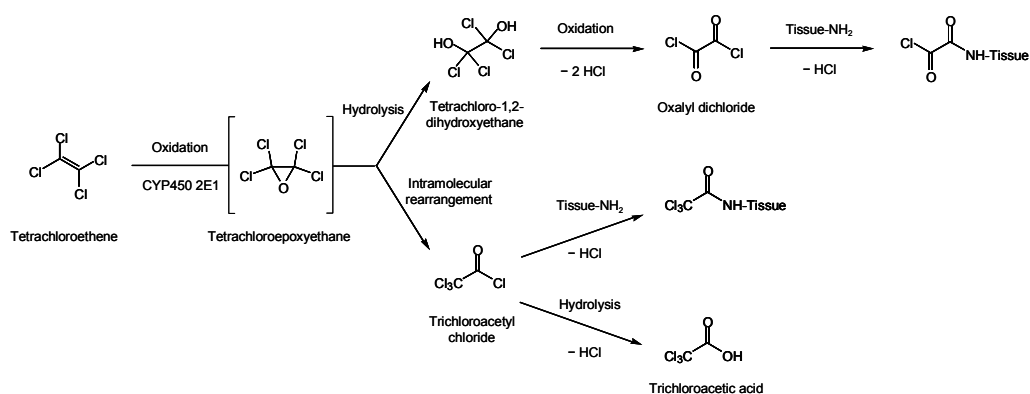


Figure 2: CYP450 mediated bioactivation of tetrachloroethene yields electrophilic acetyl and oxalyl chloride and toxic trichloroacetic acid. Other pathways of biotransformation and bioactivation of tetrachloroethene not shown in this figure.

The electrophilicity of an acyl halide is effected by the presence of a strongly electron withdrawing halogen and oxygen atom on the carbonyl carbon which consequently possesses a large partial positive charge. Since halogens are good leaving groups, they are readily replaced by nucleophiles. Detoxification reactions include hydrolysis of the vinyl halogen oxide by epoxide hydrolase and reduction of haloacetaldehyde by aldehyde and alcohol dehydrogenase to give a carboxylic acid. Non-enzymatically, acyl halides may be detoxicated by reaction with water to give carboxylic acids. Beside bioactivation of haloalkenes to electrophilic intermediates, CYP450 mediated reactions may also yield stable, but toxic metabolites, such as ketones and halogenated acetic acids which display toxicity by interfering with essential enzyme systems in the body [35-37].

1.3.2 Glutathione-dependent bioactivation

Beside cytochrome P450-dependent bioactivation of haloalkenes, glutathione conjugation is another important metabolic way of initializing the formation of potentially toxic intermediates. Although glutathione conjugation of electrophilic and therefore potentially toxic chemicals or intermediates is generally regarded as a detoxication pathway, some glutathione S-conjugates can lead to toxicity. Both addition and addition-elimination mechanisms are observed in the glutathione S-transferase-catalyzed reaction of glutathione with haloolefines (Figure 3).

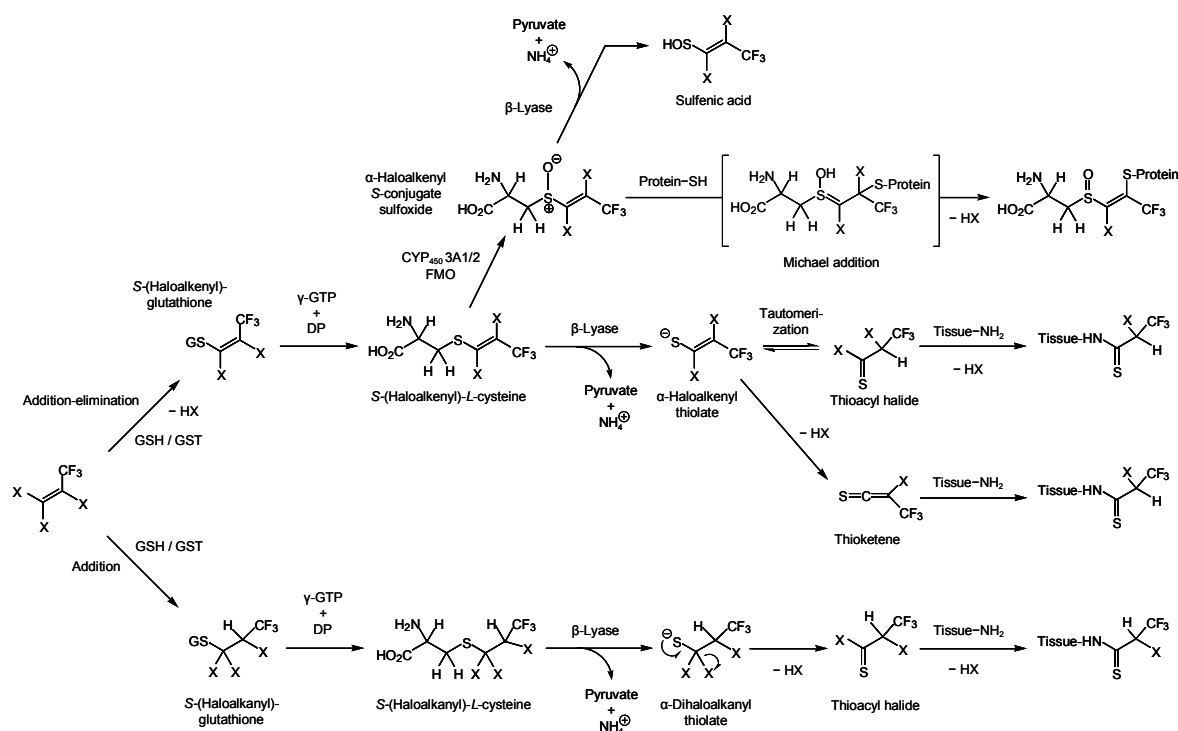


Figure 3: Bioactivation of haloalkene derived cysteine S-conjugates. Electrophilic intermediates (thioacyl halide and thioketene) are formed in the course of bioactivation of the cysteine S-conjugates after β -elimination reaction and bind covalently to tissue nucleophiles. Moreover, sulfoxidation of S-haloalkenyl cysteine yields electrophilic S-oxides acting as Michael Acceptors in the presence of cellular thiols. S-Oxides may also be processed by β -lyase to give toxic sulfenic acids.

In general, 1,1-dichloroalkenes undergo addition-elimination reactions to give S-(1-chloroalkenyl)glutathione and 1,1-difluoroalkenes are subjected to an addition

reaction resulting in S-(1,2-difluoroalkanyl)glutathione. Some haloalkenes, e.g. hexafluoropropene, undergo both addition and addition-elimination reactions [17, 38, 39]. Cleavage of the glutathione S-conjugates by hepatic γ -glutamyltranspeptidase and dipeptidase yields cysteine S-conjugates which are translocated to the kidney and processed by renal cysteine S-conjugate β -lyase [40]. Possible mechanisms of bioactivation of haloalkene derived cysteine S-conjugates are outlined in figure 3. S-(1-Haloalkenyl)- and S-(1,1-dihaloalkanyl)-L-cysteine S-conjugates are bioactivated by renal cysteine S-conjugate β -lyase to give α -haloalkenyl and α -haloalkanyl thiolates, respectively (Figure 3). Due to their structural instability, these thiolates convert to electrophilic thioacyl halides and thioketenes which further react with tissue nucleophiles such as amino groups of protein-bound lysine residues, mitochondrial phospholipids or DNA to give covalently bound adducts [41-44]. As outlined in figure 3, one electron withdrawing substituent bond to the carbon atom next to the sulfur in alkenylthiolates is apparently needed for the expression of toxicity, whereas two electronegative substituents are required to form reactive intermediates from alkanylthiolates. Bromine-containing thioacyl halides additionally form reactive thiiranes and thiolactones which are not derivatives of haloolefins without bromine [45]. Bioactivation of cysteine S-conjugates by β -lyase explains the target-organ specific toxicity and tumorigenicity observed with several haloalkenes.

Another mechanism of bioactivation of haloalkene derived cysteine S-conjugates is the CYP450- and FMO-mediated oxidation of α -haloalkenyl S-conjugates to give reactive sulfoxides (Figure 3). Sulfoxides were shown to be formed by rodent liver and kidney microsomes and were further highly reactive renal tubular cell nephrotoxics in rats *in vitro* and *in vivo* [46-48]. Electrophilic α -haloalkenyl S-conjugate sulfoxides react as Michael acceptors with tissue nucleophiles, thus contributing to the target-organ specific toxicity observed with several haloalkene derived S-conjugates, such as S-(1,2,3,4,4-pentachlorobutadienyl)-L-cysteine and S-(1,2-dichlorovinyl)-L-cysteine (DCVC) [19, 20]. In rats, DCVC S-oxide is a potent nephrotoxicant and has been shown to deplete cellular thiols. The presence of a C-C double bond next to the sulfur is obviously needed for the expression of toxicity, since aliphatic cysteine S-conjugate S-oxides are not known to react as Michael acceptors. Moreover, bioactivation of haloalkene derived cysteine S-conjugates is catalyzed by β -elimination of the corresponding S-oxides to give potentially toxic

sulfenic acids [49-51]. The formation of 1,2-dichlorovinyl sulfenic acid and DCVC S-oxide has been delineated in the biotransformation of trichloroethene and may contribute to the observed nephrotoxicity, in addition to the β -elimination of the corresponding cysteine S-conjugate (Figure 3).

In addition to bioactivation of the parent haloolefinic compound by direct reaction with glutathione, alkylating intermediates may also be formed by conjugation of initially CYP450-formed epoxides with glutathione (Figure 4). Depending on number and position of the halogen substituents, glutathione S-conjugates derived of an addition-elimination reaction of the epoxide with the tripeptide may be processed to α -dihaloalkanyl thiolates which can convert to alkylating thioacyl halides.

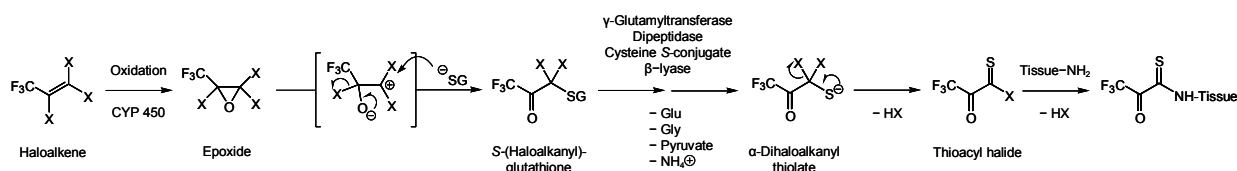


Figure 4: Bioactivation of haloalkenes by glutathione conjugation with an initially formed epoxide may yield α -dihaloalkanyl thiolates which can convert to alkylating agents and cause toxicity.

1.4 Toxicity testing results with 2,3,3,3-tetrafluoropropene (HFO-1234yf) and *trans*-1,1,1,3-tetrafluoropropene (HFO-1234ze)

Refrigerants and blowing agents which are developed to replace CFCs, HCFCs and HFCs have to meet several attributes. They have to have good environmental characteristics, like a global warming potential of less than 150, and zero ozone layer depletion potential. Other parameters to be met are low flammability, low toxicity, no impact on human health risk, energy efficiency, economic viability and compatibility to existing technical systems. 2,3,3,3-Tetrafluoropropene (HFO-1234yf) and *trans*-1,1,1,3-tetrafluoropropene (HFO-1234ze) are newly developed refrigerants and blowing agents from Honeywell. They have excellent environmental characteristics (Table 1) and are safe for both domestic and commercial usage, due to their low potentials of flammability and toxicity.

1.4.1 Toxicity testing of HFO-1234yf in rats and mice

The available toxicity data on HFO-1234yf demonstrate a low potential for toxicity in rats and mice. In a 90-day study with inhalation exposures up to concentrations of 50,000 ppm, (8 h/day, 5 days/week), no changes in clinical chemistry occurred and no histopathological effects due to HFO-1234yf were observed with the highest exposure level thus representing the NOAEL [52]. In a 90-day inhalation study integrating a toxicogenomic assessment of the carcinogenic potential of HFO-1234yf to the liver in male mice and the kidney in male rats, statistical classification analysis predicted HFO-1234yf to be non-carcinogenic to these target organs [52]. Despite the non-carcinogenic prediction, gene expression changes in the male kidney suggested a potential for endocrine-related effects and were consistent with a reduction in circulating androgens. In addition, a significant HFO-1234yf-mediated upregulation of the SA rat hypertension-associated gene (*Sah*) was observed in the male rat kidney. Increased expression of the human homolog of this gene has been linked to changes in body mass index, triglyceride levels, cholesterol, and blood pressure status. Moreover, HFO-1234yf showed absence of genotoxicity in mammalian cells, but gave a positive response in bacterial mutagenicity testing [52].

1.4.2 Developmental toxicity testing of HFO-1234yf with rabbits

In a developmental toxicity study on HFO-1234yf with New Zealand White rabbits, mortality and moribundity were noted at exposure levels of 10,000 and 50,000 ppm, whereas lethality was not observed at the 2 500 ppm level [53]. The inhalation exposures were conducted for 6 h/day and the first maternal animals died after day 14 at 10,000 ppm and 7 days at 50,000 ppm. The maternal toxicity did not result in effects on embryo/fetal development or external fetal morphology, although exposures were terminated early (gestation days 20 or 21 in the 10,000 ppm group and gestation days 13 or 14 in the 50,000 ppm group). Intrauterine growth, survival and external fetal morphology were not affected by maternal test substance exposures. Mortality and moribundity in females were associated with reduced mean body weight gains, decreases in food consumption, mild cardiomyopathy and mild renal tubular necrosis [53]. A majority of the females in the 10,000 and 50,000 ppm

groups that were found dead or euthanized in extremis were noted with decreased defecation at the daily examinations and hypoactivity and labored and/or decreased respiration at the daily examinations, at the mid-point of exposure and approximately 1 h following exposure. Following the cessation of exposure no further test substance-related clinical signs were noted and mean body weight and food consumption were similar to that of the control group throughout the remainder of the study. However, these do not provide an explanation of the cause of moribundity or death.

1.4.3 Toxicity testing of HFO-1234ze in rats and mice

The available toxicity data on HFO-1234ze also demonstrate a low potential for toxicity. Inhalation exposures for 90 days were used to assess the possible carcinogenic potential of HFO-1234ze to female mouse liver and male rat kidney using genomics [54]. No treatment related histopathological lesions were observed after exposure to HFO-1234ze at 10,000 ppm, and statistical classification analysis predicted HFO-1234ze to be non-carcinogenic to mouse liver and rat kidney. At the 2 000 ppm level, the expression of only one gene (RGD1308612), was altered in the male rat kidney, whereas at the 10,000 ppm level, this gene remained unchanged. The functional role of this gene is unknown. In contrast, large-scale gene expression changes were observed in liver of female mice after 2 000 and 10,000 ppm exposure concentrations. At the high dose, the expression of 1 318 genes was significantly changed with 38 genes showing increased expression and 1 280 genes which were downregulated. The changes were related to a variety of cellular functions such as RNA metabolism and processing, protein transport and ubiquitination, cell replication, and protein translation and the majority of changes were similar between the low and high doses of HFO-1234ze. The large scale changes in expression in the mouse liver were unexpected given the lack of histopathological lesions and the lack of gene expression changes for HFO-1234ze in the rat kidney [54].

1.4.4 Toxicity testing of HFO-1225yeZ

The development of 1,2,3,3,3-pentafluoropropene (HFO-1225yeZ) as foam blowing agent has been discontinued after the observation of several adverse effects in the test animals. In a 28-day inhalation toxicity study, rats were exposed to HFO-1225yeZ by inhalation (nose only) for 6 hours per day, 5 days per week for 4 weeks. No deaths were reported in rats, but statistically significant decreases in body weight gain, pale incisors, ameloblastic dysplasia, increased heart weights and reduced thymus weights were found after inhalation exposures to 1 000 ppm HFO-1225yeZ. Moreover, the compound showed male reproductive effects in rats at the 500 ppm level, whereas liver and kidney were not found to be target organs at exposure levels of up to 50,000 ppm HFO-1225yeZ. In mice, HFO-1225yeZ exhibited acute toxic effects after 4 hours inhalation exposure (LC₅₀: ~10,430 - 20,200 ppm). No detailed information about the findings of toxicity testing of HFO-1225yeZ can be provided, since the contents of the internal reports are confidential.

1.5 Task and scope

The objective of this thesis was to investigate the metabolic fate of 2,3,3,3-tetrafluoropropene (HFO-1234yf) and *trans*-1,1,1,3-tetrafluoropropene (HFO-1234ze) in order to predict health risks of human inhalation exposures to the parent compounds. Rats and mice were intended to be exposed by whole body inhalation to different concentrations of HFO-1234yf and HFO-1234ze. Due to lethality observed in a developmental toxicity study with rabbits, inhalation exposures of this species with HFO-1234yf were additionally projected to possibly detect differences in biotransformation. Qualitative analyses of urinary metabolites derivative of HFO-1234yf and HFO-1234ze were aimed for the delineation of schemes of biotransformation of the parent compounds in the test species. In order to estimate the extent of biotransformation of the different doses of HFO-1234yf and HFO-1234ze administered by inhalation, quantitation of major metabolites in urines from rabbits, rats and mice were also proposed. In addition to the *in vivo* experiments, investigations on biotransformation of HFO-1234yf and HFO-1234ze were also performed in incubations with rabbit, rat and human liver subcellular fractions and rat liver microsomes. The formation of metabolites and its dependence on time, cofactors and protein concentration was intended to determine the kinetics of biotransformation of HFO-1234yf and HFO-1234ze. Regarding the metabolites of the parent compounds formed *in vitro*, the role of CYP450 and glutathione pathway were aimed for comparison with the *in vivo* findings. The results of qualitative and quantitative considerations of biotransformation are required for the commercial development and interpretation of the toxicity findings of HFO-1234yf and HFO-1234ze.

Comparisons of biotransformation of HFO-1234yf and 1,2,3,3,3-pentafluoropropene (HFO-1225yeZ) were performed to investigate a possible influence of HFO-1234yf and its metabolites upon the metabolism of HFO-1225yeZ. The latter exhibits acute toxic effects in mice (LC₅₀: ~10,430 - 20,200 ppm) after 4 h of inhalation. A mixture of both gases (JDH), containing equal quantities of HFO-1234yf and HFO-1225yeZ was developed for refrigeration. Possibly, lower toxicity may occur *in vivo* with JDH than with pure HFO-1225yeZ due to metabolic competition with HFO-1234yf. Comparisons of the ¹⁹F-NMR spectra of rat urines after exposure to comparable

concentrations of HFO-1234yf, HFO-1225yeZ and JDH were intended to look for additional or absent metabolites and to determine a quantitative change in metabolite excretion in JDH urine relative to that of the HFO-1234yf and HFO-1225yeZ urines.

2 Materials and methods

2.1 Chemicals

- 2,3,3,3-Tetrafluoropropene (HFO-1234yf), *trans*-1,1,1,3-tetrafluoropropene (HFO-1234ze), 1,2,3,3,3-pentafluoropropene (HFO-1225yeZ) and JDH were supplied by Honeywell (Morristown, NJ) with a purity of 99.8% (based on FID GC analysis).
- 3,3,3-Trifluoro-2-propanol was purchased from Fluorochem (Derbyshire, Great Britain).
- 3,3,3-Trifluoro-1,2-epoxypropane and 1-bromo-3,3,3-trifluoro-2-propanol were bought from Matrix Scientific (Columbia, SC).
- 3,3,3-Trifluorolactic acid was obtained from Lancaster Synthesis Ltd., Windham, NH.
- 3,3,3-Trifluoroacetone, trifluoroacetic acid, 3,3,3-trifluoropropionic acid, enzymes and cofactors and all other chemicals were acquired from Sigma-Aldrich (Deisenhofen, Germany or St Louis, MO, USA) in the highest purity available.

2.2 Chemical syntheses

2.2.1 Metabolites of HFO-1234ze

2.2.1.1 S-(3,3,3-Trifluoro-*trans*-propenyl)-L-cysteine

Synthesis of S-(3,3,3-trifluoro-*trans*-propenyl)-L-cysteine was achieved by reacting *trans*-1,1,1,3-tetrafluoropropene with 500 mg L-cysteine in 5 mL methanol/water (5/1, v/v) adjusted to pH ~ 9 with NaOH. The solution was filled into a high pressure reaction vial which was then placed into liquid nitrogen. After condensing approximately 1 mL of *trans*-1,1,1,3-tetrafluoropropene to the frozen solution, the vial was tightly closed with a screw cap and thawed at room temperature. After stirring over night the vial was frozen in liquid nitrogen again and then opened to remove HFO-1234ze from the solution by evaporation at room temperature. Cystine was

removed from the solution by centrifugation. *S*-(3,3,3-Trifluoro-*trans*-propenyl)-*L*-cysteine was purified by HPLC on a Bischoff Chromatography Partisil ODS III column (125 mm × 8 mm) with a non linear gradient of 100% water for 1 min, then ramping to 100% methanol in 10 min. First, the gradient was driven to 50% methanol in 9 min, then to 100% methanol in 1 min and held there for another 2 min. The flow rate was maintained at 3.5 mL/min throughout the analysis. The eluate was monitored for *S*-(3,3,3-trifluoro-*trans*-propenyl)-*L*-cysteine at 240 nm. *S*-(3,3,3-Trifluoro-*trans*-propenyl)-*L*-cysteine was obtained with a purity of 90% based on ¹H and ¹³C-NMR. ¹H-NMR (CDCl₃): δ = 3.07-3.26 (m), 3.71-3.74 (dd), 5.73-5.82 (qq), 7.09-7.15 (qq). ¹³C-NMR (CDCl₃): δ = 34.3 (s), 54.0 (s), 112.1-113.2 (q, *J* = 34.1 Hz) 118.9-126.9 (q, *J* = 269 Hz, CF₃), 137.0-137.2 (q, *J* = 7.13 Hz), 175.5 (s); ¹⁹F-NMR (CFCl₃): δ = -62.1 ppm (dd, ²*J*_{HF} = 6.5 Hz, ³*J*_{HF} = 2.1 Hz).

2.2.1.2 *N*-Acetyl-*S*-(3,3,3-trifluoro-*trans*-propenyl)-*L*-cysteine

N-Acetyl-*S*-(3,3,3-trifluoro-*trans*-propenyl)-*L*-cysteine was synthesized by dissolving 50 mg of purified *S*-(3,3,3-trifluoro-*trans*-propenyl)-*L*-cysteine in 1.6 mL of acetic acid. Cold acetic anhydride (1 mL) was slowly dropped into the solution and the mixture was stirred for 5 min on ice. The reaction was then continued overnight at room temperature and the product purified by HPLC as described for *S*-(3,3,3-trifluoro-*trans*-propenyl)-*L*-cysteine. *d*₃-*N*-Acetyl-*S*-(3,3,3-trifluoro-*trans*-propenyl)-*L*-cysteine was used as internal standard and synthesized analogously as described above, but using *d*₄-acetic acid and *d*₆-acetic anhydride. ¹H-NMR (CDCl₃): δ = 1.88 (s), 2.96-3.2 (m), 4.32-4.35 (dd), 5.63-5.72 (qq), 7.02-7.07 (qq). ¹³C-NMR (CDCl₃): δ = 21.83 (s), 34.05 (s), 54.26 (s), 111.35-112.37 (q, *J* = 34.1 Hz), 119-127 (q, *J* = 268 Hz, CF₃), 137.93-138.14 (q, *J* = 7.1 Hz), 173.68 (s), 176.04 (s). ¹⁹F-NMR (CFCl₃): δ = -62.0 ppm (dd, ²*J*_{HF} = 6.5 Hz, ³*J*_{HF} = 2.0 Hz).

2.2.1.3 *S*-(3,3,3-Trifluoro-*trans*-propenyl)mercaptolactic acid

S-(3,3,3-Trifluoro-*trans*-propenyl)mercaptolactic acid was synthesized in low yields by diazotation of 40 mg *S*-(3,3,3-trifluoro-*trans*-propenyl)-*L*-cysteine (0.19 mmol) in

1 mL of ice cold water containing 69 mg NaNO₂ (0.19 mmol). Sulfuric acid (33-36%; 0.5 mL) was added dropwise to avoid an increase in temperature. Release of molecular nitrogen from the diazonium ion and hydrolysis of the resulting carbenium ion was performed by stirring on ice for 1 h and subsequent heating at flux for 30 min. *S*-(3,3,3-Trifluoro-*trans*-propenyl)mercaptolactic acid was monitored at 340 nm and eluted after 15.7 min from a Nucleosil C18 column (8 mm × 12 mm, Macherey-Nagel) when a gradient was applied from 100% water (0.1% formic acid) to 100% methanol under the following conditions: 0-1 min: 0-45% MeOH; 1-18 min: 45-48% MeOH; 18-19 min: 48-100% MeOH; 19-20 min: 100-0% MeOH. The flow rate was maintained at 3.0 mL/min throughout the analysis. Due to coeluting byproducts, the collected fractions were purified by HPLC several times in order to reduce contamination. ¹H and ¹³C-NMR spectra indicated a purity of approx. 95% of the *S*-(3,3,3-trifluoro-*trans*-propenyl)mercaptolactic acid. ¹H-NMR (CDCl₃): δ = 3.07-3.25 (qq), 4.40 (s), 5.72-5.78 (qq), 7.15-7.17 (d). ¹³C-NMR (CDCl₃): δ = 35.83 (s, CH₂), 69.59 (s, HCOH), 111.62-112.29 (q, *J* = 34.1 Hz, CH), 120.35-125.68 (q, *J* = 268.1 Hz, CF₃), 137.89-138.03 (q, *J* = 7.1 Hz, CH), 176.35 (s, CO₂H). ¹⁹F-NMR (CFCl₃): δ = -61.8 ppm (dd, ²*J*_{HF} = 6.6 Hz, ³*J*_{HF} = 2.1 Hz).

2.2.2 Metabolites of HFO-1234yf

2.2.2.1 *S*-(3,3,3-Trifluoro-2-hydroxypropenyl)-*L*-cysteine

Synthesis of *S*-(3,3,3-trifluoro-2-hydroxypropenyl)-*L*-cysteine was performed by reacting 860 μL (8.26 mmol) 1-bromo-3,3,3-trifluoro-2-propanol with 1 g (8.26 mmol) *L*-cysteine in 5 mL water adjusted to pH ~ 9 with NaOH. After stirring the solution over night, the solution was purified by HPLC as described for the cysteine *S*-conjugate of HFO-1234ze [55]. The eluate was monitored for *S*-(3,3,3-trifluoro-2-hydroxypropenyl)-*L*-cysteine at 220 nm which was obtained with a purity of >95% based on ¹H and ¹³C-NMR. ¹H-NMR (CDCl₃): δ = 2.85-3.1 (m), 2.62-2.69 (q), 3.79-3.82 (q), 4.10-4.18 (m). ¹³C-NMR (CDCl₃): δ = 31.2 (s), 32.7 (s), 53.6 (s), 68.4-69.3 (q, *J* = 30.6 Hz), 120.18-128.6 (q, *J* = 281 Hz, CF₃), 172.73 (s). ¹⁹F-NMR (CFCl₃): δ = -79.0 ppm (d, *J*_{HF} = 6.6 Hz).

2.2.2.2 S-(3,3,3-Trifluoro-2-hydroxypropanyl)mercaptolactic acid

S-(3,3,3-Trifluoro-2-hydroxypropanyl)mercaptolactic was synthesized by diazotation as described for S-(3,3,3-trifluoro-*trans*-propenyl)-L-cysteine [55]. S-(3,3,3-Trifluoro-2-hydroxypropanyl)mercaptolactic acid eluted after 5 min from a Nucleosil C18 column (8 mm x 12 mm, Macherey-Nagel) when a gradient from 100% water (0.1% formic acid) to 100% methanol in 12 min was applied. Due to coeluting byproducts, the collected eluent was again purified under the following separation conditions: 0-1 min: 0% MeOH; 1-2 min: 0-39% MeOH; 2-15 min: 39-40.5% MeOH; 15-16 min: 40.5-100% MeOH; 16-20 min: 100% MeOH. 20-21 min: 100-0% MeOH; The flow rate was maintained at 3.0 mL/min throughout the analysis and S-(3,3,3-trifluoro-2-hydroxypropanyl)mercaptolactic acid eluted after 13 min. Even though different HPLC-gradients were applied, S-(3,3,3-trifluoro-2-hydroxypropanyl)mercaptolactic acid could not be purified satisfactorily and ^1H and ^{13}C -NMR spectra indicated a purity of approx. 50%. A major doublet was present in ^1H -coupled ^{19}F -NMR spectra at $\delta = -78.9$ ($J_{\text{HF}} = 7.0$ Hz) and LC/MS analyses confirmed the presence of fragments likely yielded by the ionization of S-(3,3,3-trifluoro-2-hydroxypropanyl)mercaptolactic acid.

2.2.2.3 N-Acetyl-S-(3,3,3-trifluoro-2-hydroxypropanyl)-L-cysteine

N-Acetyl-S-(3,3,3-trifluoro-2-hydroxypropanyl)-L-cysteine acid was synthesized by slowly adding 3,3,3-trifluoro-1,2-epoxypropane to a well stirred solution of N-acetyl-L-cysteine in ethanol/water (1/2, v/v) adjusted to pH >9 with triethylamine. The reaction mixture was cooled to 4 °C during the reaction. After neutralizing by addition of 2 N HCl and evaporation of the ethanol under reduced pressure, the water phase was extracted with ethyl acetate. Two diastereomers of N-acetyl-S-(3,3,3-trifluoro-2-hydroxypropanyl)-L-cysteine were obtained in a ratio of 2:1 as an oil with a purity of >95% based on HPLC-separation with UV-detection at 225 nm.

^1H -NMR (CDCl_3): $\delta = 1.13$ -1.20 (t, $J = 7.18$ Hz), 1.97-1.98 (s), 2.69-2.73 (m), 2.88-2.95 (m), 3.01-3.12 (m), 4.02-4.07 (q, $J = 7.1$ Hz), 4.13-4.18 (m), 4.51-4.54 (q, $J = 4.8$ Hz). ^{13}C -NMR (CDCl_3): $\delta = 20.5$ (s), 21.6 (s), 33.1 (s), 52.6 (s), 68.0-70.0 (q, $J = 30.6$ Hz).

Hz), 120.1-128.7 (q, $J = 283$ Hz, CF_3), 173.8 (s), 174.2 (s). ^{19}F -NMR (CFCl_3): $\delta = -78.7$ ppm (d, $J_{\text{HF}} = 6.6$ Hz).

2.2.2.4 S-(3,3,3-Trifluoro-2-hydroxypropanyl)glutathione

S-(3,3,3-Trifluoro-2-hydroxypropanyl)glutathione was synthesized as described for S-(3,3,3-trifluoro-2-oxopropanyl)glutathione [56, 57] but using 1-bromo-3,3,3-trifluoro-2-propanol as starting material. ^1H -NMR (CDCl_3): $\delta = 2.13$ -2.17 (q; $J = 7.6$ Hz), 2.47-2.57 (m), 2.73-2.79 (m), 2.91-2.97 (m), 3.09-3.13 (m), 3.31 (s), 3.83-3.86 (t; $J = 6.5$ Hz), 3.96 (s), 4.20-4.23 (m), 4.57-4.60 (m). ^{13}C -NMR (CDCl_3): $\delta = 28.4$ (s), 33.6 (s), 34.0 (s), 35.9 (s), 43.9 (s), 55.6 (s), 56.0 (s), 71.2-71.8 (q; $J = 30.6$ Hz), 124.2-129.8 (q; $J = 277$ Hz; CF_3), 175.2 (s), 175.68 (s), 175.71 (s), 177.2 (s). ^{19}F -NMR (CFCl_3): $\delta = -78.8$ ppm (d, $J_{\text{HF}} = 6.8$ Hz).

2.2.2.5 S-(3,3,3-Trifluoro-2-oxopropanyl)glutathione

S-(3,3,3-Trifluoro-2-oxopropanyl)glutathione was synthesized by stirring glutathione (2.62 mmoles) and 2 equivalents of 3,3,3-trifluoro-1-bromoacetone in a phase transfer reaction using aqueous tetrabutylammonium hydroxide (10%) and chloroform (total of 7 mL; 1/1, v/v) at room temperature for 40 h [56]. After acidification to pH ~ 3 with HCl, the product was extracted with ethyl acetate and isolated as an oil after removal of the solvent under reduced pressure. ^{13}C -NMR (CDCl_3): $\delta = 26.0$ (s), 30.2 (s), 31.14 (s), 34.47 (s), 36.6 (s), 41.41 (s), 53.3 (s), 53.65 (s), 117.4-126.0 (q; $J = 285$ Hz, CF_3), 173.48 (s), 174.78 (s), 215.4 (s). ^1H -NMR (CDCl_3): $\delta = 2.05$ -2.1 (q, $J = 7.5$ Hz), 2.12 (s), 2.46-2.5 (m), 2.88-2.94 (m), 3.08-3.12 (m), 3.73-3.76 (t, $J = 6.37$ Hz), 3.88 (s). ^{19}F -NMR (CFCl_3): $\delta = -84.6$ ppm (s).

2.2.2.6 3,3,3-Trifluoro-1,2-dihydroxypropane

Synthesis of 3,3,3-trifluoro-1,2-dihydroxypropane was achieved by hydrolysis of 3,3,3-trifluoro-1,2-epoxypropane (Fluorochem Ltd, Derbyshire, UK). A mixture of

3,3,3-trifluoro-1,2-epoxypropane and water, containing 1% H₂SO₄, was kept at 100 °C for 2 h in a sealed tube. After extraction with ethyl acetate, the product was distilled using a Kugelrohr apparatus (temperature 100 °C/25 mmHg) [58].

¹H-NMR (CDCl₃): δ = 3.6-3.8 (m), 4.05-4.1 (m). ¹³C-NMR (CDCl₃): δ = 120.3-128.7 (q, *J* = 282 Hz; CF₃), 69.3-70.2 (q, *J* = 29.6 Hz; C₂), 59.6-59.7 (q, *J* = 2.3 Hz; C₁). ¹⁹F-NMR (CFCl₃): δ = -77.2 ppm (d, *J*_{HF} = 7.4 Hz).

2.3 Animals

Female New Zealand White rabbits (2.3-3.1 kg body weight), Male Sprague-Dawley rats (220-250 g body weight) and male B6C3F1 mice (27-30 g body weight) were purchased from Harlan-Winkelmann, Borchon, Germany) and used for all studies. All animals were kept for at least 1 week at constant humidity and temperature in the animal facility of the university with a controlled 12 h light/dark cycle in order to ensure acclimatization before the experiments.

2.4 Pretreatment of animals to induce CYP450 2E1

To induce CYP450 2E1, rats were given pyridine (100 mg/kg b.w., ip, dissolved in isotonic sodium chloride solution) once daily for 5 days [59-61]. All animals were fasted 18 h before sacrifice and preparation of microsomes.

2.5 Oral gavage of metabolites of HFO-1234yf and HFO-1234ze to rats

In order to elucidate the metabolic fate of intermediates of HFO-1234yf and HFO-1234ze, several synthesized compounds were dissolved in 2 mL of isotonic sodium chloride solution and administered by oral gavage to male Sprague-Dawley rats at dose levels of 5 mg/kg body weight. The animals were transferred to metabolism cages, and urines were collected in 24 h intervals. Urine samples were analyzed by ¹⁹F-NMR and GC/MS.

2.6 Procedure of inhalation exposures

Female rabbits (n=3/concentration) were exposed to targeted concentrations of 2 000, 10,000, and 50,000 ppm HFO-1234yf. Male rats (n=5/concentration) were exposed to targeted concentrations of 2 000, 10,000, and 50,000 ppm HFO-1234yf or HFO-1234ze; 10,000 ppm HFO-1225yeZ; and 20,000 ppm JDH. For inhalation exposures of male mice (n=5) to HFO-1234yf or HFO-1234ze, a concentration of 50,000 ppm was projected. All inhalations were conducted for 6 h in a dynamic exposure system consisting of a 20.6 L desiccator (rats and mice) or a 350 L inhalation chamber (rabbits). The air-gas-mixtures constantly passed through the inhalation systems with a flow rate of 200 L/h (rats and mice) and 350 L/h (rabbits), respectively. Air-gas-mixtures were additionally circulated inside by a magnetic stirrer (20.6 L dessicator) or an electric fan (350 L chamber) to ensure equal distribution of the parent compound. Metered amounts of the gaseous compounds were mixed with air and introduced to the exposure chamber. Chamber concentrations of the gases were monitored at 15 min intervals by taking samples (100 μ L) of the chamber atmosphere with a gastight syringe. The content of the parent compound in these samples was determined by GC/MS. Quantitation of the parent compounds were based on calibration curves with air samples containing known concentrations of the parent compounds. After the end of the exposures, the animals were transferred to metabolism cages, and urines were individually collected on ice for 48 h at 6 and 12 h intervals (rats and mice) or for 60 h at 12 h intervals (rabbits) in the biotransformation studies with HFO-1234ze and HFO-1234yf. In the comparative biotransformation study with HFO-1225yeZ, JDH and HFO-1234yf, urines were individually collected in a single interval for 24 h. Urine samples were analyzed by 19 F-NMR spectroscopy and LC/MS or GC/MS.

2.7 Enzymatic reactions *in vitro*

Pooled liver subcellular fractions or microsomes from rat (with or without pyridine pretreatment), rabbit and human were obtained either from Xeno Tech (Lenexa, KS), BD Biosciences (Woburn, MA) or self-prepared in the institut [62]. Incubations with HFO-1234yf or HFO-1234ze contained microsomes or S9, a NADPH-generating

system and/or glutathione as noted in a total volume of 1.0 mL of 0.1 M phosphate buffer containing 1 mM EDTA (pH 7.4) [19]. The final concentration of the cofactors was 10 mM for glutathione, NADP⁺ and glucose-6-phosphate (G-6-P). G-6-P-dehydrogenase was added to a final concentration of 0.25 Units/mL. Diethyl dithiocarbamate, a selective inhibitor of CYP450 2E1 [63], was used in final concentrations of 50, 100 and 300 μ M. Microsomes or S9, cofactors, and the corresponding amount of buffer were placed in sealed 2 mL GC vials and incubated for 10 min at 37 °C before addition of substrate. Gaseous HFO-1234yf or HFO-1234ze (10-100 μ L) were removed from Tedlar[®] bags (SKC Inc., Eighty Four, PA) and added through the septum with a gastight microliter syringe. Final protein concentrations were 0.5-2.5 mg/mL (rat and human S9 or rat microsomes) or 1-15 mg/mL (rabbit S9). Each reaction was repeated three times. Reaction mixtures were incubated at 37 °C in a water bath above a magnetic stirrer for 1-2 h. The vials were submerged in water to ensure constant temperatures in the vials. The reactions were stopped by placing the vials on ice. After centrifugation at 14,000 rpm and 4 °C for 10 min, the supernatants were used for determination of inorganic fluoride content and for recording ¹⁹F-NMR spectra. For LC/MS-MS analyses, the soluble proteins in these supernatants were denatured by the addition of 2 volumes of cold acetonitrile. After incubation overnight at 4 °C, the samples were centrifuged in a Beckmann TL-100 Ultracentrifuge at 80,000 rpm for 20 min. The clear supernatant was dried in vacuum and the remaining pellet dissolved in an identical volume of water. Hydroxylation of *p*-nitrophenol was determined as described [64] [65]. The absorbance of the formed product 4-nitrocatechol was measured spectrophotometrically at 510 nm with a molar extinction coefficient ϵ , determined to be 14.6 mmol⁻¹ cm⁻¹. Final protein concentrations were 1 and 2 mg/mL for rabbit, rat and human liver samples. No microsomal or S9 incubations were performed with HFO-1225yeZ and JDH.

2.8 Instrumental analyses

2.8.1 ^{19}F -NMR spectroscopy

^{19}F -NMR spectra were recorded with a Bruker DRX 300 NMR spectrometer with a 5 mm fluoride probe operating at 376 MHz. ^{19}F chemical shifts were referenced to external CFCl_3 . ^{19}F -NMR spectra were recorded with a 90° pulse length of 11 μs and a recycle delay of 1 s. The acquisition time was 1.5 s and 2 000 up to 5 000 scans were recorded for a good signal to noise (S/N) ratio. For comparison purposes the ^{19}F -NMR spectra were acquired with and without proton decoupling. Before the Fourier transformation a line broadening of 1 Hz was applied. To record NMR spectra, 720 μL of rat urine were diluted with 80 μL of D_2O , and samples were analyzed without further progressing. To analyze incubation mixtures, proteins were sedimented by centrifugation at 14,000 rpm at 4 $^\circ\text{C}$ for 10 min, and 80 μL of D_2O was added to the supernatants (720 μL). The mixtures were analyzed by ^{19}F -NMR spectroscopy without further workup. ^{19}F -NMR data were analyzed with the MestRe-C software (Mestrelab Research). Table 2 shows the ^{19}F -NMR characteristics of the compounds that were used or synthesized in this work.

Table 2: ^{19}F -NMR characteristics (chemical shift, multiplicity and ^1H - ^{19}F coupling) of compounds used in experiments or identified as metabolites in this thesis.

Compound	Chemical shift rel. to CFCl_3 [ppm]	^1H - ^{19}F Multiplicity	^1H - ^{19}F Coupling [Hz]
3,3,3-Trifluorolactic acid	-77.3	d	8.2
3,3,3-Trifluoropyruvic acid	-82.6	s	—
3,3,3-Trifluoroacetic acid	-75.4	s	—
3,3,3-Trifluoropropan-1-al	-63.2	t	10.9
3,3,3-Trifluoro-2-propanol	-80.8	d	7.0
3,3,3-Trifluoroacetone	-86.4	s	—
3,3,3-Trifluoro-1-hydroxyacetone	-83.4	s	—
3,3,3-Trifluoro-1-propanol	-64.3	t	11.2
3,3,3-Trifluoro-1,2-dihydroxypropane	-77.2	d	7.4
2,3,3,3-Tetrafluoropropene (HFO-1234yf)	-73.0; -125.6	d, m	n.a.
<i>trans</i> -1,1,1,3-Tetrafluoropropene (HFO-1234ze)	-61.2; -120	m, m	n.a.
1,2,3,3,3-Pentafluoropropene (HFO-1225yc)	n.a.	n.a.	n.a.
S-(3,3,3-Trifluoro-2-hydroxypropanyl)glutathione	-78.8	d	6.8
S-(3,3,3-Trifluoro-2-oxopropanyl)glutathione	-84.6	s	—
S-(3,3,3-Trifluoro-2-hydroxypropanyl)-L-cysteine	-79.0	d	6.6
S-(3,3,3-Trifluoro- <i>trans</i> -propenyl)-L-cysteine	-62.1	dd	$^2J_{\text{HF}} = 6.5$; $^3J_{\text{HF}} = 2.1$
<i>N</i> -Acetyl-S-(3,3,3-trifluoro-2-hydroxypropanyl)-L-cysteine	-78.7	d	6.6
<i>N</i> -Acetyl-S-(3,3,3-trifluoro- <i>trans</i> -propenyl)-L-cysteine	-62.0	dd	$^2J_{\text{HF}} = 6.5$; $^3J_{\text{HF}} = 2.0$
S-(3,3,3-trifluoro-2-hydroxypropanyl)mercaptoplactic acid	-78.9	d	7.0
S-(3,3,3-Trifluoro- <i>trans</i> -propenyl)mercaptoplactic acid	-61.8	dd	$^2J_{\text{HF}} = 6.6$; $^3J_{\text{HF}} = 2.1$
3,3,3-Trifluoropropionic acid	-63.5	t	11.4
1-Bromo-3,3,3-trifluoroacetone	-83.6	s	—

2.8.2 Mass Spectrometry, coupled with Liquid or Gas Chromatography

GC/MS analyses were performed with an Agilent 5973 mass spectrometer coupled to an Agilent 6890 GC. For the detection of volatile metabolites in incubations and urines, samples were heated in sealed 1 mL GC-vials and headspace samples were removed with a warmed syringe. Metabolites with a higher boiling point were extracted with dichloromethane from the samples before injection. For all LC/MS-MS analyses a Q Trap 2000 mass spectrometer (Applied Biosciences) was used in combination with an Agilent HPLC pump + 100 μ L autosampler (1100 series). After dilution with water (1:100 or 1000) and centrifugation 10 μ L of the sample were injected and negative ions were analyzed. For purification of synthesized substances, a Hewlett Packard Liquid Chromatograph (1090 series) was used in combination with a DAD-detector (H.P. 1046A).

2.8.3 Fluoride selective electrode

Inorganic fluoride in microsomal or S9 incubations and urine samples were analyzed with a fluoride-selective electrode combined with a reference electrode (WTW, Weilheim, Germany). For sample preparation, 800 μ L supernatant or urine was combined with an equal volume of total-ionic-strength-adjustment buffer (TISAB: 1 M acetic acid, 1 M sodium chloride, 0.012 M (\pm)-*trans*-1,2-diaminocyclohexane-*N,N,N',N'*-tetraacetic acid monohydrate in deionized water, pH 5.5).

2.9 Qualitative analysis of metabolites by mass spectrometry

Several urinary metabolites of HFO-1234yf and HFO-1234ze were identified by GC/MS or LC/MS-MS (IDA EPI), since they were found to be identical in fragmentation patterns and retention times to those of their synthetic reference compounds. Moreover, the signals were not observed in analyses of control urine samples.

2.9.1 Qualitative analysis of metabolites by GC/MS

2.9.1.1 3,3,3-Trifluoroacetone

3,3,3-Trifluoroacetone was identified by GC/MS using an Agilent Q-Plot fused-silica capillary column (30 m x 0.32 mm i.d.; film thickness, 20 μm) in the head-space from samples (100 μL) heated to 28 $^{\circ}\text{C}$. The typical intensities of m/z 43 [CO-CH_3 ; 76%] and 69 [CF_3 ; 24%] were detected with a retention time of 4.25 min when a linear temperature program from 100 $^{\circ}\text{C}$ to 170 $^{\circ}\text{C}$ with a heating rate of 10 $^{\circ}\text{C}/\text{min}$ was applied using helium as carrier gas with a flow rate of 2 mL/min.

2.9.1.2 3,3,3-Trifluoro-2-propanol

The presence of 3,3,3-trifluoro-2-propanol was confirmed by headspace GC/MS analysis. Vials were heated at 85 $^{\circ}\text{C}$ for 1 h and headspace samples were removed with a warmed syringe. Analyses were performed using an Agilent DB-WAX capillary column (30 m x 0.25 mm i.d.; film thickness, 25 μm) using a linear temperature program from 40 $^{\circ}\text{C}$ (hold for 1 min) to 160 $^{\circ}\text{C}$ (hold for 1 min) with a heating rate of 15 $^{\circ}\text{C}/\text{min}$; helium at 2 mL/min as carrier gas; and splitless injection. During the chromatographic separation, the intensities of m/z 45 [CHOHCH_3 ; 68%], 69 [CF_3 ; 17%] and 99 [CF_3CHOH ; 15%] eluted after 4.5 min and were monitored with a dwell time of 100 ms.

2.9.1.3 3,3,3-Trifluoroacetic acid

The presence of trifluoroacetic acid was confirmed by GC/MS after transformation to the methyl ester. Samples of urine (1 mL) were mixed with 80 μL 0.1 M NaOH and taken to dryness in an evacuated desiccator containing anhydrous P_2O_5 . The organic acids in the dried residues were converted to methyl esters by addition of methanol and concentrated (97%) sulfuric acid (100 μL each) and heated for 1 h at 80 $^{\circ}\text{C}$ in gas-tight reaction vials. Head-space samples (250 μL) were removed with a warmed (80 $^{\circ}\text{C}$) gastight syringe. Analysis was performed using an Agilent Q-Plot fused-silica

capillary column (30 m x 0.32 mm i.d.; film thickness, 20 μm) using a linear temperature program from 100 $^{\circ}\text{C}$ to 220 $^{\circ}\text{C}$ with a heating rate of 15 $^{\circ}\text{C}/\text{min}$; helium at 2 mL/min; and split injection with a split ratio of 5:1. During the chromatographic separation, the intensities of m/z 59 [COOCH_3 ; 48%] and 69 [CF_3 ; 52%] were monitored with a dwell time of 100 msec and were eluted after 4.75 min.

2.9.1.4 3,3,3-Trifluoro-1,2-dihydroxypropane

3,3,3-Trifluoro-1,2-dihydroxypropane was extracted from samples (1 mL) with dichloromethane. The organic solvent was evaporated and the residue was dissolved in 50 μL of dichloromethane. Samples (1 μL) were analysed by GC/MS using a Agilent DB-WAX column. Using a temperature gradient from 40 $^{\circ}\text{C}$ to 220 $^{\circ}\text{C}$, a heating rate of 10 $^{\circ}\text{C}/\text{min}$ and helium as carrier gas with a flow rate of 2 mL/min, the peaks of m/z 31 [CH_2OH], 69 [CF_3] and 80 [CF_2CHOH] characteristic of 3,3,3-trifluoro-1,2-dihydroxypropane were eluted after 13.0 min.

2.9.2 Qualitative analysis of metabolites by LC/MS-MS

2.9.2.1 3,3,3-Trifluorolactic acid

Qualitative analysis of 3,3,3-trifluorolactic acid was performed in the negative ion mode and peaks of characteristic fragments (m/z 59, 79 and 143) eluted from a ReproSil-Pur C18 column (AQ 5 μm) at a retention time of 4.28 min when a flow rate of 200 $\mu\text{L}/\text{min}$ and a linear gradient (from 98% water to 50% water in methanol in 20 min) was applied. Method setpoints were adjusted as follows: source temperature: 400 $^{\circ}\text{C}$; scan rate: 4000 amu/s; spray voltage: -4200 V; collision energy: -10 V; declustering potential: -30 V; entrance potential: -10 V; injection volume: 10 μL .

2.9.2.2 Glutathione S-conjugates and derivatives of cysteine S-conjugates

Several metabolites of HFO-1234ze or HFO-1234yf in urine samples or incubations with liver proteins were identified by LC/MS-MS in the negative ion mode, performing sensitive MRM (IDA EPI) analyses (Table 3). Method setpoints were adjusted as follows: source temperature: 400 °C; scan rate: 4000 amu/s; spray voltage: -4200 V; collision energy: -30 V; declustering potential: -26 V; entrance potential: -3.5 V. Volumes of 10 µL were injected and separated on a ReproSil-Pur C18 column (150 mm x 3 mm; AQ 3 µm). Samples were separated by different gradient elutions using 0.1% formic acid in water (eluent A) and acetonitrile (eluent B).

Gradient A: 98% eluent A holding for 5 min, then ramping first to 50% eluent B over 20 min and second to 90% eluent B over 2 min. The final concentration of 90% eluent B was held for 2 min.

Gradient B: 98% eluent A holding for 1 min, then ramping to 90% eluent B over 5 min and holding 90% eluent B for 3 min.

Gradient C: 100% eluent A holding for 3 min, then ramping to 100% eluent B in 12 min.

Table 3: Metabolites of HFO-1234yf or HFO-1234ze identified by LC/MS-MS in urine samples or incubations with liver protein.

Name	Transition detected for identification [m/z]	Characteristic fragments of EPI [m/z]	Retention time [min]	Gradient
S-(3,3,3-Trifluoro-2-oxopropanyl)glutathione	416/272	416, 272, 254 and 143	6.19	A
N-Acetyl-S-(3,3,3-trifluoro-2-hydroxypropanyl)-L-cysteine S-oxide	290/161	290, 161, 75 and 69	5.1	A
S-(3,3,3-Trifluoro-2-hydroxypropanyl)-mercaptolactic acid	233/145	233, 145, 75 and 69	14.3	A
S-(3,3,3-Trifluoro-2-hydroxypropanyl)glutathione	418/272	418, 272, 254 and 145	6.75	A
S-(3,3,3-Trifluoro-2-hydroxypropanyl)-mercaptolactic acid S-oxide	249/161	249, 161, 75 and 69	3.6	A
S-(3,3,3Trifluoro- <i>trans</i> -propenyl)-L-cysteine	214/127	214, 127, 107 and 87	6.79	B
2-S-(1-Carboxy-3,3,3-trifluoropropanyl)glutathione	432/272	432, 272 and 254	10.7	C
S-(3,3,3-Trifluoro- <i>trans</i> -propenyl)glutathione	400/272	400, 272 and 254	14.0	C

2.10 Quantitation of metabolites

2.10.1 Quantitation by GC/MS

2.10.1.1 HFO-1234yf , HFO-1234ze, HFO-1225yeZ and JDH

Quantitations of the gaseous compounds were performed in the course of the inhalation experiments. Head-space samples (100 μL) were removed with a gastight syringe from Tedlar[®] bags (SKC Inc., Eighty Four, PA) for calibration curves or from the inside of the inhalation chamber to monitor the projected gas concentration during the inhalation exposures. Analysis was performed using a Agilent Q-Plot fused-silica capillary column (30 m x 0.32 mm i.d.; film thickness, 20 μm) using a linear temperature program from 60 $^{\circ}\text{C}$ (hold for 1 min) to 130 $^{\circ}\text{C}$ (hold for 1 min) with a heating rate of 15 $^{\circ}\text{C}/\text{min}$; helium at 2 mL/min; and split injection with a split ratio of 5:1. All intensities were monitored with a dwell time of 100 msec. During the chromatographic separation, the intensities of m/z 45 [CFCH_2 ; 22%], 69 [CF_3 ; 40%], 95 [CF_3CCH_2 ; 18%] and 114 [CF_3CFCH_2 ; 19%] of HFO-1234yf eluted after 5.5 min. The intensities of m/z 45 [CHCHF ; 5%], 69 [CF_3 ; 40%], 95 [CF_3CHCH ; 33%] and 114 [CF_3CHCHF ; 22%] of HFO-1234ze eluted after 6.1 min. For both analytes, m/z 69 was monitored for quantitation. Typical fragments after ionization of HFO-1225yeZ were m/z 69 [CF_3 ; 36%], 82 [CF_2CHF ; 28%] and 113 [CF_3CFCH ; 36%]. For quantitation of HFO-1225yeZ and JDH which contains HFO-1225yeZ, m/z 69 was used. Calibration curves were prepared with air samples fortified with known concentrations of HFO-1234yf, HFO-1234ze or HFO-1225yeZ and by plotting the quotient m/z 32 [O_2 ; internal standard] and the chosen ionization fragment vs. the concentration of the parent compound. Quantitations were performed relative to the content of O_2 which eluted after 1.8 min. The use of O_2 as internal standard was acceptable, since all inhalation exposures were performed in a dynamic inhalation system with a high flow-through of the air-gas-mixture. Deviations between repeatedly analyzed reference samples were 10% and the response of the detector was linear in the concentration ranges used.

2.10.1.2 3,3,3-Trifluoropropionic acid

3,3,3-Trifluoropropionic acid was quantified by GC/MS after derivatization to the methyl ester, as described for the qualitative analysis of trifluoroacetic acid [66]. This method permitted the quantitation of 250 pmol/mL of 3,3,3-trifluoropropionic acid with a signal to noise ratio of 10:1. Deviations between repeatedly analyzed reference samples were 10% and the response of the detector was linear in the concentration ranges used. During the chromatographic separation, the intensities of m/z 69 [CF_3 ; 9%], 83 [CF_3CH_2 ; 16%], 111 [$\text{CF}_3\text{CH}_2\text{CO}$; 69%] and 142 [$\text{CF}_3\text{CH}_2\text{COOCH}_3$; 7%] were monitored after 7.5 min with a dwell time of 100 msec. Quantitation was performed relative to the content of difluoroacetic acid as internal standard which showed the characteristic fragment of m/z 51 [CF_2H] eluting after 5.8 min. Samples were analyzed in triplicate and calibration curves were measured before every sample sequence.

2.10.2. Quantitations by LC/MS

Several metabolites of HFO-1234yf and HFO-1234ze in urine samples of rabbits, rats and mice or in incubations with rabbit liver S9 fractions were quantified by LC/MS-MS (MRM) in the negative ion mode (Table 4). Method setpoints were adjusted as follows: source temperature: 400 °C; spray voltage: -4200 V; collision energy: -30 V; declustering potential: -26 V; entrance potential: -9.5 V. Samples were separated on a ReproSil-Pur C18 column (150 mm x 3 mm; AQ 3 μm) by a gradient elution using 98% eluent A (0.1% formic acid in water) holding for 1 min, then ramping to 90% eluent B (acetonitrile) over 5 min. After 3 min at 90% eluent B, the concentration of eluent A was elevated to 98% over 1 min. The flow rate was maintained at 300 $\mu\text{L}/\text{min}$ throughout the analysis. For quantitation of urinary metabolites, calibration curves were prepared with urine samples fortified with known concentrations of the analyte. *N*-Acetyl-*S*-(2-chloro-1,1,2-trifluoroethyl)-*L*-cysteine was used as internal standard for quantitation *N*-acetyl-*S*-(3,3,3-trifluoro-2-hydroxypropenyl)-*L*-cysteine. d_3 -*N*-Acetyl-*S*-(3,3,3-trifluoro-*trans*-propenyl)-*L*-cysteine was used as internal standard for quantitation of *N*-acetyl-*S*-(3,3,3-trifluoro-*trans*-propenyl)-*L*-cysteine and *S*-(3,3,3-trifluoro-*trans*-propenyl)mercaptolactic acid. All metabolites were quantified

with a signal to noise ratio of 10:1. Deviations between repeatedly analyzed reference samples were <10% and the response of the detector was linear in the concentration ranges used.

Table 4: Quantitation of metabolites of HFO-1234yf or HFO-1234ze by LC/MS-MS.

Name of analyte	Range of analyte in calibration curve [pmol/mL]	Lowest quantified concentration of analyte [pmol/mL]	Retention time [min]	Transition used for quantitation [<i>m/z</i>]	Characteristic fragments of EPI [<i>m/z</i>]
<i>N</i> -Acetyl- <i>S</i> -(3,3,3-trifluoro-2-hydroxypropanyl)- <i>L</i> -cysteine	0–218	1.8	7.47	274/145	274, 145, 75, 69
<i>N</i> -Acetyl- <i>S</i> -(3,3,3-trifluoro- <i>trans</i> -propenyl)- <i>L</i> -cysteine	0–117	1.2	8.35	256/127	256, 127, 107, 87
<i>S</i> -(3,3,3-Trifluoro- <i>trans</i> -propenyl)mercaptolactic acid	0–926	2.9	8.52	215/127	215, 127, 107, 87
Name of internal standard					
<i>d</i> ₃ - <i>N</i> -Acetyl- <i>S</i> -(3,3,3-trifluoro- <i>trans</i> -propenyl)- <i>L</i> -cysteine	—	—	8.35	259/127	259, 127, 107, 87
<i>N</i> -Acetyl- <i>S</i> -(2-chloro-1,1,2-trifluoroethyl)- <i>L</i> -cysteine	—	—	8.18	278/149	278, 149, 129

2.10.3. Quantitation of inorganic fluoride

For quantitation, the fluoride-selective electrode was calibrated daily with freshly prepared solutions containing 0.125, 0.25, 0.5, 1, 2, 3, 4, 5, 6, 7, 8, 9 and 10 ppm sodium fluoride. Samples were constantly stirred during analysis, and values for response (mV) were noted after 10 min. Calibration curves were prepared by plotting the voltage vs. the fluoride concentration. Inorganic fluoride was quantified in urine samples and in incubations with liver proteins. This method permitted the quantitation of 12 nmol/mL of inorganic fluoride and deviations between repeatedly analyzed reference samples were <10%.

3 Results

3.1 Biotransformation of HFO-1234ze in rats and mice

3.1.1 Inhalation exposures

In order to identify urinary metabolites of HFO-1234ze, male Sprague-Dawley rats (n=5/concentration) were exposed for 6 h by inhalation to 2 000, 10,000, and 50,000 ppm in a dynamic inhalation system. Male B6C3F1 mice (n=5) were exposed for 6 h to a single concentration of 50,000 ppm to obtain a comparison of the metabolite profiles. Concentrations of HFO-1234ze in the exposure chamber were monitored by GC/MS throughout the inhalation exposure. In the inhalation exposures with rats, measured concentrations of HFO-1234ze were 755 ± 283 ppm (target 2 000 ppm), $12,797 \pm 5\,249$ ppm (target 10,000 ppm) and $51,091 \pm 486$ ppm (target 50,000 ppm), based on mean \pm SD from 15 determinations of HFO-1234ze air concentrations over the exposure time. In the inhalation exposure with mice, the mean concentration of HFO-1234ze was determined to be $47,405 \pm 9\,254$ ppm (target 50,000 ppm). After the end of the exposures, animals were transferred to metabolism cages to individually collect urine in 6 or 12 h intervals for 48 h (Figure 5). Additionally, control urines had been collected before the exposures.

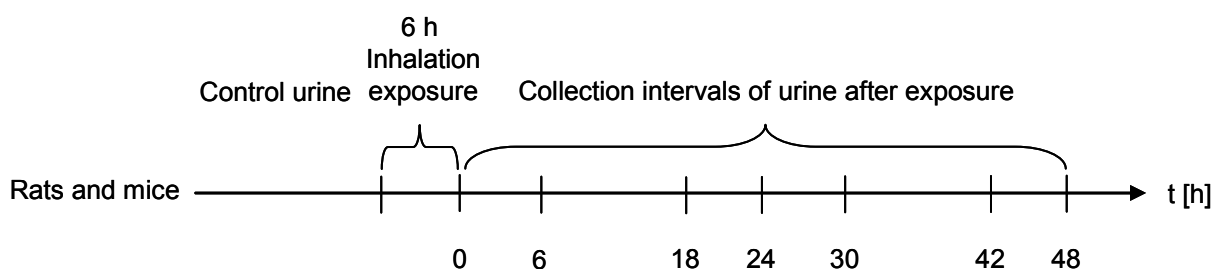


Figure 5: Design of urine collections from rats and mice after exposure to HFO-1234ze.

3.1.2 Qualitative analyses of urine samples by ^{19}F -NMR

After the inhalation exposures, collected urines of rats and mice were analyzed by ^{19}F -NMR spectroscopy, recording ^1H -coupled and ^1H -decoupled spectra. In order to detect small traces of fluorine-containing metabolites by this approach, up to 4 000 scans were recorded of each urine sample. In ^{19}F -NMR spectra of urines from rats and mice exposed to 50,000 ppm HFO-1234ze (Figures 6 and 7), several resonances were present and could be allocated to metabolites formed from HFO-1234ze, since ^{19}F -NMR spectra from urine samples collected before the inhalation exposures did not contain any signals. Moreover, no signals were present in ^{19}F -NMR spectra of rat urine samples collected after exposure to 2 000 and 10,000 ppm HFO-1234ze.

3.1.2.1 ^1H -decoupled ^{19}F -NMR spectra

In ^1H -decoupled ^{19}F -NMR spectra from urines of rats and mice (Figure 6), all metabolite signals were singlets, indicating the presence of three magnetically equivalent fluorine atoms and the absence of a fluorine atom at the carbon in β -position to the CF_3 -moiety which would yield complex signals due to ^{19}F - ^{19}F couplings. Even though the loss of inorganic fluoride from the carbon atom in β -position to the CF_3 -moiety is obvious regarding ^1H -decoupled ^{19}F -NMR spectra, only a small signal at $\delta = -119.6$ ppm was present in ^{19}F -NMR spectra of urine samples, likely due to efficient incorporation of inorganic fluoride in teeth and bones.

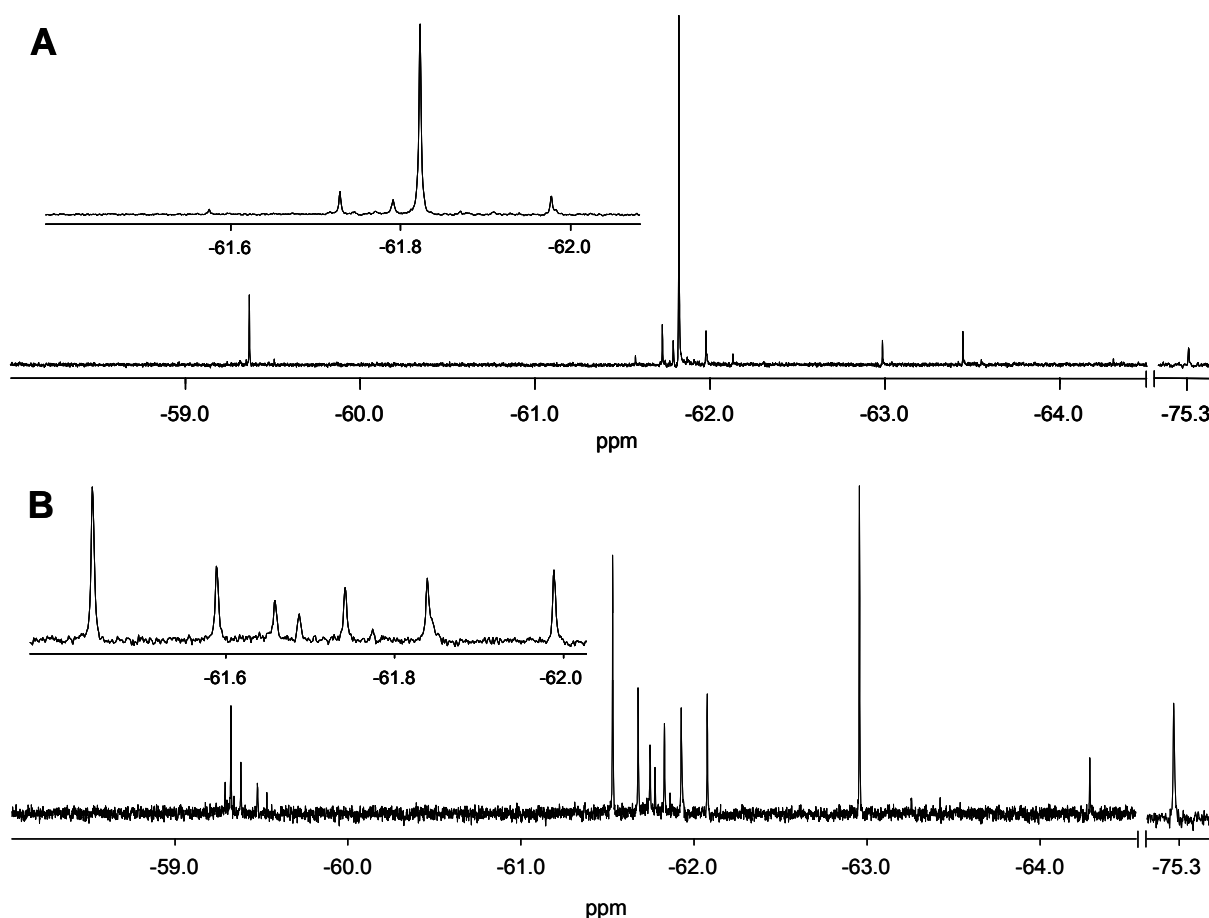


Figure 6: ^1H -decoupled ^{19}F -NMR spectra from urine samples of a rat (A) and a mouse (B), collected within the first 6 h after the end of the inhalation exposure to 50,000 ppm HFO-1234ze. A zoom of the range between -61.6 and -62.0 ppm of each spectrum was placed above the main scale.

3.1.2.2 ^1H -coupled ^{19}F -NMR spectra

In ^1H -coupled ^{19}F -NMR spectra of urine samples from rats and mice collected after exposure to 50,000 ppm HFO-1234ze (Figure 7), signals were split into doublets, triplets or doublet of doublets with characteristic ^1H - ^{19}F couplings. In general, doublets are indicative of the presence of one proton at the carbon atom in α -position to the CF_3 -moiety, triplets are associated with structures possessing a CH_2 -group next to the CF_3 -moiety and doublets of structures containing a vinylic CF_3 -moiety are likely split into doublets of doublets due to the coupling of the fluorine atoms with a proton at the carbon atom in β -position to the CF_3 -group [67]. Moreover, structures showing a chemical shift in the range of approx. -55 to -65 ppm do not contain a

hydroxy group or an oxygen atom bond to the carbon in α -position to the CF_3 -moiety, since these substituents would yield chemical shifts of approx. -70 to -80 ppm and -80 to -90 ppm, respectively.

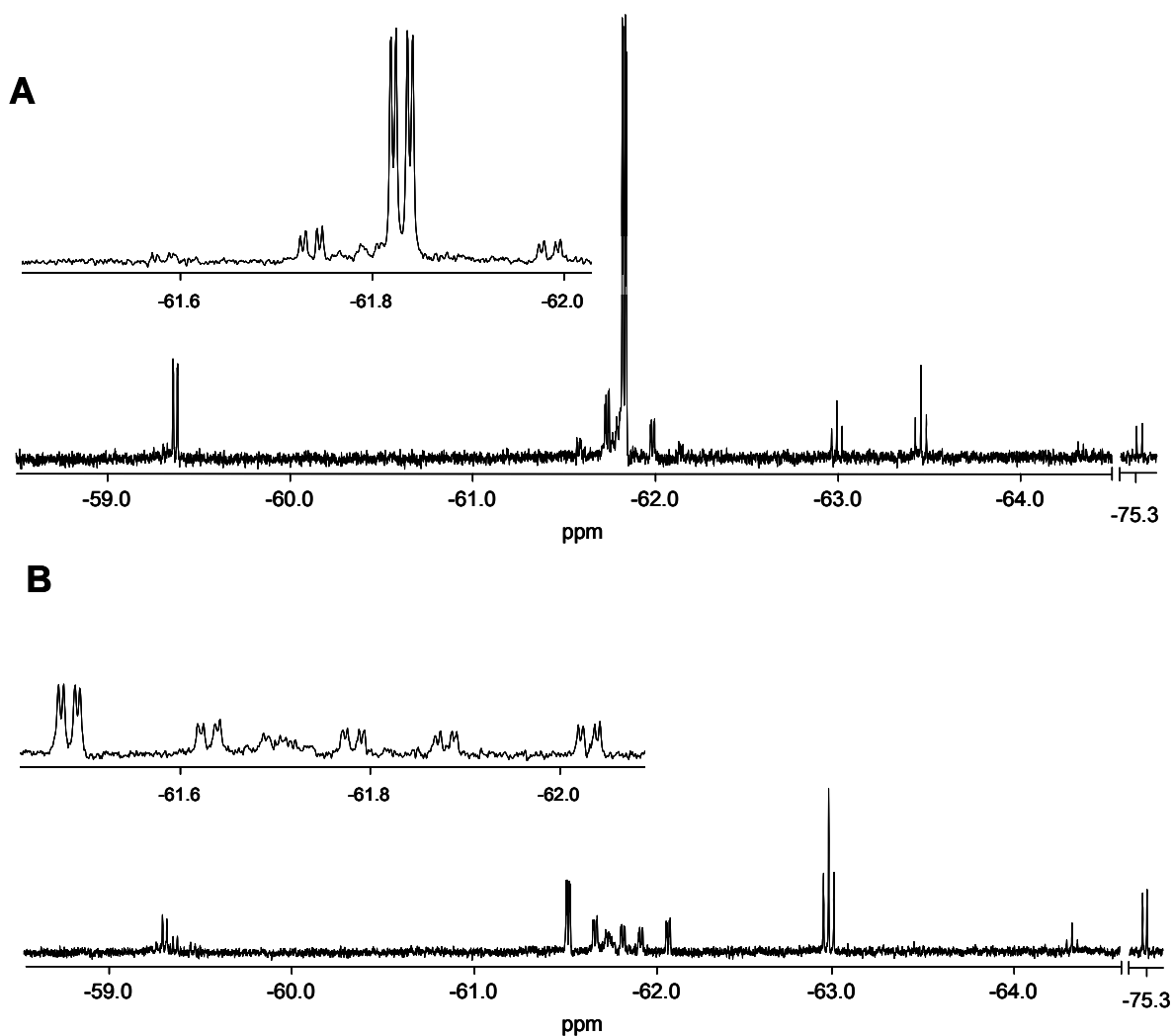


Figure 7: ^1H -coupled ^{19}F -NMR spectra from urine samples of a rat (A) and a mouse (B), collected within the first 6 h after the end of the inhalation exposure to 50,000 ppm HFO-1234ze. A zoom of the range between -61.6 and -62.0 ppm of each spectrum was placed on top of the main scale.

3.1.2.3 Identification of metabolites of HFO-1234ze by ^{19}F -NMR

Beside qualitative analyses by mass spectrometry, urinary metabolites were identified by comparison of their ^{19}F -NMR characteristics (chemical shift, multiplicity, ^1H - ^{19}F coupling) to those of their synthetical reference compounds (Table 5). The major resonance in the ^1H -coupled ^{19}F -NMR spectrum of rat urine after exposure to HFO-1234ze (Figure 7 A) was a doublet of doublet at $\delta = -61.8$ ppm that was identical in chemical shift and fluorine-proton coupling ($^2J_{\text{HF}} = 6.6$ Hz; $^3J_{\text{HF}} = 2.1$ Hz) to that of synthetic *S*-(3,3,3-trifluoro-*trans*-propenyl)mercaptolactic acid (**6**, Scheme 1). The resonance at $\delta = -62.1$ ppm (dd; $^2J_{\text{HF}} = 6.5$ Hz, $^3J_{\text{HF}} = 2.1$) was identical in chemical shift and fluorine-proton coupling to that of *S*-(3,3,3-trifluoro-*trans*-propenyl)-*L*-cysteine (**4**, Scheme 1), whereas the resonance at $\delta = -62.0$ ppm (dd; $^2J_{\text{HF}} = 6.5$ Hz, $^3J_{\text{HF}} = 2.0$) was allocated to *N*-acetyl-*S*-(3,3,3-trifluoro-*trans*-propenyl)-*L*-cysteine (**7**, Scheme 1). The triplet at $\delta = -63.5$ ppm ($J_{\text{HF}} = 11.4$ Hz) represents 3,3,3-trifluoropropionic acid (**11**, Scheme 1). Moreover, the resonance at $\delta = -75.3$ ppm (d, $J_{\text{HF}} = 8.2$ Hz) is identical in chemical shift and fluorine-proton coupling to that of 3,3,3-trifluorolactic acid (**17**, Scheme 1).

Most of the resonances seen in ^{19}F -NMR spectra of urine samples collected from rats after exposure to 50,000 ppm HFO-1234ze were also present in mouse urine (Figures 6 B and 7 B). However, *S*-(3,3,3-trifluoro-*trans*-propenyl)mercaptolactic acid (**6**, Scheme 1) was only present as a minor metabolite. Biotransformation of HFO-1234ze in mice mainly yielded a hypothesized 3,3,3-trifluoropropionamide (**12**, Scheme 1) at $\delta = -63.0$ ppm (t, $J_{\text{HF}} = 10.7$ Hz) which is likely a product of an amino acid conjugation of 3,3,3-trifluoropropionic acid (**11**, Scheme 1). An appropriate structure represents (3,3,3-trifluoropropionylamino)-acetic acid, as carbon acids may be conjugated with glycine in rodents [68]. The formation of a metabolite possessing identical ^{19}F -NMR characteristics as the presumed 3,3,3-trifluoropropionamide was observed after oral gavage of 3,3,3-trifluoropropionic acid to rats [66]. The triplet representing 3,3,3-trifluoropropionic acid was not present in ^{19}F -NMR spectra of mouse urine samples after exposure to HFO-1234ze (Figures 6 B and 7 B), indicating a possible quantitative conjugation of 3,3,3-trifluoropropionic acid or catabolism. The signal at $\delta = -64.3$ ppm (t; $J_{\text{HF}} = 11.2$ Hz) is identical in ^{19}F -NMR characteristics to those of 3,3,3-trifluoro-1-propanol (**18**, Scheme 1). The

biotransformation product of HFO-1234ze in urine samples of rats and mice showing a doublet in ^1H -coupled ^{19}F -NMR spectra at $\delta = -59.4$ ppm (d, $J_{\text{HF}} = 8.9$ Hz) may be a metabolic successor of 2-S-(1-carboxy-3,3,3-trifluoropropenyl)glutathione (**15**, Scheme 1), whose presence is indicated by LC/MS-MS in incubations of rat liver microsomes containing NADPH, glutathione and HFO-1234ze (Figure 13).

Table 5: Metabolites of HFO-1234ze in urines of rats and mice, identified by ^{19}F -NMR.

Name of metabolite	Structure	Chem. shift [ppm]	Multiplicity	^1H - ^{19}F Coupling [Hz]
S-(3,3,3-Trifluoro- <i>trans</i> -propenyl)mercaptolactic acid		-61.8	dd	$^2J_{\text{HF}} = 6.6$ $^3J_{\text{HF}} = 2.1$
<i>N</i> -Acetyl-S-(3,3,3-trifluoro- <i>trans</i> -propenyl)-L-cysteine		-62.0	dd	$^2J_{\text{HF}} = 6.5$ $^3J_{\text{HF}} = 2.0$
S-(3,3,3-Trifluoro- <i>trans</i> -propenyl)-L-cysteine		-62.1	dd	$^2J_{\text{HF}} = 6.5$ $^3J_{\text{HF}} = 2.1$
3,3,3-Trifluoropropionamide		-63.0	t	$J_{\text{HF}} = 10.7$
3,3,3-Trifluoropropionic acid		-63.5	t	$J_{\text{HF}} = 11.2$
3,3,3-Trifluoro-1-propanol		-64.3	t	$J_{\text{HF}} = 11.2$
3,3,3-Trifluorolactic acid		-75.3	d	$J_{\text{HF}} = 8.2$

3.1.2.4 Oral gavage of 3,3,3-trifluoro-1-propanol to a rat

In order to investigate the metabolic fate of 3,3,3-trifluoro-1-propanol which was identified by ^{19}F -NMR as metabolite of HFO-1234ze in urines of rats and mice, the metabolite was administered by oral gavage to a male Sprague-Dawley rat. Urine was collected for 24 h after the administration and analyzed by ^{19}F -NMR spectroscopy (Figure 8). Biotransformation of 3,3,3-trifluoro-1-propanol yielded three triplets in the ^1H -coupled ^{19}F -NMR spectrum. The triplet at $\delta = -64.4$ ppm ($J_{\text{HF}} = 11.2$ Hz) could be allocated to 3,3,3-trifluoro-1-propanol. The main metabolite of 3,3,3-

trifluoro-1-propanol showed a triplet at $\delta = -63.5$ ppm ($J_{\text{HF}} = 11.4$ Hz) and was identical to ^{19}F -NMR characteristics of 3,3,3-trifluoropropionic acid. The third triplet at $\delta = -63.0$ ppm ($J_{\text{HF}} = 10.7$ Hz) was identical in chemical shift, multiplicity and ^1H - ^{19}F -coupling to the presumed 3,3,3-trifluoropropionamide present in urines of rats and mice after exposure to HFO-1234ze. The 3,3,3-trifluoropropionamide may be formed by conjugation of 3,3,3-trifluoropropionic acid with an amino acid which is likely to be glycine in rodents [68].

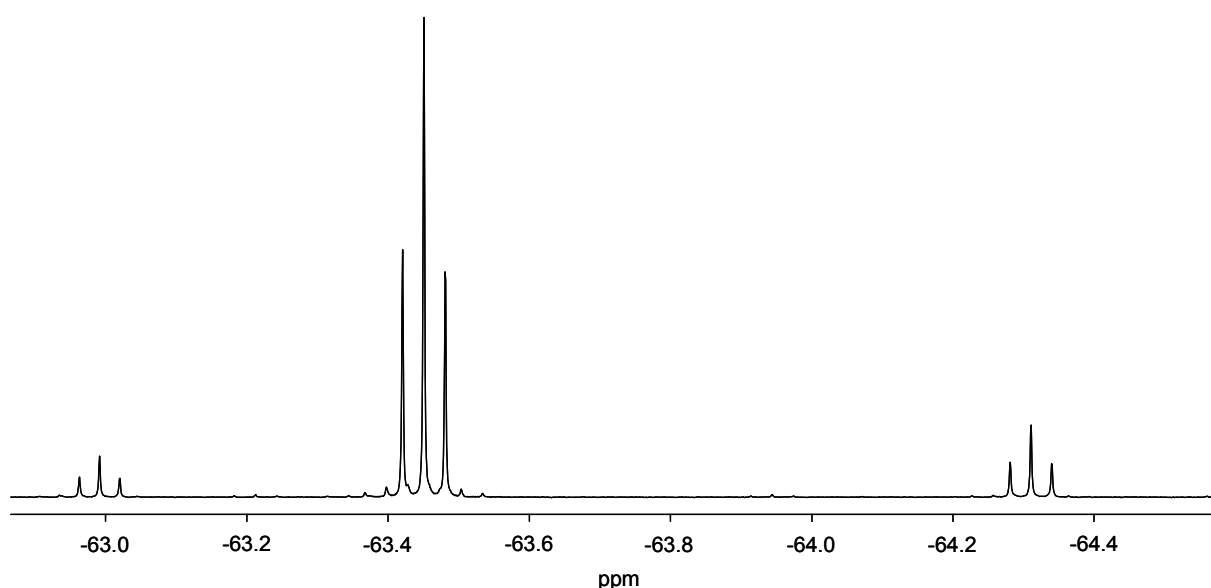


Figure 8: ^1H -coupled ^{19}F -NMR spectrum of urine collected from a rat after oral gavage of 3,3,3-trifluoro-1-propanol. The triplet at $\delta = -64.4$ ($J_{\text{HF}} = 11.2$ Hz) was allocated to 3,3,3-trifluoro-1-propanol, the signal at $\delta = -63.5$ (t; $J_{\text{HF}} = 11.4$ Hz) was identified as 3,3,3-trifluoropropionic acid and the triplet at $\delta = -63.0$ (t; $J_{\text{HF}} = 10.7$ Hz) represents the presumed 3,3,3-trifluoropropionamid.

3.1.2.5 Conjugation of 3,3,3-trifluoropropanal with urea

Even though ^{19}F -NMR considerations did not indicate the presence of 3,3,3-trifluoropropanal in urines from rats and mice after exposure to HFO-1234ze, the aldehyde is likely to be the metabolic precursor of 3,3,3-trifluoropropionic acid, conclusively identified by ^{19}F -NMR spectroscopy and mass spectrometry. As shown for the structural similar 3,3,3-trifluoroethanal, aldehydes excreted with urine may

conjugate with urea [69]. Therefore, 2 μL 3,3,3-trifluoropropanal were incubated in 1 mL of an aqueous urea solution (1 M) and incubated at 37 $^{\circ}\text{C}$ overnight. Subsequent analysis by ^{19}F -NMR spectroscopy showed the presence of two additional fluorine-containing substances in the incubation (Figure 9). Beside the triplet of 3,3,3-trifluoropropanal at $\delta = -63.2$ ppm ($J_{\text{HF}} = 10.9$ Hz), signals at $\delta = -63.6$ ppm ($J_{\text{HF}} = 10.65$ Hz) and at $\delta = -64.1$ ppm ($J_{\text{HF}} = 10.54$ Hz) may be allocated to 3,3,3-trifluoropropanal-urea and bis-(3,3,3-trifluoropropanal)-urea adducts. Since no metabolite of HFO-1234ze present in urines of rats and mice showed identical ^{19}F -NMR characteristics, mass spectrometric analyses of the presumed urea-conjugates were not performed.

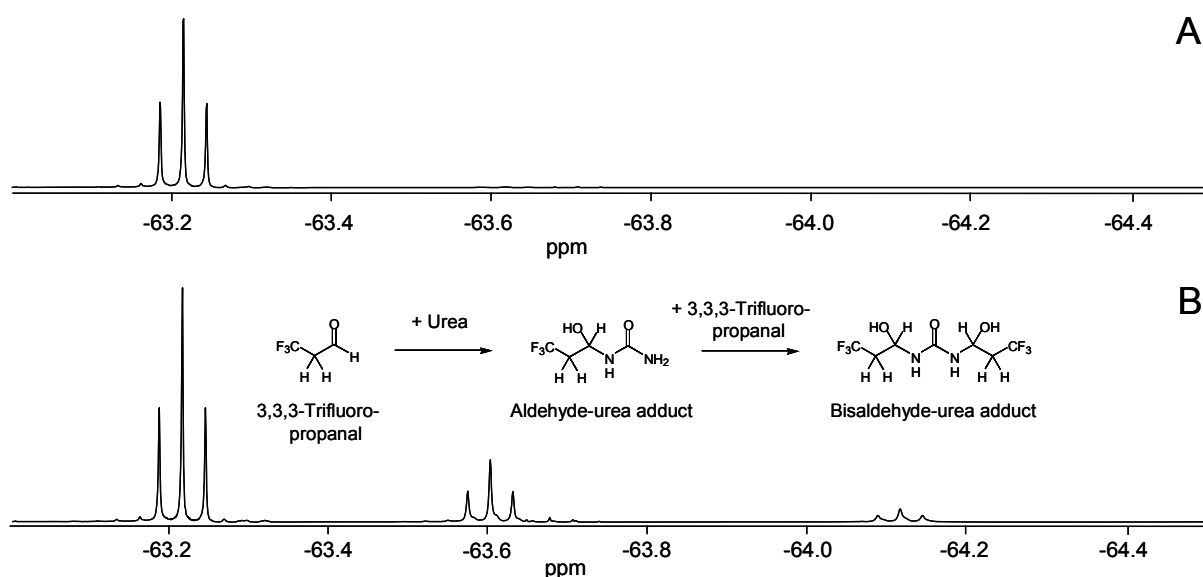


Figure 9: ^1H -coupled ^{19}F -NMR spectra of 3,3,3-trifluoropropanal in water (A) and in aqueous urea solution (B). The resonances at $\delta = -63.6$ and -64.1 ppm may be attributable to urea conjugates of the aldehyde.

3.1.3 Qualitative analyses of urine samples by mass spectrometry

In addition to ^{19}F -NMR analyses, structures of urinary metabolites were confirmed by LC/MS or GC/MS. In urine samples of both rats and mice, the presence of *S*-(3,3,3-trifluoro-*trans*-propenyl)mercaptolactic acid, *N*-acetyl-*S*-(3,3,3-trifluoro-*trans*-

propenyl)-L-cysteine and S-(3,3,3-trifluoro-*trans*-propenyl)-L-cysteine were confirmed by LC/MS-MS (IDA EPI), whereas 3,3,3-trifluoropropionic acid was identified by GC/MS. The synthetic reference compounds and the urinary metabolites showed identical retention times and mass fragments after ionization. Moreover, the identified metabolites were shown to be absent in samples of control urines.

3.1.3.1. Identification of urinary metabolites of HFO-1234ze by LC/MS

The characteristic EPIs of S-(3,3,3-trifluoro-*trans*-propenyl)-L-cysteine (A), N-acetyl-S-(3,3,3-trifluoro-*trans*-propenyl)-L-cysteine (B) and S-(3,3,3-trifluoro-*trans*-propenyl)mercaptolactic acid (C) show losses of neutral fragments (NL) which are typical of thioethers of cysteine (NL 87 amu), lactic acid (NL 88 amu) and N-acetyl-L-cysteine (NL 129 amu) (Figure 10 and Table 6). The ionization fragments of m/z 87 and 107 in the EPIs (A–C) are likely formed by releasing two times HF (m/z 20) from the common S-(3,3,3-trifluorovinyl)-ion (m/z 127).

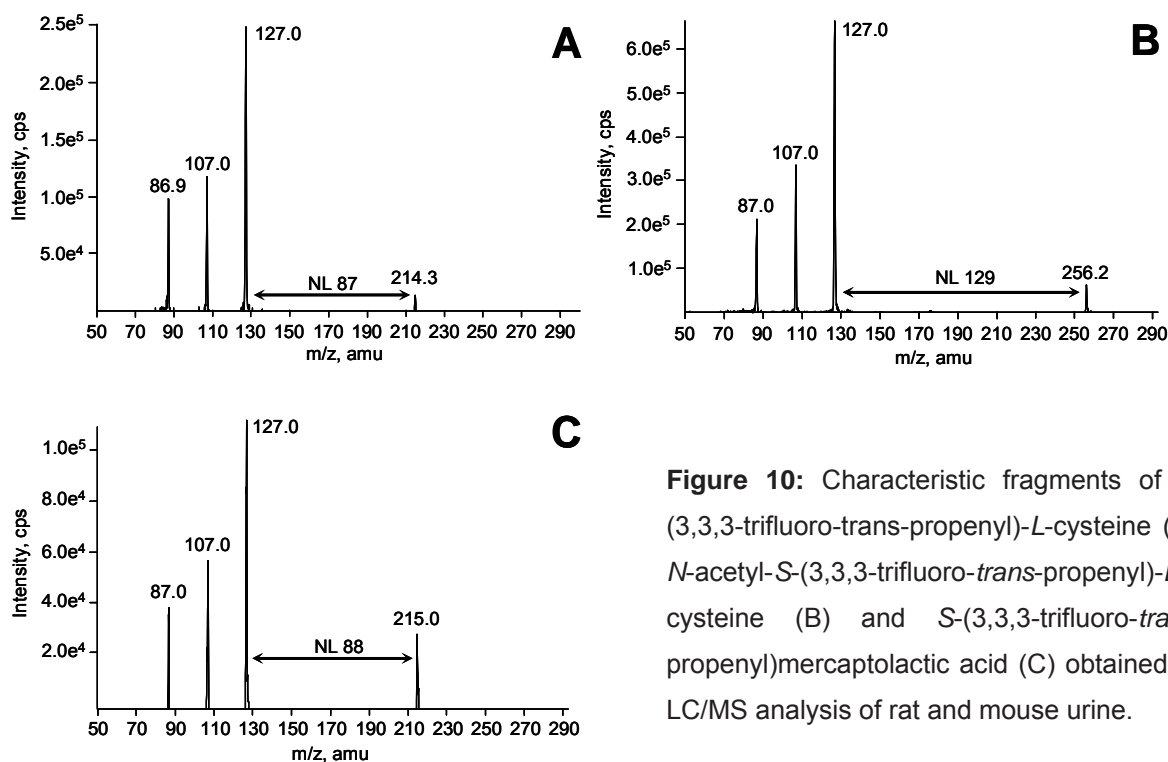
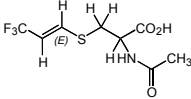
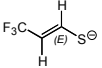
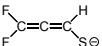
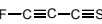
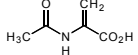
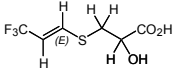
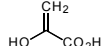
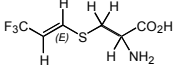
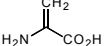


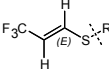
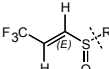
Figure 10: Characteristic fragments of S-(3,3,3-trifluoro-*trans*-propenyl)-L-cysteine (A), N-acetyl-S-(3,3,3-trifluoro-*trans*-propenyl)-L-cysteine (B) and S-(3,3,3-trifluoro-*trans*-propenyl)mercaptolactic acid (C) obtained by LC/MS analysis of rat and mouse urine.

Table 6: Interpretation of EPIs of urinary metabolites of HFO-1234ze identified by LC/MS, explaining the losses of neutral fragments.

Name of metabolite	Structure	Fragments after ionization	
		Thiolate ions	Neutral fragment
<i>N</i> -Acetyl- <i>S</i> (3,3,3-trifluoro- <i>trans</i> -propenyl)- <i>L</i> -cysteine		 <i>m/z</i> 127  <i>m/z</i> 107  <i>m/z</i> 87	 <i>m/z</i> 129
<i>S</i> -(3,3,3-Trifluoro- <i>trans</i> -propenyl)mercaptolactic acid		—//—	 <i>m/z</i> 88
<i>S</i> -(3,3,3-Trifluoro- <i>trans</i> -propenyl)- <i>L</i> -cysteine		—//—	 <i>m/z</i> 87

In order to identify further metabolites derivative of the cysteine *S*-conjugate of HFO-1234ze, LC/MS analyses of urines from rats and mice were performed in the sensitive MRM mode, using the transitions of the appropriate molecular ions to *m/z* 127 for 3,3,3-trifluorovinyl *S*-conjugates and to *m/z* 143 for 3,3,3-trifluorovinyl *S*-conjugates *S*-oxides (Table 7).

Table 7: Search for possible derivatives of *S*-(3,3,3-trifluoro-*trans*-propenyl)-*L*-cysteine by LC/MS (MRM).

Metabolite		
Name	Structure	Transition used for identification
3,3,3-Trifluorovinyl <i>S</i> -conjugate		<i>m/z</i> [molecular ion] to <i>m/z</i> 127
3,3,3-Trifluorovinyl <i>S</i> -conjugate <i>S</i> -oxide		<i>m/z</i> [molecular ion] to <i>m/z</i> 143

In the chromatograms of urine samples of rats and mice exposed to HFO-1234ze, the signals of the cysteine *S*-conjugate and *N*-acetyl-*L*-cysteine *S*-conjugate of HFO-1234ze were present, but no signals were indicative of the presence of sulfoxides.

The mercaptolactic acid *S*-conjugate was also observed, whereas its metabolic precursor mercaptopyruvic acid *S*-conjugate could not be detected. Moreover, this approach gave no evidence for the presence of the mercaptoacetic acid *S*-conjugate, the *S*-methyl conjugate and the *S*-glucuronide in urine samples.

3.1.3.2. Identification of urinary metabolites of HFO-1234ze by GC/MS

3,3,3-Trifluoropropionic acid was present as a minor metabolite in urines of rats and mice after inhalation exposure to HFO-1234ze and identified by GC/MS after derivatization to the methyl ester. In the chromatogram, recorded in the Single Ion Monitoring (SIM) scan, typical ionization fragments were present and were allocated to the CF_2H -residue (m/z 51; 4%), the CF_3 -group (m/z 69; 8%), the CF_3CH_2 -residue (m/z 83; 14%), the $\text{CF}_3\text{CH}_2\text{CO}$ -residue (m/z 111; 66%) and the non-ionized methyl ester (m/z 142; 8%) (Figure 11 A). The chromatograms showing the absence and presence of selected m/z 111 after 7.5 min in urine samples of rats collected before and after the inhalation are presented in figure 11 B.

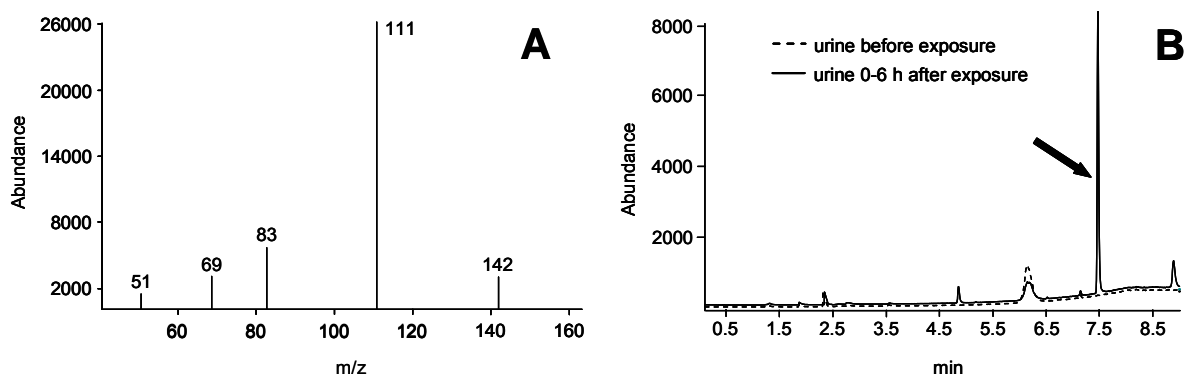


Figure 11: Identification of 3,3,3-trifluoropropionic acid as methyl ester in urine of rats and mice after exposure to 50,000 ppm HFO-1234ze. Typical fragments of the methyl ester recorded in a SIM scan (A); overlay of chromatograms showing absence and presence of m/z 111 at 7.5 min in urine collected before and after the exposure, respectively (B).

3.1.4 Quantitation of urinary metabolites of HFO-1234ze

^{19}F -NMR spectra indicated that *S*-(3,3,3-trifluoro-*trans*-propenyl)mercaptolactic acid was the major metabolite of HFO-1234ze in rat urine after inhalation exposure to 50,000 ppm. This *S*-conjugate was therefore quantified to determine the kinetics of excretion. In rats, the recovery of *S*-(3,3,3-trifluoro-*trans*-propenyl)mercaptolactic acid excreted within 48 h in urine was determined as 349 ± 169 , 309 ± 111 and $7\,137 \pm 2\,115$ nmol at 2 000, 10,000 and 50,000 ppm. In mice, the recovery of this metabolite was $2\,027 \pm 458$ nmol at 50,000 ppm (Figure 12 and Table 8). Quantitative analysis of rat urine samples from the three different exposure concentrations over time shows that *S*-(3,3,3-trifluoro-*trans*-propenyl)mercaptolactic acid is rapidly excreted, since 95% of total excretion occurred within 18 h after the end of exposure ($t_{1/2}$ approx. 6 h). After the 2 000 and 10,000 ppm inhalations, only very small quantities of *S*-(3,3,3-trifluoro-*trans*-propenyl)mercaptolactic acid were detected by LC/MS in the sensitive MRM mode and no signals were present in the ^{19}F -NMR spectra.

After inhalation exposure of mice to 50,000 ppm HFO-1234ze, *S*-(3,3,3-trifluoro-*trans*-propenyl)mercaptolactic acid was present as a minor metabolite accounting for 8% of total ^{19}F -related signals in contrast to 66% in rat urine (50,000 ppm). In all urine samples of rats and mice, *N*-acetyl-*S*-(3,3,3-trifluoro-*trans*-propenyl)-*L*-cysteine and 3,3,3-trifluoropropionic acid were present as minor metabolites. For *N*-acetyl-*S*-(3,3,3-trifluoro-*trans*-propenyl)-*L*-cysteine, urinary recovery was calculated to be 23 ± 7 , 27 ± 12 and 452 ± 98 nmol at 2 000, 10,000 and 50,000 ppm in rats and 4 ± 1 nmol at 50,000 ppm in mice. The urinary recovery of 3,3,3-trifluoropropionic acid amounted to 18 ± 4 , 26 ± 8 and 402 ± 60 nmol at 2 000, 10,000 and 50,000 ppm in rats and to 61 ± 16 nmol at 50,000 ppm in mice (Figure 12 and Table 8). Both *N*-acetyl-*S*-(3,3,3-trifluoro-*trans*-propenyl)-*L*-cysteine and 3,3,3-trifluoropropionic acid were also rapidly excreted and 95% of the total were recovered within 18 h after the end of exposure ($t_{1/2}$ approx. 6 h). The extent of biotransformation of HFO-1234ze in rats and mice at the 50,000 ppm level were assessed, using the individual respiratory minute volumes of 0.8 and $1.3 \text{ L min}^{-1} \text{ kg}^{-1}$ [70] and body weights of 230 and 30 g for rats and mice, respectively. Total amounts of HFO-1234ze received by inhalation for 6 h were calculated to be 149 mmol in rats and

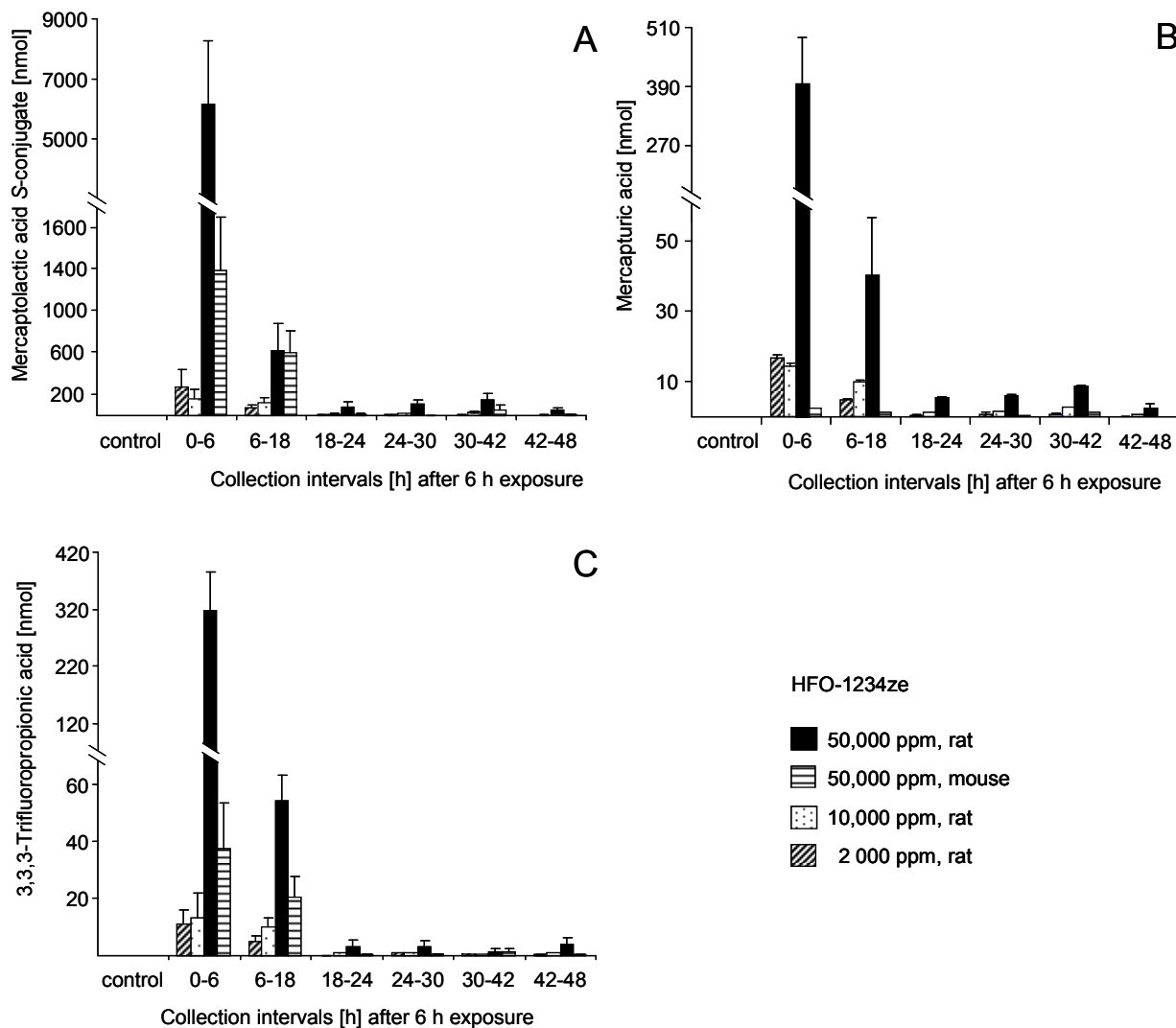


Figure 12: Time course of urine excretion of *S*-(3,3,3-trifluoro-*trans*-propenyl)mercaptolactic acid (A), *N*-acetyl-*S*-(3,3,3-trifluoro-*trans*-propenyl)-*L*-cysteine (B) and 3,3,3-trifluoropropionic acid (C) in rats and mice after inhalation exposure to different concentrations of HFO-1234ze.

31.3 mmol in mice. Quantified amounts of *S*-(3,3,3-trifluoro-*trans*-propenyl)mercaptolactic acid were 7 137 and 2 027 nmol in rats and mice (Table 8), representing 66 and 8% of total ^{19}F -related signal intensities, respectively. Thus, the extents to which biotransformation of HFO-1234ze occurred were 0.007 (rats) and 0.08% (mice) of the total dose received by inhalation.

Table 8: Recovery of *S*-(3,3,3-trifluoro-*trans*-propenyl)mercaptolactic acid, *N*-acetyl-*S*-(3,3,3-trifluoro-*trans*-propenyl)-*L*-cysteine and 3,3,3-trifluoropropionic acid in urines of rats and mice excreted within 48 h after inhalation exposure to HFO-1234ze for 6 h.

n.a. inhalation exposures not performed.

Exposure concentration ppm	<i>S</i> -(3,3,3-Trifluoro- <i>trans</i> -propenyl)mercaptolactic acid [nmol]		<i>N</i> -Acetyl- <i>S</i> -(3,3,3-trifluoro- <i>trans</i> -propenyl)- <i>L</i> -cysteine [nmol]		3,3,3-Trifluoropropionic acid [nmol]	
	Rats	Mice	Rats	Mice	Rats	Mice
2 000	349 ± 169	n.a.	23 ± 7	n.a.	18 ± 4	n.a.
10,000	309 ± 111	n.a.	27 ± 12	n.a.	26 ± 8	n.a.
50,000	7 137 ± 2115	2 027 ± 458	452 ± 98	4 ± 1	402 ± 60	61 ± 16

3.1.5 Qualitative analyses of metabolites of HFO-1234ze in incubations with liver protein

To characterize biotransformation by rat liver microsomes (native and pyridine induced) and human S9 fractions, incubations with HFO-1234ze and appropriate cofactors were performed.

3.1.5.1 Identification of metabolites by ¹⁹F-NMR

Besides the signals of the parent compound, no additional resonances were apparent in ¹⁹F-NMR spectra (not shown) of incubation mixtures containing NADPH and/or glutathione after reaction times of up to 1 h, even when protein concentrations of 4 mg/mL were used. However, the microsomal preparations exhibited *p*-nitrophenol oxidase activity which is a marker for the activity of CYP450 2E1 [64]. Oxidation rates of *p*-nitrophenol were 0.18 ± 0.05 nmol mg⁻¹ min⁻¹ in liver microsomes from rats without pretreatment, 3.22 ± 1.2 nmol mg⁻¹ min⁻¹ in liver microsomes from pyridine-pretreated rats, and 0.11 ± 0.02 nmol mg⁻¹ protein min⁻¹ in human S9 fractions. Moreover, when 2,3,3,3-tetrafluoropropene (HFO-1234yf) was used as a positive control, ¹⁹F-NMR signals were observed as reported [57].

3.1.5.2 Identification of metabolites by LC/MS

A more sensitive analysis of incubations containing rat liver microsomes and S9 fractions, a NADPH-regenerating system, glutathione, and HFO-1234ze was performed by LC/MS in the sensitive MRM mode. Potential glutathione S-conjugates formed from HFO-1234ze were searched using the transitions of the appropriate molecular ions to m/z 272 and 254, typical fragments of glutathione S-conjugates after electrospray ionization [71]. By this approach, S-(3,3,3-trifluoro-*trans*-propenyl)glutathione (**2**, Scheme 1) a presumed precursor of the S-conjugates present in urine samples of rats and mice was tentatively identified, as well as 2-S-(1-carboxy-3,3,3-trifluoropropyl)glutathione (**15**, Scheme 1), a reaction product of glutathione and HFO-1234ze (Figure 13). Due to low intensities of both glutathione S-conjugates in incubations, no EPIs could be recorded. A comparison with the reference compounds could not be performed, since the glutathione S-conjugates were not synthesized. Moreover, no information on the reaction rates could be

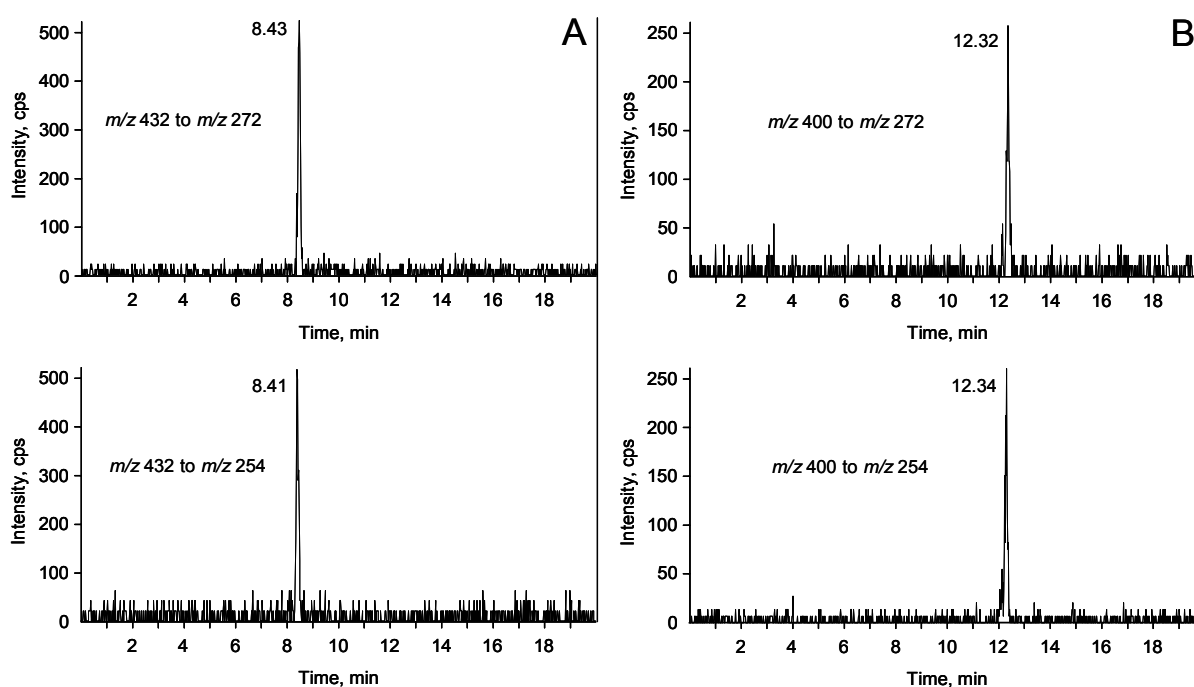


Figure 13: LC/MS-MS analyses of incubations of rat liver protein with HFO-1234ze, indicating the presence of 2-S-(1-carboxy-3,3,3-trifluoropropenyl)glutathione (A) and S-(3,3,3-trifluoro-*trans*-propenyl)glutathione (B) by the transitions of the molecular ions to m/z 272 and 254 at identical retention times. Due to low signal intensities, no EPIs could be recorded.

obtained, since small signals representing these metabolites were only observed in samples from incubation with high concentrations of liver protein (4 mg/mL), after an incubation time of 1 hour or more.

3.1.5.3 Analysis by a fluoride selective electrode

As indicated by ^1H -decoupled ^{19}F -NMR spectra of urine samples from rats and mice, biotransformation of HFO-1234ze exclusively yielded metabolites containing a CF_3 group but lacking a fluorine atom in β -position to the CF_3 -moiety. Due to the low reaction rates of HFO-1234ze observed in incubations with liver proteins, the presumed loss of inorganic fluoride during biotransformation could not be confirmed using a fluoride selective electrode, due to low sensitivity.

3.2 Biotransformation of HFO-1234yf in rabbits, rats and mice

3.2.1 Inhalation exposures

In order to identify metabolites formed from HFO-1234yf and excreted with urine, rabbits, rat and mice were exposed by inhalation to different concentrations of the parent compound. Female New Zealand White rabbits (n=3/concentration) and male Sprague-Dawley rats (n=5/concentration) were exposed for 6 h to 2 000, 10,000, and 50,000 ppm, whereas 5 male B6C3F1 mice were only exposed for 3.5 h to 50,000 ppm. Concentrations of HFO-1234yf in the exposure chamber were monitored by GC/MS throughout the inhalations. Measured concentrations of HFO-1234yf in the exposure chamber of rabbits were $2\,051 \pm 259$ ppm (target 2 000 ppm), $9\,869 \pm 258$ ppm (target 10,000 ppm) and $49,709 \pm 3\,069$ ppm (target 50,000 ppm), based on mean \pm SD from 15 determinations of HFO-1234yf air concentrations over the exposure time. Measured concentrations of HFO-1234yf in the exposure chamber of rats were $1\,900 \pm 192$ ppm (target 2 000 ppm), $11,279 \pm 1\,876$ ppm (target 10,000 ppm) and $50,647 \pm 5\,304$ ppm (target 50,000 ppm). The mean concentration of HFO-1234yf in the inhalation exposures with mice was $48,193 \pm 2\,412$ ppm (target 50,000 ppm). After the end of the exposures, urine samples were collected at 12 h (rabbits) or 6 and 12 h (rats and mice) time intervals for 60 h (rabbits) or 48 h (rats and mice) (Figure 14). Fluorine-containing metabolites were identified by ^{19}F -NMR spectroscopy and by LC/MS and GC/MS.

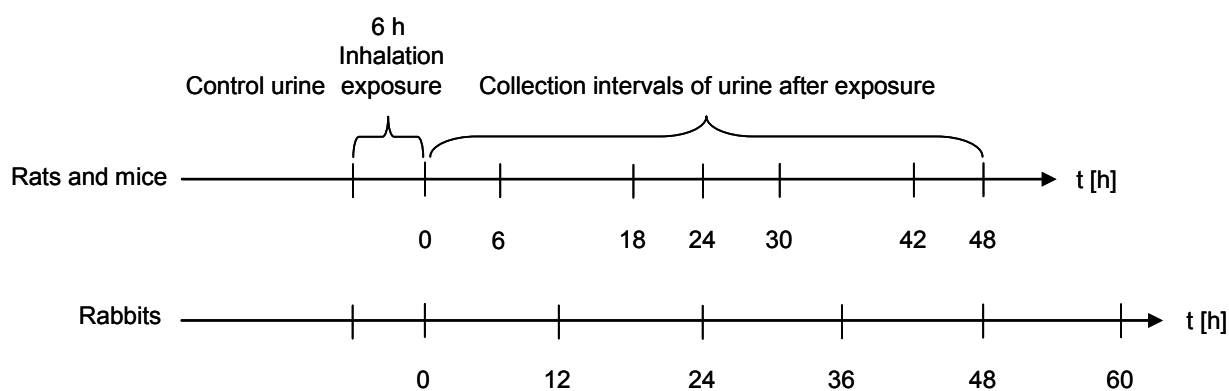


Figure 14: Design of urine collections from rabbits, rats and mice after exposure to HFO-1234yf.

3.2.2 Qualitative analyses of urine samples by ^{19}F -NMR

After the inhalation exposures, collected urines from rabbits rats and mice were analyzed by ^{19}F -NMR spectroscopy, recording ^1H -coupled and ^1H -decoupled spectra. In order to afford the detection of small traces of fluorine-containing metabolites by this approach, up to 4 000 scans were recorded of each urine sample. ^{19}F -NMR spectra of urines from all exposure levels showed several resonances which could be allocated to metabolites formed from HFO-1234yf (Figures 15 and 16; Table 9) since ^{19}F -NMR spectra from urine samples collected before the inhalation exposures did not contain any signals.

3.2.2.1 ^1H -decoupled ^{19}F -NMR spectra

In ^1H -decoupled ^{19}F -NMR spectra of urines from rabbits, rats and mice (Figure 15), all metabolite signals were singlets, indicating the presence of three magnetically equivalent fluorine atoms and the absence of a fluorine atom in α -position to the CF_3 -moiety which would yield complex signals due to ^{19}F - ^{19}F couplings. ^{19}F -NMR spectra from all urines lacked the signal of inorganic fluoride at $\delta = -119.6$ ppm, possibly due to its incorporation in teeth and bones. However, the loss of inorganic fluoride from the carbon atom in α -position to the CF_3 -group is indicated by the absence of ^{19}F - ^{19}F couplings in ^1H -decoupled spectra.

3.2.2.2 ^1H -coupled ^{19}F -NMR spectra

In ^1H -coupled ^{19}F -NMR spectra of urine samples from rabbits, rats and mice (Figure 16) collected after exposure to different concentrations of HFO-1234yf, some signals were split into doublets with characteristic ^1H - ^{19}F couplings. In general, singlets with a chemical shift in the range from approx. -70 to -80 ppm are indicative of a carbonyl group in α -position to the CF_3 -moiety. Doublets with a chemical shift in the range of approx. -70 to -80 ppm can be allocated to structures possessing one proton and a hydroxy group at the carbon atom next to the CF_3 -moiety.

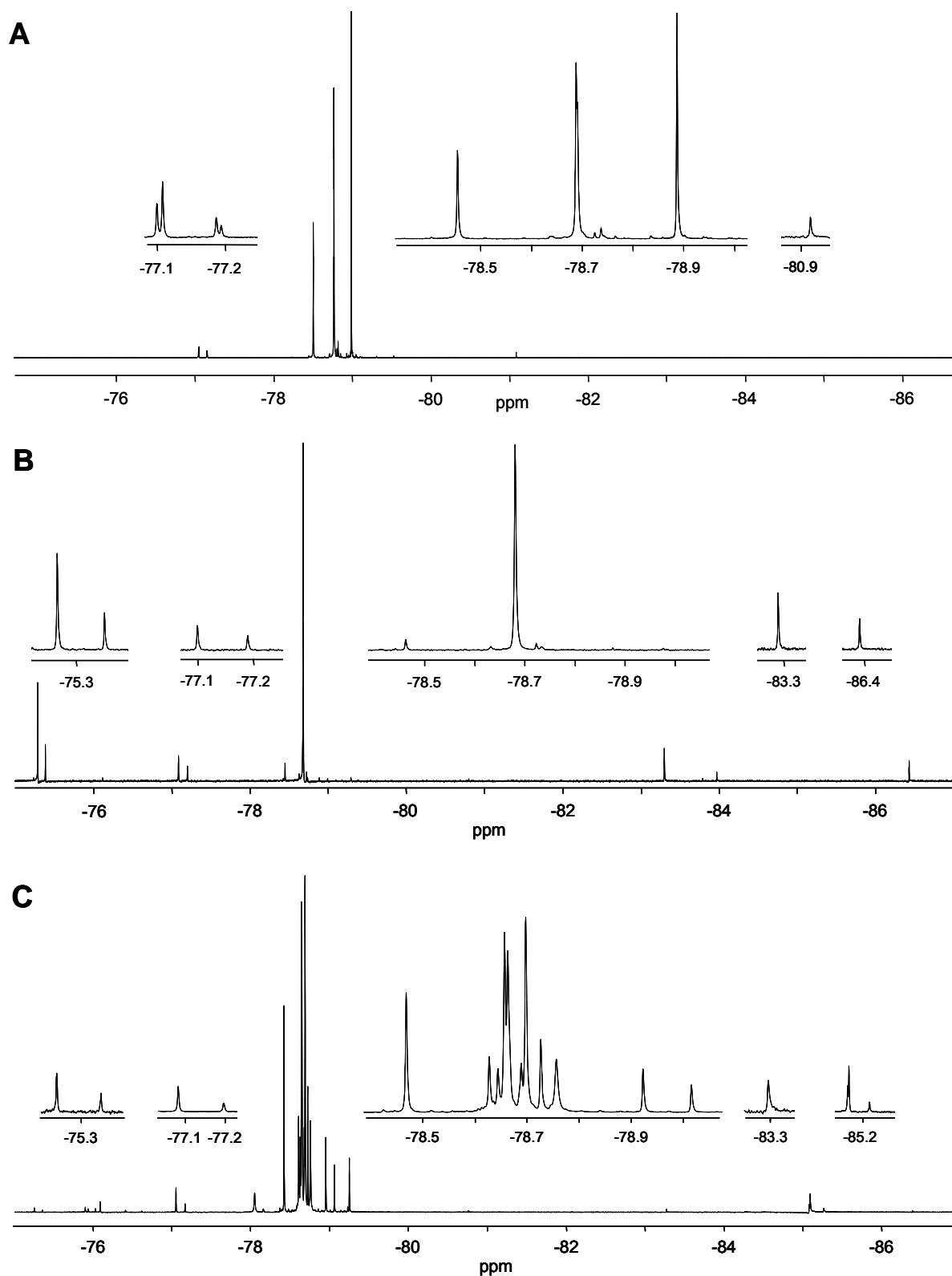


Figure 15: ^1H -decoupled ^{19}F -NMR spectra from urine samples of a rabbit (A), a rat (B) and a mouse (C) collected after the end of the inhalation exposure to HFO-1234yf. Rat and mouse urine collected from 6 to 18 hours after the end of the exposures and rabbit urine from the first 12 hours were analyzed.

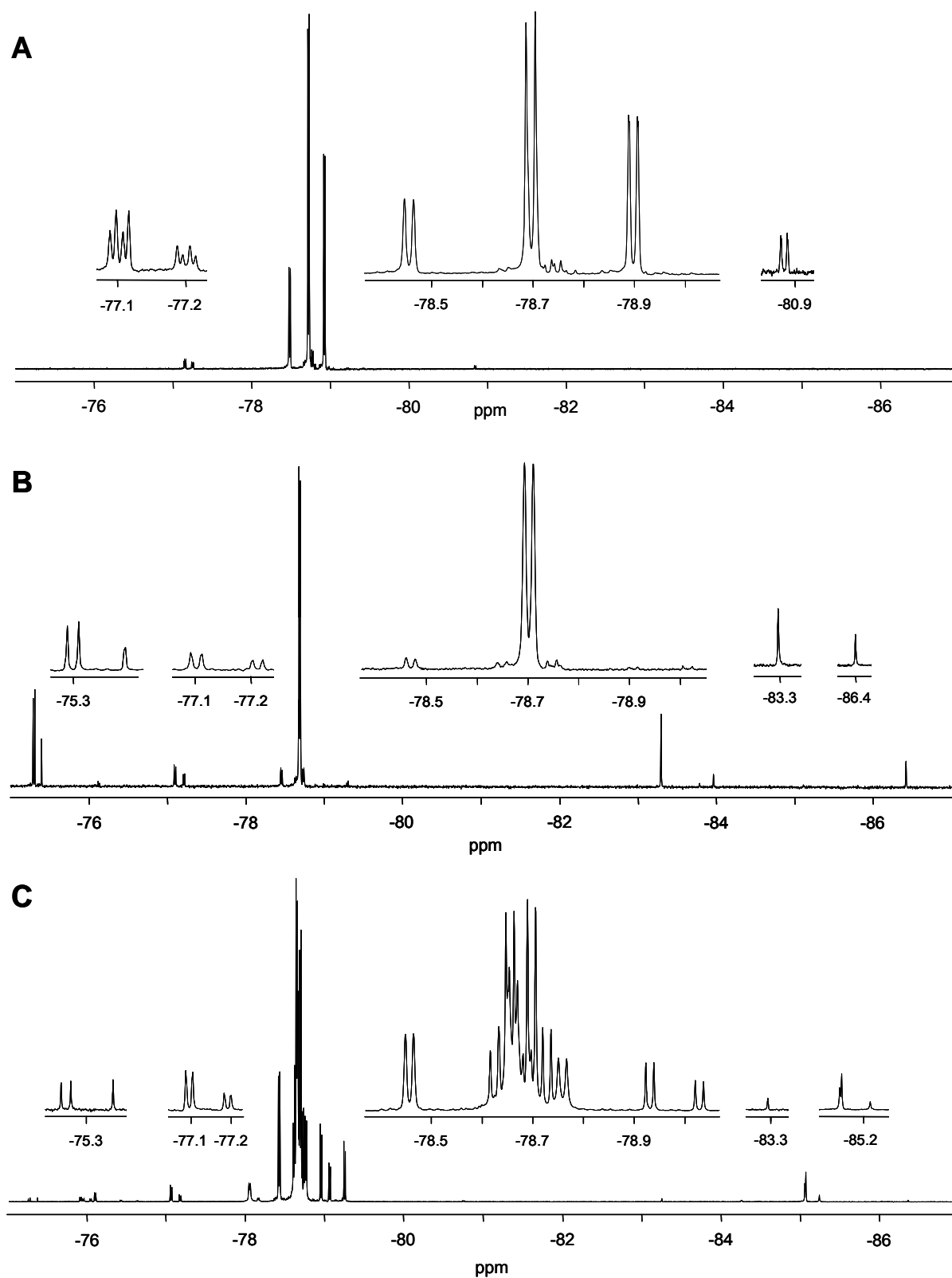


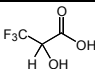
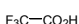
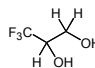
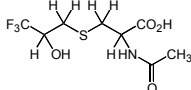
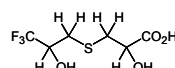
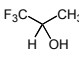
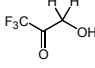
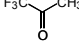
Figure 16: ^1H -coupled ^{19}F -NMR spectra from urine samples of a rabbit (A), a rat (B) and a mouse (C) collected after the end of the inhalation exposure to HFO-1234yf. Rat and mouse urine collected from 6 to 18 hours after the end of the exposures and rabbit urine from the first 12 hours were analyzed.

3.2.2.3 Identification of metabolites of HFO-1234yf by ^{19}F -NMR

Beside qualitative analyses by mass spectrometry, urinary metabolites were identified by comparison of their ^{19}F -NMR characteristics (chemical shift, multiplicity, ^1H - ^{19}F coupling constant) to those of their synthetic reference compounds (Table 9). In ^1H -coupled ^{19}F -NMR spectra of urines from rabbits, rats and mice (Figure 16), the major resonance in the ^1H -coupled ^{19}F -NMR spectrum was a signal at $\delta = -78.7$ ppm that was identical in chemical shift and fluorine-proton coupling ($J_{\text{HF}} = 6.5$ Hz) to those of synthetic *N*-acetyl-*S*-(3,3,3-trifluoro-2-hydroxypropyl)-*L*-cysteine (**15**, Scheme 2). In addition, LC/MS analysis confirmed the presence of *N*-acetyl-*S*-(3,3,3-trifluoro-2-hydroxypropyl)-*L*-cysteine as two separate peaks, most likely as diastereomers, in the urine samples [57]. Several minor metabolites of HFO-1234yf in urine samples were identified by ^{19}F -NMR characteristics and the assigned structures were confirmed by LC/MS or GC/MS by comparisons with synthetic reference compounds (Figures 20 and 21). The doublet at $\delta = -75.3$ ppm was identical in chemical shift and fluorine-proton coupling ($J_{\text{HF}} = 8.2$ Hz) to that of 3,3,3-trifluorolactic acid (**20**, Scheme 2). LC/MS-MS confirmed the formation of 3,3,3-trifluorolactic acid as a minor metabolite of HFO-1234yf excreted in urines from rats and mice. Another resonance at $\delta = -75.4$ ppm remained a singlet in ^1H -coupled spectra and is identical in chemical shift to that of trifluoroacetic acid (**26**, Scheme 2) which was confirmed by GC/MS. 3,3,3-Trifluorolactic acid and 3,3,3-trifluoroacetic acid were not observed in ^{19}F -NMR spectra of rabbit urines. A third metabolite showed a doublet in ^1H -coupled ^{19}F -spectra at $\delta = -77.0$ ppm ($J_{\text{HF}} = 7.4$ Hz). This chemical shift and the coupling constant is identical to the ^{19}F -NMR spectra of synthesized 3,3,3-trifluoro-1,2-dihydroxypropane (**14**, Scheme 2). Subsequent GC/MS analysis of urine samples confirmed 3,3,3-trifluoro-1,2-dihydroxypropane as a minor metabolite of HFO-1234yf in urines from all species. The signal at $\delta = -78.9$ ppm was split into a doublet ($J_{\text{HF}} = 6.4$ Hz) and could be allocated to *S*-(3,3,3-trifluoro-2-hydroxypropyl)mercaptolactic acid (**11**, Scheme 2). The presence of *S*-(3,3,3-trifluoro-2-hydroxypropyl)mercaptolactic acid in urines from rabbits, rats and mice was confirmed by LC/MS. Identical fragments of the urinary metabolite were found after ionization of the synthetic reference compound. The small resonance at $\delta = -80.8$ ppm (d, $J_{\text{HF}} = 7.0$ Hz) in ^{19}F -NMR spectra of rabbit urine samples was identical in chemical shift and ^1H - ^{19}F coupling to that of synthetic

3,3,3-trifluoro-2-propanol (**7**, Scheme 2). Analysis by GC/MS confirmed the presence of 3,3,3-trifluoro-2-propanol in rabbit urine, but not in urines from rats and mice. The singlet at $\delta = -86.4$ ppm in the ^{19}F -NMR spectrum of rat and mouse urines was allocated to 3,3,3-trifluoroacetone (**6**, Scheme 2) and further confirmed by GC/MS.

Table 9: Metabolites of HFO-1234yf in urines of rabbits, rats and/or mice, identified by ^{19}F -NMR.

Name of metabolite	Structure	Chemical shift [ppm]	Multiplicity	^1H - ^{19}F coupling [Hz]
3,3,3-Trifluorolactic acid		-75.3	d	8.2
3,3,3-Trifluoroacetic acid		-75.4	s	-
3,3,3-Trifluoro-1,2-dihydroxypropane		-77.1	d	7.4
<i>N</i> -Acetyl- <i>S</i> -(3,3,3-trifluoro-2-hydroxypropanyl)- <i>L</i> -cysteine		-78.7	d	6.5
<i>S</i> -(3,3,3-Trifluoro-2-hydroxypropanyl)-mercaptolactic acid		-78.9	d	6.4
3,3,3-Trifluoro-2-propanol		-80.8	d	7.0
3,3,3-Trifluoro-1-hydroxyacetone		-83.3	s	-
3,3,3-Trifluoroacetone		-86.4	s	-

The signal at $\delta = -83.3$ ppm was a singlet in both proton coupled and decoupled ^{19}F -NMR spectra and tentatively allocated to 3,3,3-trifluoro-1-hydroxyacetone (**17**, Scheme 2), probably present as hydrate. Isolation of this substance failed, thus neither mass analysis nor a comparison to the chemical shift of the authentic standard could be performed. However, when 3,3,3-trifluoro-1,2-dihydroxypropane (**14**, Scheme 2) was orally administered to a rat, a resonance with an identical ^{19}F -NMR characteristics was present in urine in addition to a signal representing 3,3,3-trifluorolactic acid (**20**, Scheme 2; Figure 18). 3,3,3-Trifluoro-1-hydroxyacetone is an expected oxidation product of 3,3,3-trifluoro-1,2-dihydroxypropane. Moreover, when reacting 3,3,3-trifluoro-1-bromoacetone with water at pH >9, a reaction product, likely 3,3,3-trifluoro-1-hydroxyacetone, was formed further supporting the structure

assignment. This reaction product showed an identical chemical shift as the urinary metabolite in ^{19}F -NMR spectra (Figures 15 B and 16 B).

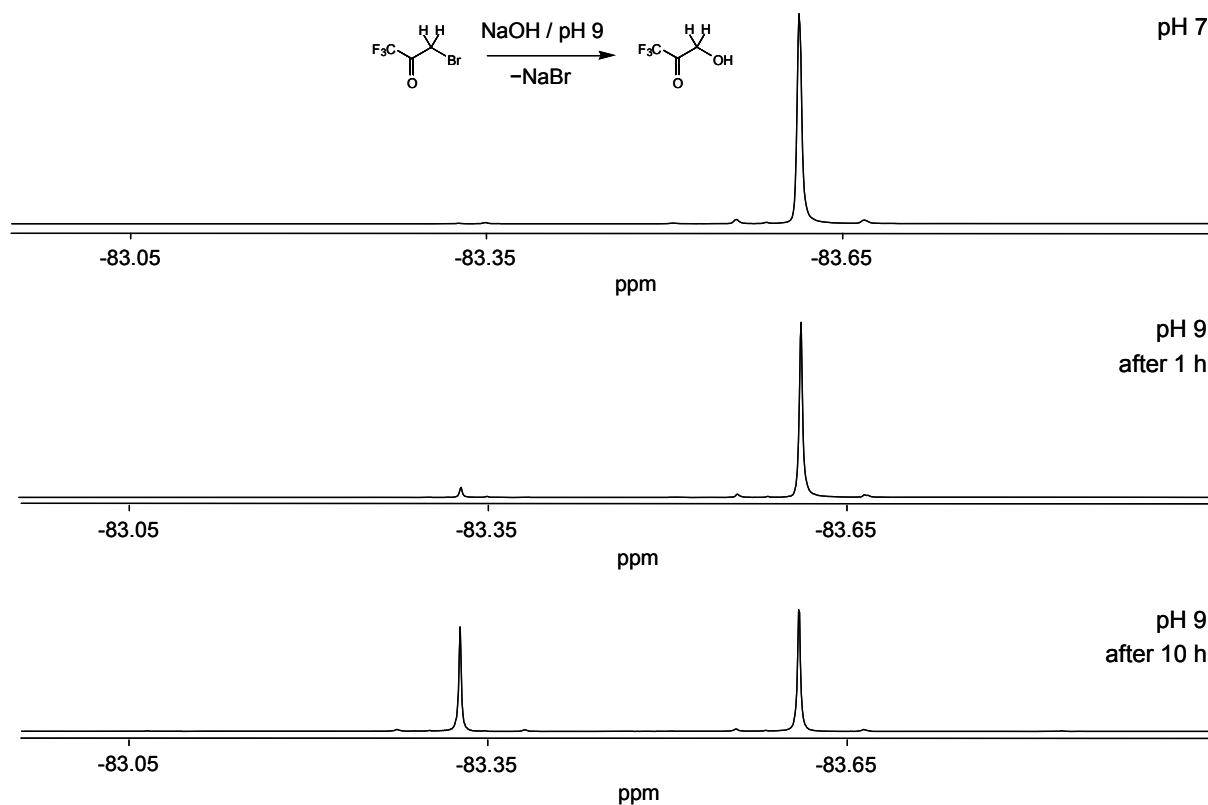


Figure 17: ^{19}F -NMR spectra of a solution of 1-bromo-3,3,3-trifluoroacetone ($\delta = -83.6$ ppm) in water which is probably transformed to 3,3,3-trifluoro-1-hydroxyacetone ($\delta = -83.3$ ppm) after adjusting to pH 9 with NaOH.

3.2.2.4 Oral gavage of 3,3,3-trifluoro-1,2-dihydroxypropane to a rat

3,3,3-Trifluoro-1,2-dihydroxypropane (**14**, Scheme 2) was identified as minor metabolite of HFO-1234yf in urines from rats and mice. In order to investigate its metabolic fate, 3,3,3-trifluoro-1,2-dihydroxypropane was administered to a male Sprague-Dawley rat by oral gavage, and urine was collected for 24 hours and analyzed by ^{19}F -NMR spectroscopy (Figure 18). Beside the signal of the administered compound at $\delta = -77.1$ ppm (d; $J_{\text{HF}} = 7.4$ Hz), the major metabolite was a doublet at $\delta = -75.3$ ppm with a ^1H - ^{19}F coupling of 8.2 Hz, indicative of 3,3,3-trifluorolactic acid (**20**, Scheme 2). This metabolite accounted for approx. 60%

of total ^{19}F -NMR signal intensities in the urine sample. Minor metabolites of 3,3,3-trifluoro-1,2-dihydroxypropane tentatively identified were 3,3,3-trifluoroacetic acid ($\delta = -75.4$ ppm; s) (**26**, Scheme 2) and 3,3,3-trifluoro-1-hydroxyacetone ($\delta = -83.3$ ppm; s) (**17**, Scheme 2). The small resonances at $\delta = -74.9$ (d; $J_{\text{HF}} = 7.1$ Hz) and $\delta = -77.3$ ppm (d; $J_{\text{HF}} = 7.5$ Hz) remained unidentified.

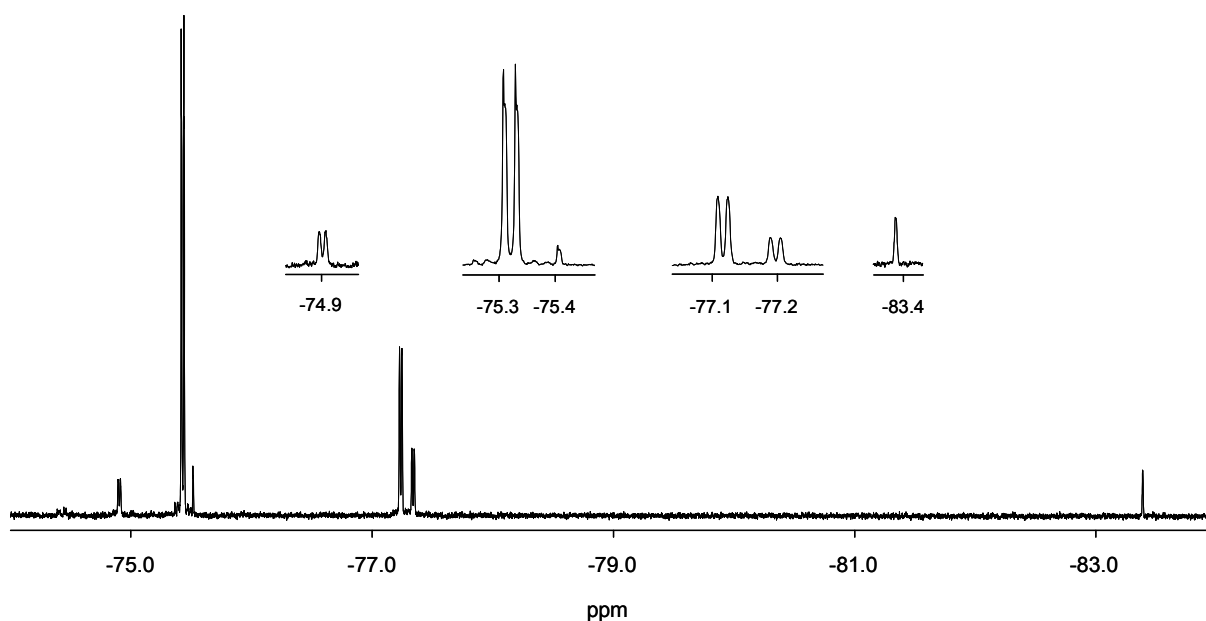


Figure 18: ^1H -coupled ^{19}F -NMR spectrum from rat urine after oral gavage of 3,3,3-trifluoro-1,2-dihydroxypropane. Signals could be allocated to: 3,3,3-trifluorolactic acid ($\delta = -75.3$ ppm); 3,3,3-trifluoroacetic acid ($\delta = -75.4$ ppm); 3,3,3-trifluoro-1,2-dihydroxypropane ($\delta = -77.1$ ppm); 3,3,3-trifluoro-1-hydroxyacetone ($\delta = -83.3$ ppm). The resonance at $\delta = -77.2$ ppm remained unidentified.

3.2.2.5 Oral gavage of 3,3,3-trifluorolactic acid to a rat

3,3,3-Trifluorolactic acid (**20**, Scheme 2) was identified by ^{19}F -NMR as minor metabolite of HFO-1234yf in urines from rats and mice. Moreover, 3,3,3-trifluorolactic acid was the major metabolite of 3,3,3-trifluoro-1,2-dihydroxypropane in rat urine after oral gavage (Figure 18). When 3,3,3-trifluorolactic acid was orally administered to a rat, the ^{19}F -NMR spectrum of the collected urine did not contain additional signals beside the doublet at $\delta = -75.3$ (d; $J_{\text{HF}} = 8.2$ Hz) of the carboxylic acid

(spectrum not shown). 3,3,3-Trifluorolactic acid was not further biotransformed in the rat and thus represents a metabolic endpoint of biotransformation of HFO-1234yf.

3.2.2.6 Oral gavage of 3,3,3-trifluoropyruvic acid to a rat

Even though ^{19}F -NMR spectra of urines from rabbits, rats and mice did not contain a signal indicative of 3,3,3-trifluoropyruvic acid (**19**, Scheme 2), this carboxylic acid is a logical metabolic precursor of 3,3,3-trifluorolactic acid (**20**, Scheme 2) which has been identified in urines of rats and mice after inhalation exposure to HFO-1234yf (Figures 15 and 16). To investigate the metabolic fate of 3,3,3-trifluoropyruvic acid in rats, the compound was orally administered to a rat and urine was analyzed by ^{19}F -NMR (Figure 19). Beside the resonance of 3,3,3-trifluoropyruvic acid at $\delta = -82.6$ ppm (s), only one additional signal was present as doublet in the ^1H -coupled ^{19}F -NMR spectrum and could be allocated to 3,3,3-trifluorolactic acid ($\delta = -75.3$ ppm; $J_{\text{HF}} = 8.2$ Hz).

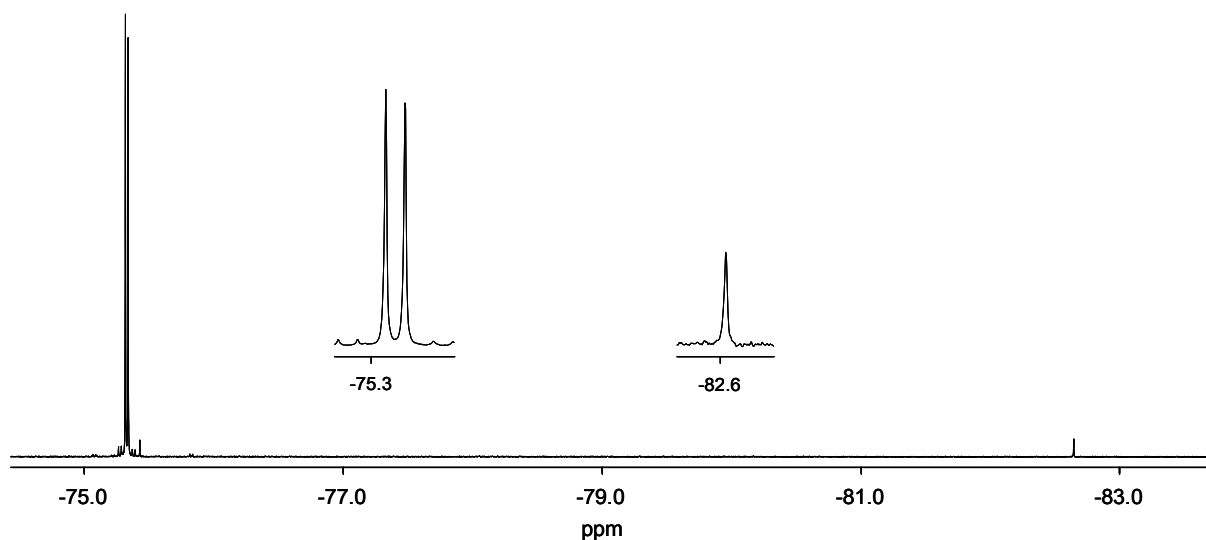


Figure 19: ^1H -coupled ^{19}F -NMR spectrum of the urine from a rat after oral gavage of 3,3,3-trifluoropyruvic acid, indicated by the singlet at $\delta = -82.6$ ppm. The only metabolite formed was 3,3,3-trifluorolactic acid at $\delta = -75.3$ ppm (d; $J_{\text{HF}} = 8.2$ Hz).

3.2.3 Qualitative analyses of urinary metabolites by mass spectrometry

In addition to ^{19}F -NMR analyses, several structures of urinary metabolites of HFO-1234yf were identified by LC/MS or GC/MS. In urine samples of rabbits, rats and mice, the presence of *N*-acetyl-*S*-(3,3,3-trifluoro-2-hydroxypropanyl)-*L*-cysteine (**15**, Scheme 2) and its *S*-oxide (**16**, Scheme 2), *S*-(3,3,3-trifluoro-2-hydroxypropanyl)-mercaptolactic acid (**11**, Scheme 2) and its *S*-oxide (**12**, Scheme 2) and 3,3,3-trifluorolactic acid (**20**, Scheme 2) were confirmed by LC/MS-MS (IDA EPI), whereas 3,3,3-trifluoroacetic acid (**26**, Scheme 2), 3,3,3-trifluoro-1,2-dihydroxypropane (**14**, Scheme 2), 3,3,3-trifluoro-2-propanol (**7**, Scheme 2) and 3,3,3-trifluoroacetone (**6**, Scheme 2) were identified by GC/MS. The synthetic reference compounds and the urinary metabolites showed identical retention times and mass fragments after ionization. Moreover, the identified metabolites were shown to be absent in samples of control urines.

3.2.3.1 Identification of urinary metabolites of HFO-1234yf by LC/MS

The characteristic fragments in the EPIs of *N*-acetyl-*S*-(3,3,3-trifluoro-2-hydroxypropanyl)-*L*-cysteine (A), *N*-acetyl-*S*-(3,3,3-trifluoro-2-hydroxypropanyl)-*L*-cysteine *S*-oxide (B), *S*-(3,3,3-trifluoro-2-hydroxypropanyl)mercaptolactic acid (C) and *S*-(3,3,3-trifluoro-2-hydroxypropanyl)mercaptolactic acid *S*-oxide (D) obtained by LC/MS analysis of rabbit, rat or mouse urine (Figure 20) show molecular ions and neutral losses (NL) of 129 and 88 amu which are typical of thioethers of *N*-acetyl-*L*-cysteine (mercapturic acids) (A, B) and lactic acid (C, D), respectively (Figure 20). The ionisation fragment of m/z 145 in the EPIs A and C is likely formed by the thiolate ion.

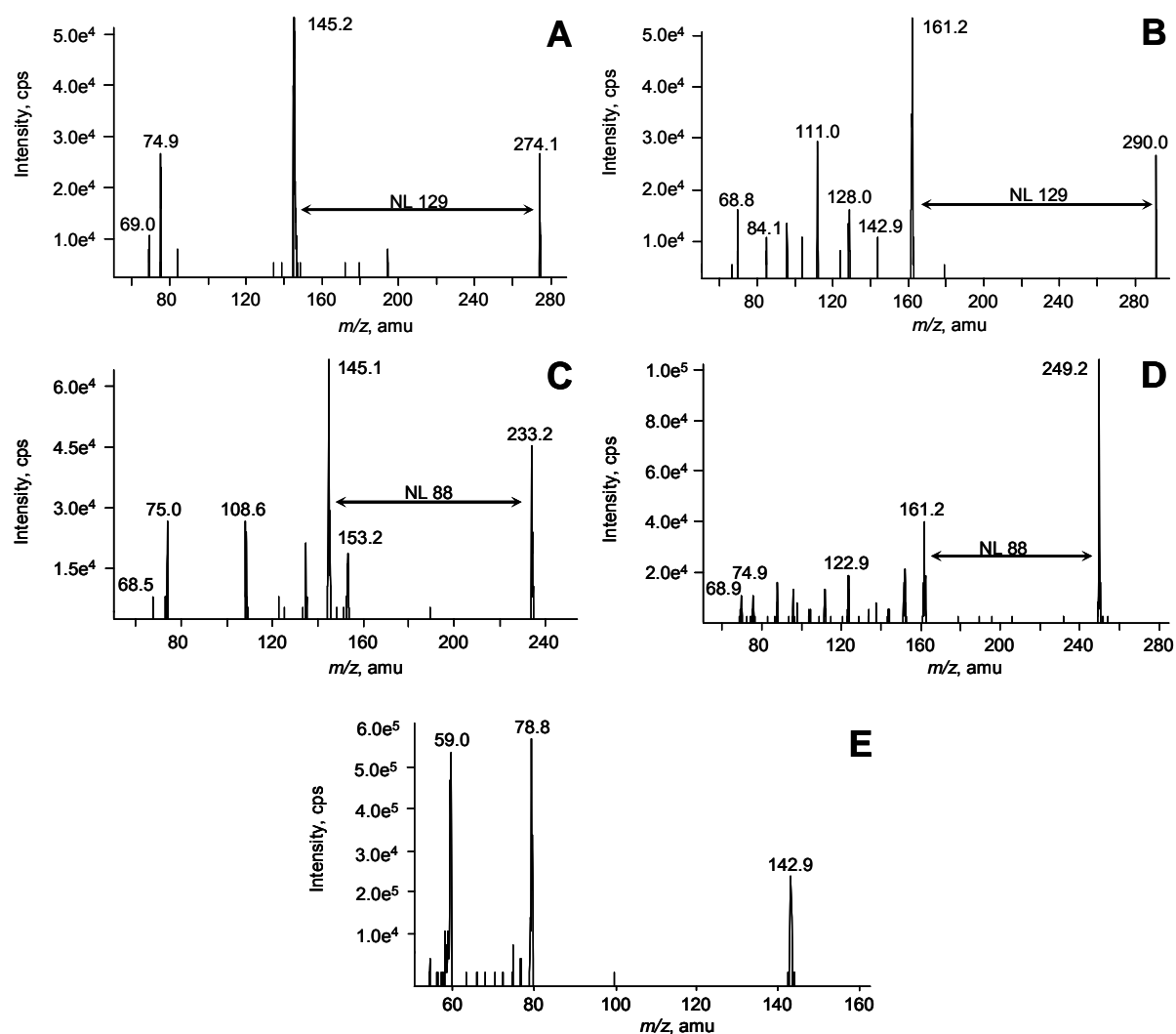


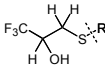
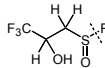
Figure 20: Characteristic fragments of *N*-acetyl-*S*-(3,3,3-trifluoro-2-hydroxypropanyl)-*L*-cysteine (A), *N*-acetyl-*S*-(3,3,3-trifluoro-2-hydroxypropanyl)-*L*-cysteine *S*-oxide (B), *S*-(3,3,3-trifluoro-2-hydroxypropanyl)mercaptolactic acid (C), *S*-(3,3,3-trifluoro-2-hydroxypropanyl)mercaptolactic acid *S*-oxide (D) and 3,3,3-trifluorolactic acid (E) obtained by LC/MS analysis of rabbit, rat or mouse.

of *S*-(3,3,3-trifluoro-2-propanol), whereas m/z 161 in the EPIs B and D may be attributable to the thiolate ion of *S*-(3,3,3-trifluoro-2-propanol) *S*-oxide. The ionization fragment m/z 79 in EPI E is attributable to the 2,2-difluoro-1-hydroxyethyl ion which is likely formed from 3,3,3-trifluorolactic acid by releasing CO_2 (m/z 44) and HF (m/z 20). A second release of HF from m/z 79 may explain the formation of m/z 59.

Further derivatives of the cysteine *S*-conjugate of HFO-1234yf were searched in urine samples by LC/MS in the sensitive MRM mode, using the transitions of the appropriate molecular ions to m/z 145 for 3,3,3-trifluoro-2-hydroxypropanyl *S*-

conjugates and to m/z 161 for 3,3,3-trifluoro-2-hydroxypropanyl S-conjugates S-oxides (Table 10). Beside the metabolites presented in Figure 20, no evidence was given for the presence of cysteine S-conjugate, cysteine S-conjugate S-oxide or the corresponding mercaptopyruvic acid S-conjugate, mercaptoacetic acid S-conjugate, S-methyl conjugate and S-glucuronide.

Table 10: Analysis of possible derivates of S-(3,3,3-trifluoro-2-hydroxypropanyl)-L-cysteine by LC/MS-MS.

Metabolite		
Name	Structure	Transition used for identification
3,3,3-Trifluoro-2-hydroxypropanyl S-conjugate		m/z [molecular ion] to m/z 145
3,3,3-Trifluoro-2-hydroxypropanyl S-conjugate S-oxide		m/z [molecular ion] to m/z 161

3.2.3.2 Identification of urinary metabolites of HFO-1234yf by GC/MS

Several minor metabolites of HFO-1234yf present in urines of rabbits, rats or mice were identified by GC/MS (Figure 21). 3,3,3-Trifluoroacetic acid (**26**, Scheme 2), 3,3,3-trifluoro-1,2-dihydroxypropane (**14**, Scheme 2) and 3,3,3-trifluoroacetone (**6**, Scheme 2) were present only in urines collected from rats and mice, whereas 3,3,3-trifluoro-2-propanol (**7**, Scheme 2) was identified exclusively in urine samples from rabbits. In the chromatogram of 3,3,3-trifluoro-2-propanol (Figure 21 A), typical ionization fragments are present and can be allocated to CHOHCH_3 (m/z 45), CF_3 (m/z 69) and CF_3CHOH (m/z 99). The chromatogram of 3,3,3-trifluoro-1,2-dihydroxypropane (Figure 21 B) contains fragments which are attributable to CH_2OH (m/z 31), CF_3 (m/z 69) and CF_2CHOH (m/z 80). Typical fragments after ionization of 3,3,3-trifluoroacetone (Figure 21 C) can be allocated to CH_3 (m/z 15), COCH_3 (m/z 43) and CF_3 (m/z 69). 3,3,3-Trifluoroacetic acid was analyzed after derivatization to the methyl ester and showed the fragments of COOCH_3 (m/z 59) and CF_3 (m/z 69) (Figure 21 D). The chromatograms showing absence and presence of an extracted fragment in urine samples collected before and after the inhalation exposures to

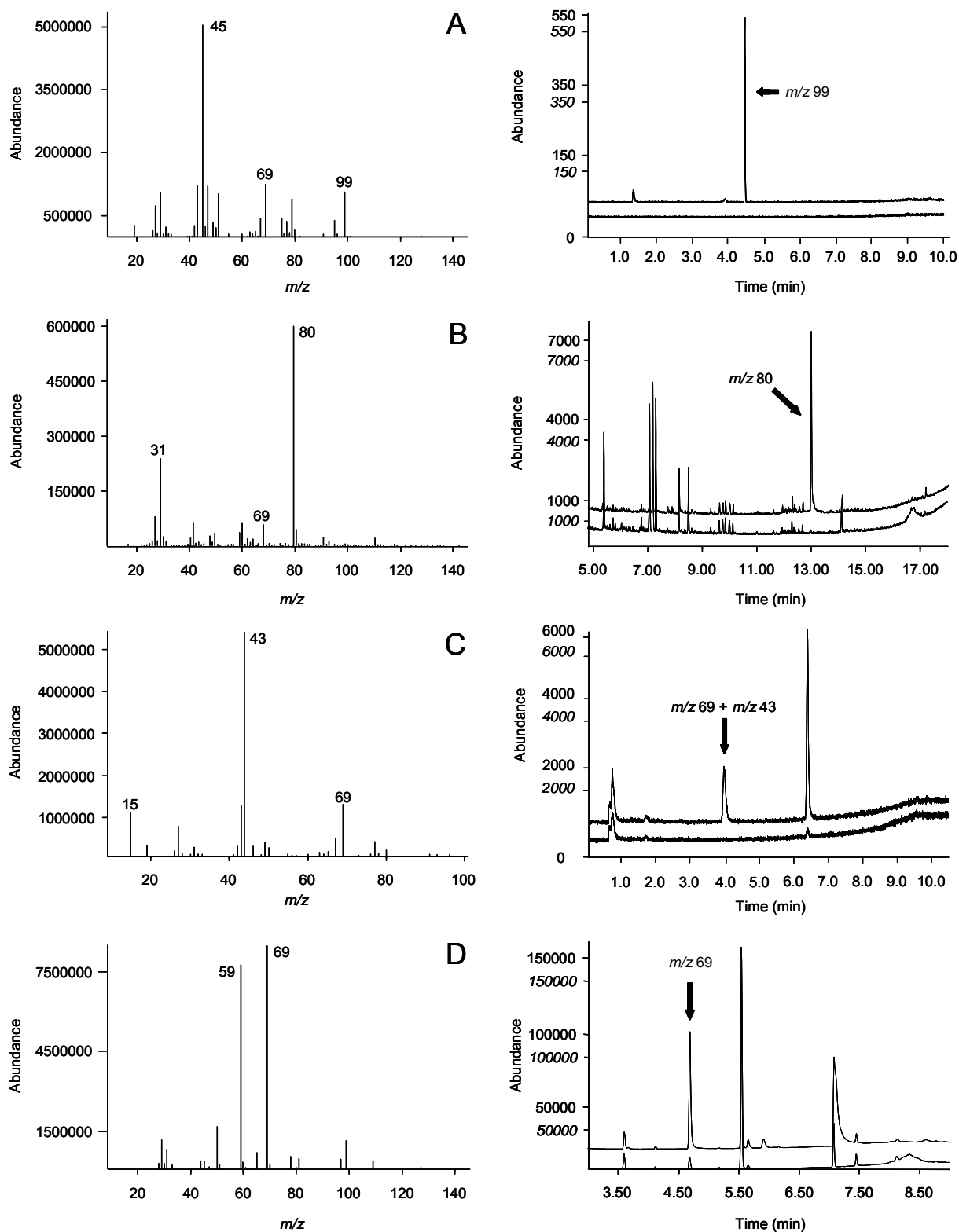


Figure 21: Identification of 3,3,3-trifluoro-2-propanol (A), 3,3,3-trifluoro-1,2-dihydroxypropane (B), 3,3,3-trifluoroacetone (C) and 3,3,3-trifluoroacetic acid (D) in urines from rabbits, rats or mice by GC/MS. Mass spectra of fullscan on the left side; chromatograms of extracted ions on the right side, showing absence and presence of extracted ions in control urines (lower line) and urines collected after the exposure to HFO-1234yf (upper line).

HFO-1234yf are placed next to their fullscan mass spectra. The presence of m/z 69 in the chromatogram of the control urine (Figure 21 D) was effected by small contaminations of 3,3,3-trifluoroacetic acid in the derivatization detergents used.

3.2.4 Quantitation of urinary metabolites of HFO-1234yf

In the urine samples collected after inhalation exposure of rabbits, rats and mice to HFO-1234yf, *N*-acetyl-*S*-(3,3,3-trifluoro-2-hydroxypropanyl)-*L*-cysteine (**15**, Scheme 2) was the major metabolite indicated by the ^{19}F -NMR spectra. This compound was therefore quantified to determine the kinetics of excretion. In rabbits, the recovery of *N*-acetyl-*S*-(3,3,3-trifluoro-2-hydroxypropanyl)-*L*-cysteine excreted within 60 h in urine was determined as 35 ± 11 , 46 ± 8 and 133 ± 20 μmol at 2 000, 10,000 and 50,000 ppm (Figure 22, Table 11). In rats, the recovery of the mercapturic acid excreted within 48 h in urine was measured to be 0.3 ± 0.03 , 0.63 ± 0.16 and 2.43 ± 0.86 μmol at 2 000, 10,000 and 50,000 ppm. Male B6C3F1 mice were only exposed to 50,000 ppm HFO-1234yf and the recovery of the *N*-acetyl-*L*-cysteine *S*-conjugate was determined as 1.77 ± 0.44 μmol .

Table 11: Recovery of *N*-acetyl-*S*-(3,3,3-trifluoro-2-hydroxypropanyl)-*L*-cysteine and inorganic fluoride in urines of rabbits, rats and mice excreted within 60 h (rabbits) or 48 h (rats and mice) after inhalation exposure to HFO-1234yf for 6 h.

Exposure concentration ppm	<i>N</i> -Acetyl- <i>S</i> -(3,3,3-trifluoro-2-hydroxypropanyl)- <i>L</i> -cysteine [μmol]			Inorganic fluoride [μmol] Rabbits
	Rabbits	Rats	Mice	
2 000	35 ± 11	0.30 ± 0.03	—	1.6 ± 0.2
10,000	46 ± 8	0.63 ± 0.16	—	3.9 ± 0.4
50,000	133 ± 20	2.43 ± 0.86	1.77 ± 0.44	14.2 ± 1.0

Quantitative analysis of rabbit and rat urine samples from the three different exposure concentrations over time showed that *N*-acetyl-*S*-(3,3,3-trifluoro-2-hydroxypropanyl)-*L*-cysteine was rapidly excreted and 97% of total excretion occurred within 12 h and 18 h following the exposure ($t_{1/2}$ approx. 9.5 and 6 h) in rabbits and rats, respectively. In all urine samples of rabbits collected within the first

12 h after the end of the inhalative exposures, inorganic fluoride was found in higher concentrations than compared to those of the control urines (Figure 22, Table 11). The recovery of inorganic fluoride was calculated to be 1.6 ± 0.2 , 3.9 ± 0.4 and 14.2 ± 1.0 μmol at 2 000, 10,000 and 50,000 ppm in contrast to 0.8 ± 0 μmol in urines which had been collected within 12 h before the inhalation exposures. Due to incorporation of inorganic fluoride in teeth and bones, no correlation between recovered quantities of *N*-acetyl-S-(3,3,3-trifluoro-2-hydroxypropanyl)-L-cysteine and inorganic fluoride is evident.

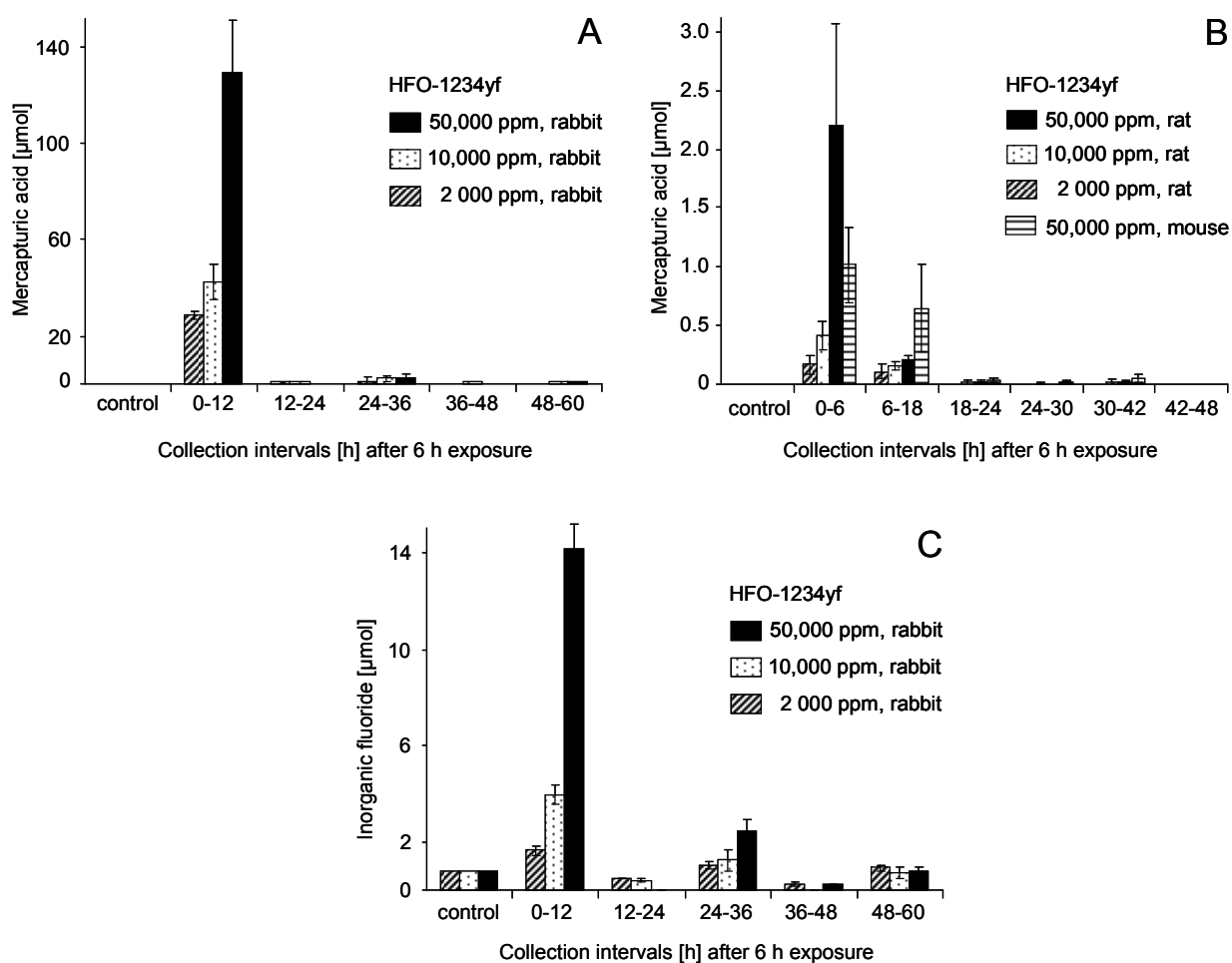


Figure 22: Time courses of urine excretion of *N*-acetyl-S-(3,3,3-trifluoro-2-hydroxypropanyl)-L-cysteine in rabbits (A), rats and mice (B) and of inorganic fluoride in rabbits (C) after exposure to different concentrations of HFO-1234yf.

Based on respiratory minute volumes of 1.3 , 0.8 and 0.26 $\text{L min}^{-1} \text{kg}^{-1}$ in mice, rats and rabbits, and mean body weights of 30 , 230 and 3000 g, calculated total doses of 18.3 , 149 and 606 mmol of HFO-1234yf were received by inhalation for 6 h (rabbits,

rats) and 3.5 h (mice) at the 50,000 ppm level, respectively [70]. Quantified amounts of *N*-acetyl-*S*-(3,3,3-trifluoro-2-hydroxypropanyl)-*L*-cysteine acid were 133, 2.43 and 1.77 μmol in rabbits, rats and mice (Table 11), representing 44, 90 and 32% of total ^{19}F -related signal intensities, respectively. Thus, extents of biotransformation of HFO-1234yf were calculated to be 0.05 (rabbits), 0.002 (rats) and 0.03% (mice) of total dose received by inhalation.

3.2.5 Qualitative analyses of metabolites in incubations with liver protein

Incubations with HFO-1234yf and appropriate cofactors were performed in order to characterize biotransformation by rat liver microsomes (native and pyridine induced) and human S9 fractions.

3.2.5.1 Identification of metabolites of HFO-1234yf by ^{19}F -NMR

To characterize biotransformation by subcellular fractions, rat liver microsomes and cytosol as well as rabbit and human S9 fractions were incubated with HFO-1234yf and appropriate cofactors. No metabolite formation was evident regarding ^{19}F -NMR spectra of incubations of HFO-1234yf with human liver S9 fractions, containing NADPH and/or glutathione. Moreover, in incubations of HFO-1234yf with rat liver cytosol or microsomes containing either glutathione or NADPH, or both, metabolite formation was not detected by ^{19}F -NMR (data not shown). Two major signals present as singlets at $\delta = -83.4$ ppm and $\delta = -119.5$ ppm and a minor singlet at $\delta = -83.9$ ppm were found to be in both ^1H -coupled and uncoupled ^{19}F -NMR spectra (Figure 23 A), when using liver microsomes from pyridine induced rats, in the presence of NADPH. Additionally, signals of HFO-1234yf (**1**, Scheme 2) were present at $\delta = -73.0$ and $\delta = -125.6$ ppm. When these incubations were performed in the presence of NADPH and glutathione, an additional signal at $\delta = -84.6$ ppm was formed (Figure 23 B). A singlet with an identical chemical shift was obtained with synthetic *S*-(3,3,3-trifluoro-2-oxopropanyl)glutathione (**3**, Scheme 1) suggesting that the metabolite is identical to *S*-(3,3,3-trifluoro-2-oxopropanyl)glutathione. The product formed at $\delta = -83.4$ ppm in the presence of NADPH, but absence of glutathione (Figure 23 A), had

an identical chemical shift as one of the minor urinary metabolites of HFO-1234yf in urines from rats and mice and is likely to represent 3,3,3-trifluoro-1-hydroxyacetone (**17**, Scheme 2). No structure could be allocated to the small signal at $\delta = -83.9$ ppm.

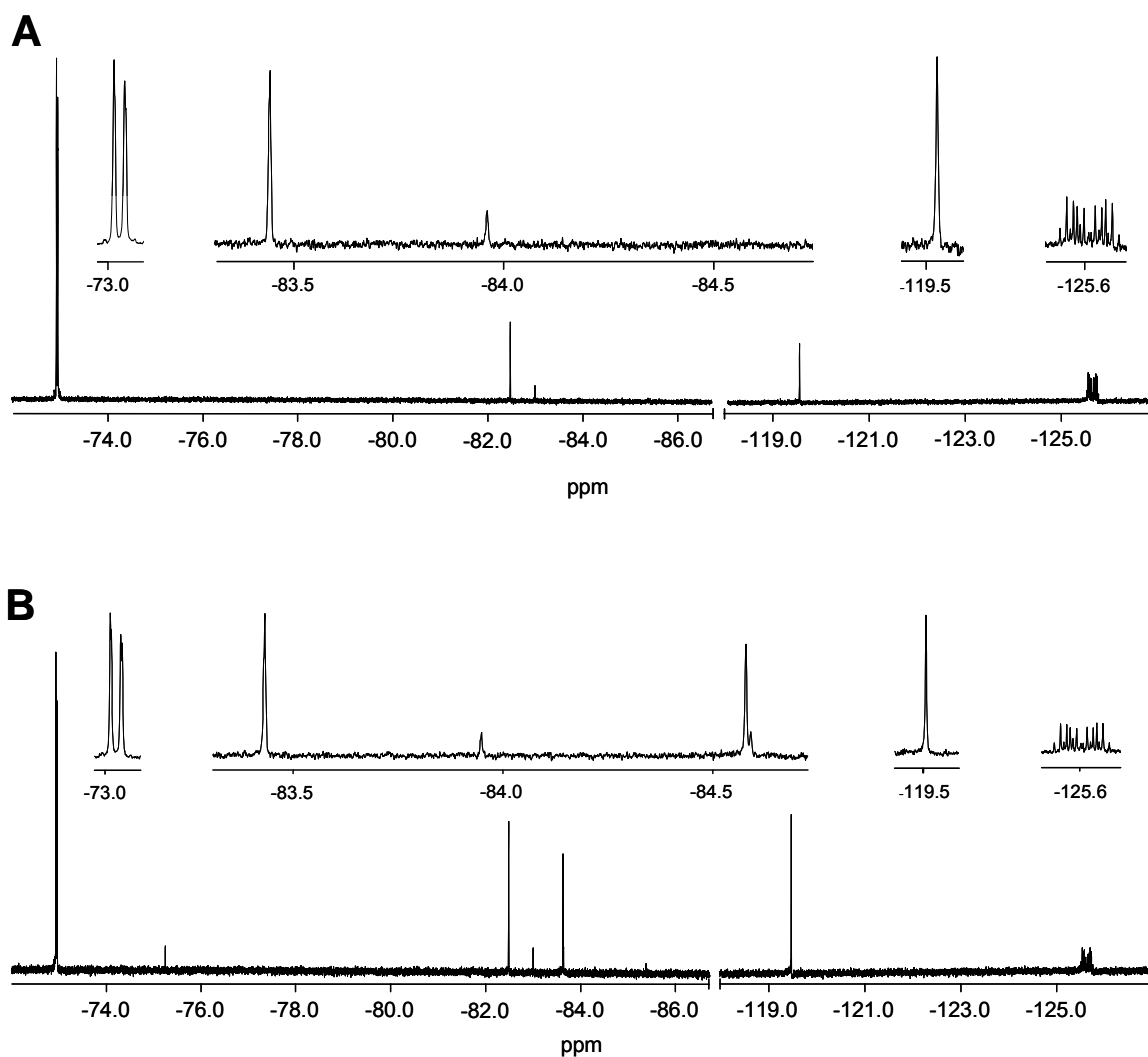


Figure 23: ^{19}F -NMR spectra (^1H -coupled) of incubations of liver microsomes from pyridine induced rats and HFO-1234yf. The singlet at $\delta = -83.3$ ppm was tentatively identified as 3,3,3-trifluoro-1-hydroxyacetone and the resonance at $\delta = -119.5$ ppm was assigned to inorganic fluoride. Another singlet at $\delta = -84.6$ ppm was formed in incubations with NADPH and glutathione (B), but was absent in incubations without glutathione (A) suggesting that this metabolite represents a glutathione S-conjugate.

Incubations with HFO-1234yf and appropriate cofactors were performed in order to characterize biotransformation by rabbit liver S9 fractions. Besides the signals of the parent compound, no additional resonances were apparent in ^{19}F -NMR spectra of incubation mixtures containing either glutathione or NADPH (Figure 24), whereas three additional ^{19}F -related signals were present in spectra of incubations containing both NADPH and glutathione. The major metabolite in ^1H -coupled ^{19}F -NMR spectra was a doublet at $\delta = -80.8$ ppm (d, $J_{\text{HF}} = 7.0$ Hz) which was identical in chemical shift and ^1H - ^{19}F coupling to that of synthetic 3,3,3-trifluoro-2-propanol (**7**, Scheme 1). A second doublet at $\delta = -78.8$ ppm (d, $J_{\text{HF}} = 6.8$ Hz) could be allocated to *S*-(3,3,3-trifluoro-2-hydroxypropanyl)glutathione (**4**, Scheme 2) and was identical in chemical shift and ^1H - ^{19}F coupling to that of the reference compound. A third signal at $\delta = -119.6$ ppm was identified as inorganic fluoride.

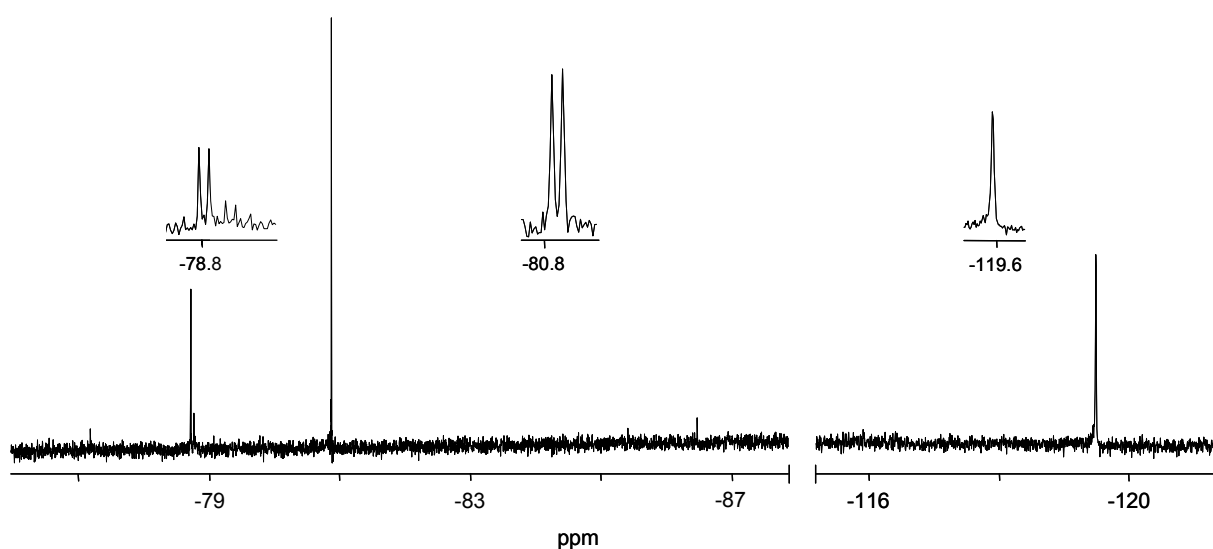


Figure 24: ^{19}F -NMR spectra (^1H -coupled) of incubations of liver S9 fractions from rabbits and HFO-1234yf with NADPH and glutathione. The doublet at $\delta = -78.8$ ppm ($J_{\text{HF}} = 6.8$ Hz) was identified as *S*-(3,3,3-trifluoro-2-hydroxypropanyl)glutathione, the resonance at $\delta = -80.8$ ppm (d; $J_{\text{HF}} = 7.0$ Hz) was assigned to 3,3,3-trifluoro-2-propanol and the presence of inorganic fluoride was indicated by the singlet at $\delta = -119.6$ ppm. Signals resulting from HFO-1234yf are not shown.

3.2.5.2 Identification of metabolites of S-(3,3,3-trifluoro-2-oxopropanyl)-glutathione by ^{19}F -NMR

S-(3,3,3-Trifluoro-2-oxopropanyl)glutathione has been identified as a derivate of HFO-1234yf in incubations with liver microsomes from pyridine induced rats (Figure 23). Synthetic S-(3,3,3-trifluoro-2-oxopropanyl)glutathione (**3**, Scheme 2) was added as substrate to incubations of rabbit liver S9 fractions with NADPH in order to confirm the metabolic fate of this glutathione S-conjugate in rabbits. In ^1H -coupled ^{19}F -NMR spectra of these incubations, several signals were present as singlet or doublets and were identified by interpretation of their ^{19}F -NMR characteristics (Figure 25). The biotransformation of S-(3,3,3-trifluoro-2-oxopropanyl)glutathione ($\delta = -84.6$ ppm; s) mainly yielded a doublet at $\delta = -78.8$ ppm ($J_{\text{HF}} = 6.8$ Hz) which could be allocated to S-(3,3,3-trifluoro-2-hydroxypropanyl)glutathione (**4**, Scheme 2).

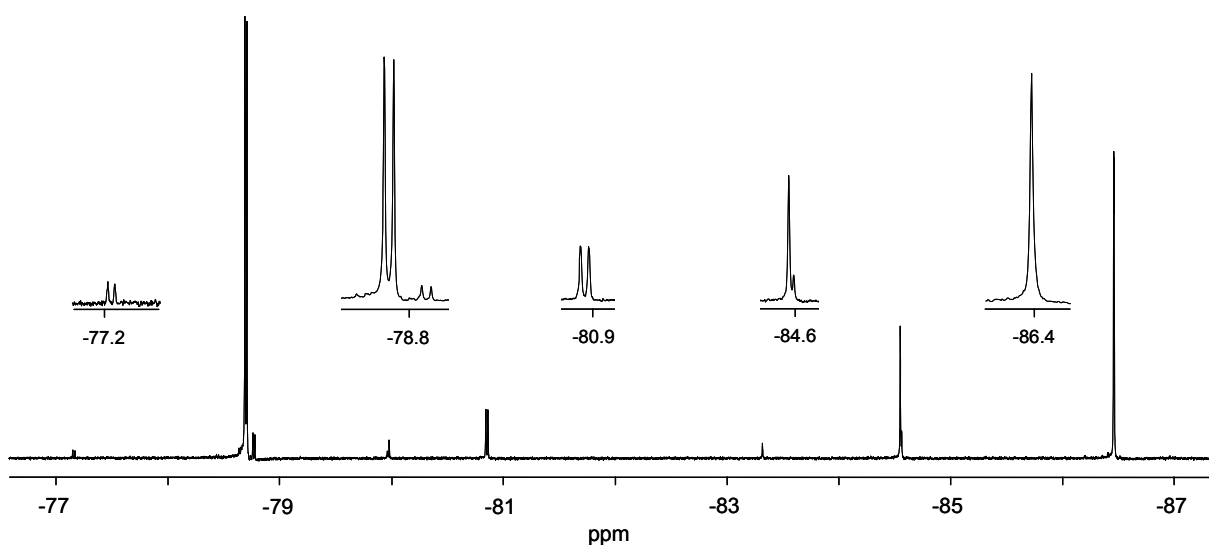


Figure 25: ^{19}F -NMR spectra (^1H -coupled) of incubations of liver S9 fractions from rabbits and synthetic S-(3,3,3-trifluoro-2-oxopropanyl)glutathione with NADPH. The doublet at $\delta = -78.8$ ppm ($J_{\text{HF}} = 6.8$ Hz) was identified as S-(3,3,3-trifluoro-2-hydroxypropanyl)glutathione, the resonance at $\delta = -80.8$ ppm (d; $J_{\text{HF}} = 7.0$ Hz) was assigned to 3,3,3-trifluoro-2-propanol, the doublet at $\delta = -77.2$ ($J_{\text{HF}} = 7.4$ Hz) was allocated to 3,3,3-trifluoro-1,2-dihydroxypropane and the presence of 3,3,3-trifluoroacetone was indicated by the singlet at $\delta = -84.6$ ppm. The small resonances at $\delta = -80.0$ and -83.3 ppm were contaminations resulting from the synthesis of S-(3,3,3-trifluoro-2-oxopropanyl)glutathione ($\delta = -84.9$ ppm; s).

Two minor doublets at $\delta = -77.2$ ($J_{\text{HF}} = 7.4$ Hz) and -80.8 ppm ($J_{\text{HF}} = 7.0$ Hz) were identified as 3,3,3-trifluoro-1,2-dihydroxypropane (**14**, Scheme 2) and 3,3,3-trifluoro-2-propanol (**7**, Scheme 2), respectively. The formation of 3,3,3-trifluoroacetone (**6**, Scheme 2) was indicated by the singlet at $\delta = -86.4$ ppm.

3.2.5.3 Identification of metabolites of HFO-1234yf by LC/MS and GC/MS

Analyses of incubations containing rabbit liver S9 fractions or microsomes from pyridine induced rats, a NADPH-regenerating system, glutathione, and HFO-1234yf were performed by LC/MS in the sensitive MRM mode, using the transitions of the appropriate molecular ions to m/z 272, a typical fragment of glutathione S-conjugates after electrospray ionization [71]. This approach allowed to confirm the presence of S-(3,3,3-trifluoro-2-hydroxypropanyl)glutathione (**4**, Scheme 2) in incubations with rabbit liver S9 fractions (Figure 26 B), whereas its metabolic precursor S-(3,3,3-trifluoro-2-oxopropanyl)glutathione (**3**, Scheme 2) could only be detected in incubations with rat liver microsomes (Figure 26 A). S-(3,3,3-Trifluoro-2-oxopropanyl)glutathione and S-(3,3,3-trifluoro-2-hydroxypropanyl)glutathione are likely precursors of *N*-acetyl-S-(3,3,3-trifluoro-2-hydroxypropanyl)-*L*-cysteine (**15**, Scheme 2) which was the main metabolite observed *in vivo*. The identified glutathione S-conjugates were identical in retention time and fragmentation after

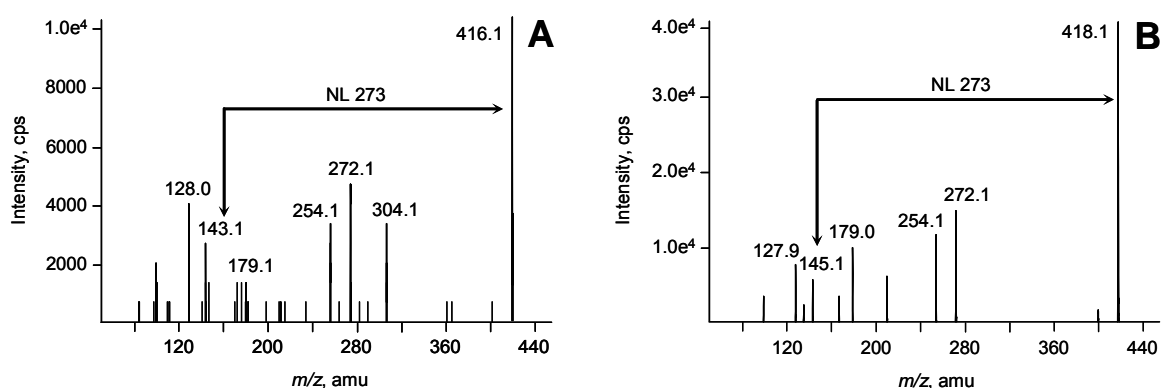


Figure 26: Identification of S-(3,3,3-trifluoro-2-oxopropanyl)-glutathione (A) and S-(3,3,3-trifluoro-2-hydroxypropanyl)-glutathione (B) by LC/MS-MS in incubations with HFO-1234yf, containing liver microsomes from pyridine induced rats (A) and rabbit liver S9 fractions (B).

ionization as compared to their synthetic reference compounds. In incubations without a NADPH-regenerating system, no glutathione S-conjugate could be detected. Moreover, this approach allowed to identify S-(3,3,3-trifluoro-2-hydroxypropyl)glutathione in incubations containing rabbit liver S9 fractions, NADPH and synthetic S-(3,3,3-trifluoro-2-oxopropyl)glutathione (Figure 26 B). The characteristic fragments in the EPIs of S-(3,3,3-trifluoro-2-oxopropyl)glutathione (A) and S-(3,3,3-trifluoro-2-hydroxypropyl)glutathione (B) (Figure 26) show the molecular ions and a neutral loss (NL) of 273 amu which is typical of thioethers of glutathione [71]. The fragment of m/z 143 in the EPI A is likely formed by the thiolate ion of S-(3,3,3-trifluoroacetone), whereas m/z 145 in EPI B may be attributable to the thiolate ion of S-(3,3,3-trifluoro-2-propanol). The fragment m/z 272 in both EPIs can be attributed to the thiolate ion of glutathione, and m/z 254 is yielded by the loss of H₂O (m/z 18) from the thiolate ion of glutathione. 2-S-(3,3,3-Trifluoropropenyl)glutathione was the presumed product of an addition-elimination reaction of HFO-1234yf with glutathione and searched in incubations of rat and rabbit liver S9 fractions using the transition of m/z 400 to m/z 272. Even though this metabolite had been identified by DuPont researches using an OrbiTrap FT-mass spectrometer [57], analyses with the less sensitive LC/MS system used within the framework of this thesis could not confirm the presence of 2-S-(3,3,3-trifluoropropenyl)glutathione in incubations of rabbit or rat liver S9 fractions.

Except for 3,3,3-trifluoro-1,2-dihydroxypropane (**14**, Scheme 2), the minor metabolites 3,3,3-trifluoro-2-propanol (**7**, Scheme 2) and 3,3,3-trifluoroacetone (**6**, Scheme 2) were confirmed by GC/MS in incubations with rabbit liver S9 fractions and HFO-1234yf (Figure 21) or synthetic S-(3,3,3-trifluoro-2-oxopropyl)glutathione (**3**, Scheme 2; Figure 25). The metabolites were found to be identical in retention times and fragmentation patterns to their reference compounds. In incubations of liver microsomes from pyridine induced rats with HFO-1234yf, the presumed metabolite 3,3,3-trifluoro-2-hydroxyacetone (**17**, Scheme 2) could not be confirmed by mass spectrometric analyses.

3.2.6 Quantitation of inorganic fluoride in incubations of HFO-1234yf with liver protein

As indicated by ^1H -decoupled ^{19}F -NMR spectra of incubations with rabbit liver S9 fractions and rat liver microsomes, biotransformation of HFO-1234yf exclusively yielded metabolites containing a CF_3 -group but lacking a fluorine atom in α -position to the CF_3 -moiety. The loss of inorganic fluoride during metabolism of HFO-1234yf was indicated by the singlet at $\delta = -119.6$ ppm in these spectra (Figures 23 and 24). In incubations with liver microsomes from untreated and pyridine induced rat liver microsomes and with human liver S9 fractions, metabolite formation from HFO-1234yf was quantified by determination of release of inorganic fluoride (Figure 27). Release of inorganic fluoride from HFO-1234yf was dependent on incubation time (B), substrate concentration (C) and concentration of enzymatically active protein (D). Reaction rates for fluoride release were 0.86 ± 0.2 nmol mg^{-1} min^{-1} (native rat liver microsomes), 2.77 ± 0.05 nmol mg^{-1} min^{-1} (pyridine induced rat liver microsomes) and 0.59 ± 0.01 nmol mg^{-1} min^{-1} (human S9 fractions). In rat microsomes, a saturation of biotransformation was apparent after addition of more than 2.67 μmoles of HFO-1234yf to the incubations (C). In low concentrations, diethyl dithiocarbamate almost completely inhibited the formation of inorganic fluoride from HFO-1234yf, suggesting that CYP450 2E1 is the major enzyme responsible for the oxidation of HFO-1234yf in rat liver microsomes. In rabbit liver S9 fractions, the formation of inorganic fluoride was determined to be 0.26 ± 0.02 nmol mg^{-1} min^{-1} . The microsomal preparations exhibited *p*-nitrophenol oxidase activity which paralleled the reaction rates obtained with HFO-1234yf. *p*-Nitrophenol oxidase activity is a marker for the activity of CYP450 2E1 [64] which is involved in the biotransformation of several other hydrochlorofluorocarbons and hydrofluorocarbons [72]. Oxidation rates of *p*-nitrophenol were 0.18 ± 0.05 nmol mg^{-1} min^{-1} in liver microsomes from rats without pretreatment, 3.22 ± 1.2 nmol mg^{-1} min^{-1} in liver microsomes from pyridine-pretreated rats, 0.11 ± 0.02 nmol mg^{-1} min^{-1} in human S9 fractions and 5.6 ± 0.5 nmol mg^{-1} min^{-1} in rabbit liver S9 fractions.

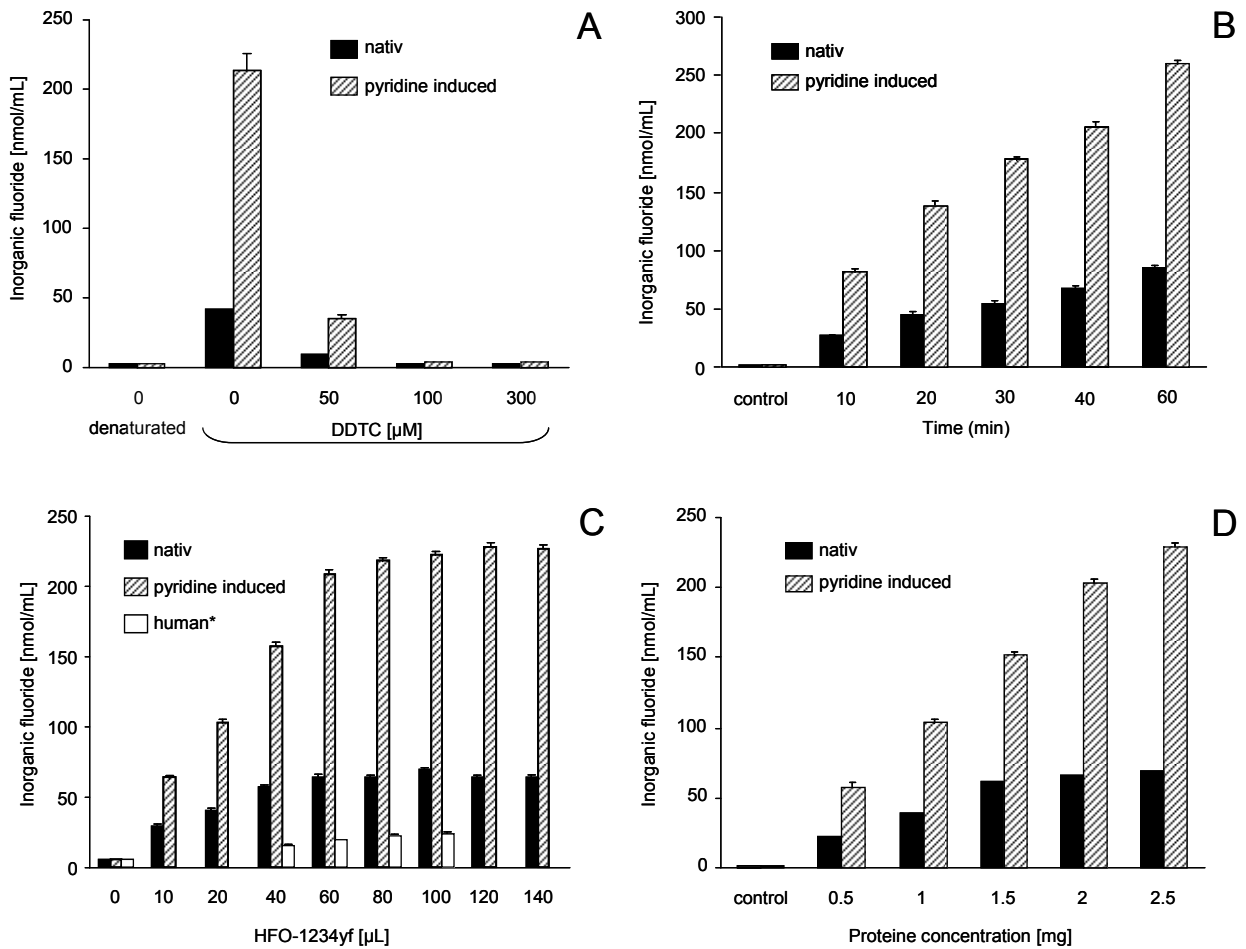


Figure 27: Release of inorganic fluoride in microsomal incubations of HFO-1234yf with liver microsomes from unpretreated rat (black bars), pyridine pretreated rats (dashed bars) and human liver S9 fractions (white bars). Inhibitory effect of diethyldithiocarbamic acid (A), dependence of fluoride release on HFO-1234yf concentration (B), protein concentration (C), and incubation time (D). * not performed with 10, 20, 120 and 140 μL HFO-1234yf.

3.3 Comparative biotransformation of pure 1,2,3,3,3-pentafluoropropene (HFO-1225yeZ) and a mixture of HFO-1225yeZ and HFO-1234yf (JDH)

The aim of the study was to investigate the possible influence of 2,3,3,3-tetrafluoropropene (HFO-1234yf) upon the biotransformation of 1,2,3,3,3-pentafluoropropene (HFO-1225yeZ). The latter exhibits acute toxic effects in mice (LC_{50} : ~10,430 - 20,200 ppm) after 4 h of inhalation. A mixture of both gases (JDH), containing equal quantities of HFO-1234yf and HFO-1225yeZ was developed for refrigeration. Comparisons of the ^{19}F -NMR spectra of rat urines after exposure to comparable concentrations of HFO-1234yf, HFO-1225yeZ and JDH were performed in order to look for additional or absent metabolites and to determine a quantitative changing in metabolite excretion in JDH urine relative to that of the HFO-1234yf and HFO-1225yeZ urines.

3.3.1 Inhalation exposures

Male Sprague-Dawley rats (n=5/concentration) were exposed for 6 h by inhalation to 10,000 ppm HFO-1225yeZ or HFO-1234yf and to 20,000 ppm JDH (HFO-1225yeZ/HFO-1234yf, 1/1, v/v) in a dynamic inhalation system. Urines were collected individually before and in a 24 h-interval after the end of the exposures. In the inhalation exposures, GC/MS measured concentrations of HFO-1225yeZ and HFO-1234yf were $10,599 \pm 1\,430$ ppm (target 10,000 ppm) and $10,113 \pm 374$ ppm (target 10,000 ppm), respectively. The concentration of JDH was calculated to be $21,275 \pm 2\,330$ ppm (target 20,000 ppm), based on mean \pm SD from 15 determinations of gas concentrations over the exposure time.

3.3.2 Qualitative analyses of urine samples by ^{19}F -NMR

After the inhalation exposures, collected urines of rats and mice were analyzed by ^{19}F -NMR spectroscopy, recording ^1H -coupled and ^1H -decoupled spectra (Figures 28 and 29). All NMR measurements were performed under the same conditions and qualitative analyses were performed by comparing the metabolite patterns. In ^1H -decoupled ^{19}F -NMR spectra of urines from rats exposed to HFO-1225yeZ, HFO-1234yf and JDH (Figure 28), all signals were present as singlets, indicating the absence of fluorine atoms in α -position and α,β -position to the CF_3 -moiety in HFO-1234yf and HFO-1225yeZ-derived metabolites, respectively. In ^1H -coupled ^{19}F -NMR spectra, some singlets were split into doublets with characteristic ^1H - ^{19}F couplings (Figure 29). In general, metabolite patterns of HFO-1225yeZ, HFO-1234yf and JDH were found to be very similar. The doublet at $\delta = -75.3$ ppm was identical in chemical shift and ^1H - ^{19}F coupling (d, $J_{\text{HF}} = 8.2$ Hz) to that of synthetic 3,3,3-trifluorolactic acid (**1**, Figure 29). 3,3,3-Trifluoroacetic acid (**2**, Figure 29) was identified by the presence of a singlet at $\delta = -75.4$ ppm, whereas the doublet at $\delta = -77.1$ ppm (d, $J_{\text{HF}} = 7.4$ Hz) could be allocated to 3,3,3-trifluoro-1,2-dihydroxypropane (**3**, Figure 29). The presence of *N*-acetyl-*S*-(3,3,3-trifluoro-2-hydroxypropanyl)-*L*-cysteine (**5**, Figure 29) was indicated by the doublet at $\delta = -78.7$ ppm (d, $J_{\text{HF}} = 6.6$ Hz) and 3,3,3-trifluoro-1-hydroxyacetone (**6**, Figure 29) was identified by the singlet at $\delta = -83.3$ ppm. The doublet (**4**, Figure 29) at $\delta = -77.2$ ppm (d, $J_{\text{HF}} = 7.2$ Hz) remained unidentified. All metabolites of HFO-1225yeZ, tentatively identified by their ^{19}F -NMR characteristics, accounted for 88% of total ^{19}F -related signals, and were also present in urines from rats exposed to HFO-1234yf and JDH, where they accounted for 84 and 86% of all ^{19}F -related signals, respectively. No predominant metabolite derivative from HFO-1234yf and from JDH was absent in the HFO-1225yeZ urines.

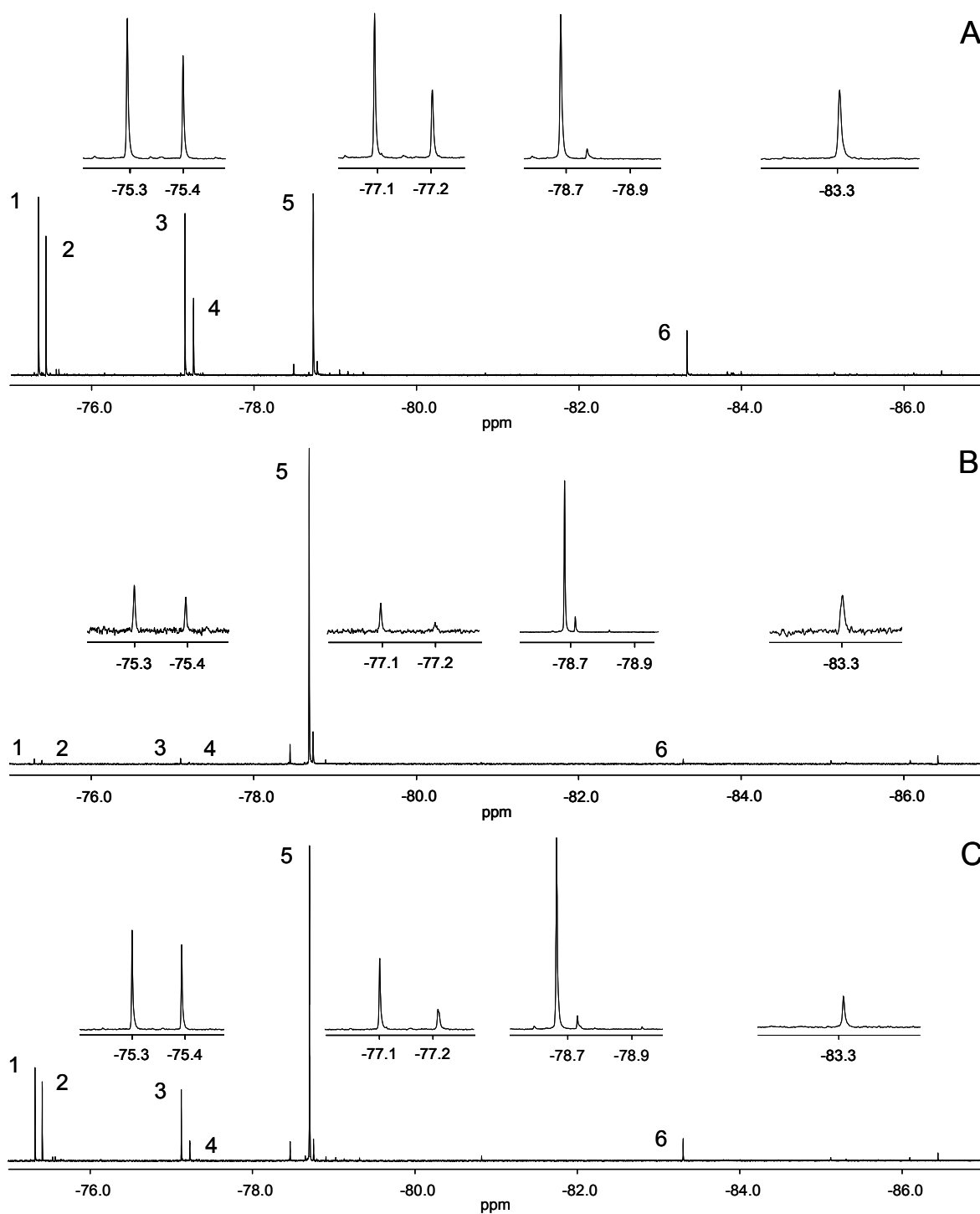


Figure 28: ^1H -decoupled ^{19}F -NMR spectra of rat urines collected after inhalation exposure for 6 h to 10,000 ppm 1,2,3,3,3-pentafluoropropene (HFO-1225yeZ) (A), 10,000 ppm 2,3,3,3-tetrafluoropropene (HFO-1234yf) (B) and 20,000 ppm JDH (HFO-1225yeZ/HFO-1234yf, 1/1, v/v) (C). The 6 major metabolites of 1,2,3,3,3-pentafluoropropene were signed by numbers and also marked in the spectrograms B and C.

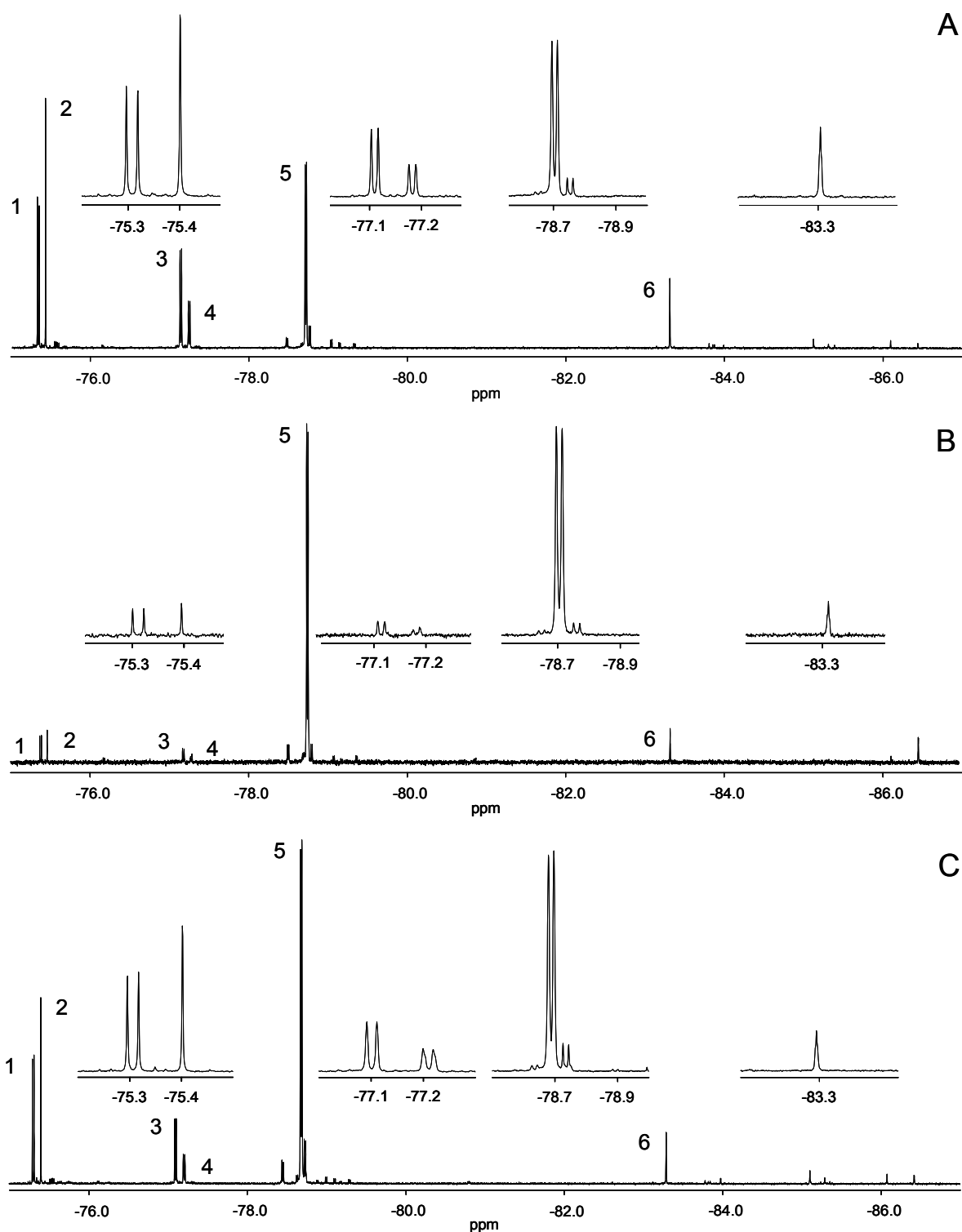


Figure 29: ^1H -coupled ^{19}F -NMR spectra of rat urines collected after inhalation exposure for 6 h to 10,000 ppm 1,2,3,3,3-pentafluoropropene (HFO-1225yeZ) (A), 10,000 ppm 2,3,3,3-tetrafluoropropene (HFO-1234yf) (B) and 20,000 ppm JDH (HFO-1225yeZ/HFO-1234yf, 1/1, v/v) (C). The 6 major metabolites of 1,2,3,3,3-pentafluoropropene were signed by numbers and also marked in the spectrograms B and C.

3.3.3 Semi-quantitative analysis of urinary metabolites by ^{19}F -NMR

A semi-quantitative determination of changes in metabolite excretion in JDH urine relative to that of the HFO-1225yeZ and HFO-1234yf urines was made by ^{19}F -NMR. Constant peak areas of an internal standard (difluoroacetic acid, DFA) spiked into the urines documented the reliability of the NMR measurements. The quotient built of integrated peak areas of the major metabolites of HFO-1225yeZ (1-6, Figures 28 and 29) and the internal standard were compared to the corresponding quotients from the HFO-1234yf and JDH urines. Metabolites chosen for this investigation were signed by numbers in ^{19}F -NMR spectra of the rat urines and could be tentatively allocated to: 3,3,3-trifluorolactic acid **1**, 3,3,3-trifluoroacetic acid **2**, 3,3,3-trifluoro-1,2-dihydroxypropane **3**, unknown metabolite **4**, *N*-acetyl-S-(3,3,3-trifluoro-2-hydroxypropyl)-*L*-cysteine **5** and 3,3,3-trifluoro-1-hydroxyacetone **6**. The normalized metabolite quantities were referenced to the total volume of urines that were individually collected from the rats within 24 h after the end of the exposures. Quantitative changings in metabolite excretion in JDH urine relative to that of the HFO-1234yf and HFO-1225yeZ urines are shown in Figure 30. Similar extents of biotransformation of HFO-1225yeZ and HFO-1234yf were detected after inhalation exposures to 10,000 ppm (approx. 1 800 rel. to DFA, both). In contrast, an inhalation exposure to 20,000 ppm JDH which is a mixture of equal volumes of HFO-1225yeZ and HFO-1234yf, did not yield the sum of metabolite quantities recovered from single inhalations with HFO-1225yeZ and HFO-1234yf. The total metabolite quantity derivative of JDH was approx. 1 400 relative to DFA, indicating an inhibitory effect of HFO-1234yf on biotransformation of HFO-1225yeZ. The percentages of the metabolites in urine collected from animals exposed to JDH represented an approximation of the mean values built of the corresponding metabolites in urines from animals exposed to HFO-1225yeZ and HFO-1234yf, indicating similar metabolite patterns in the mixture.

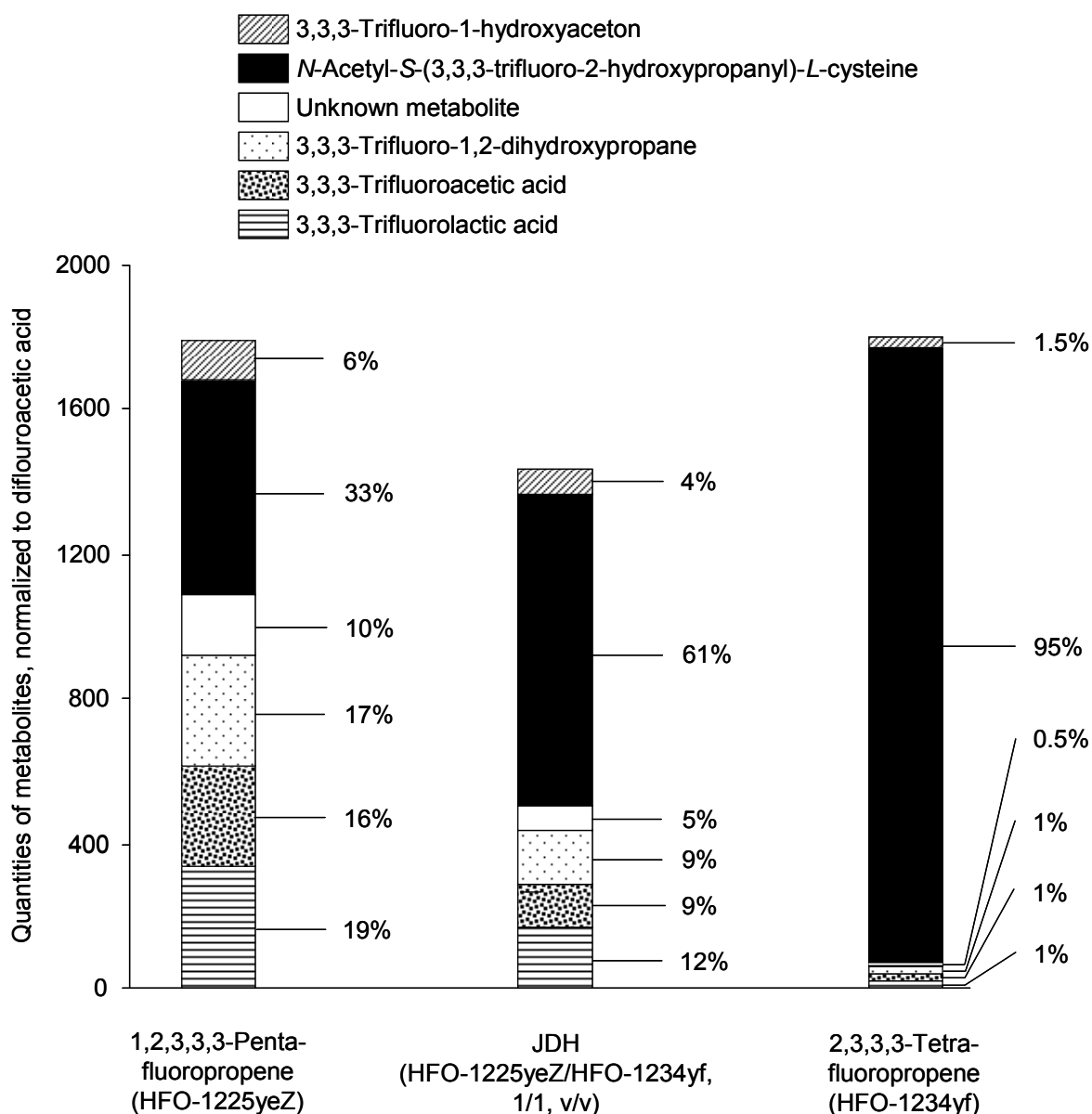


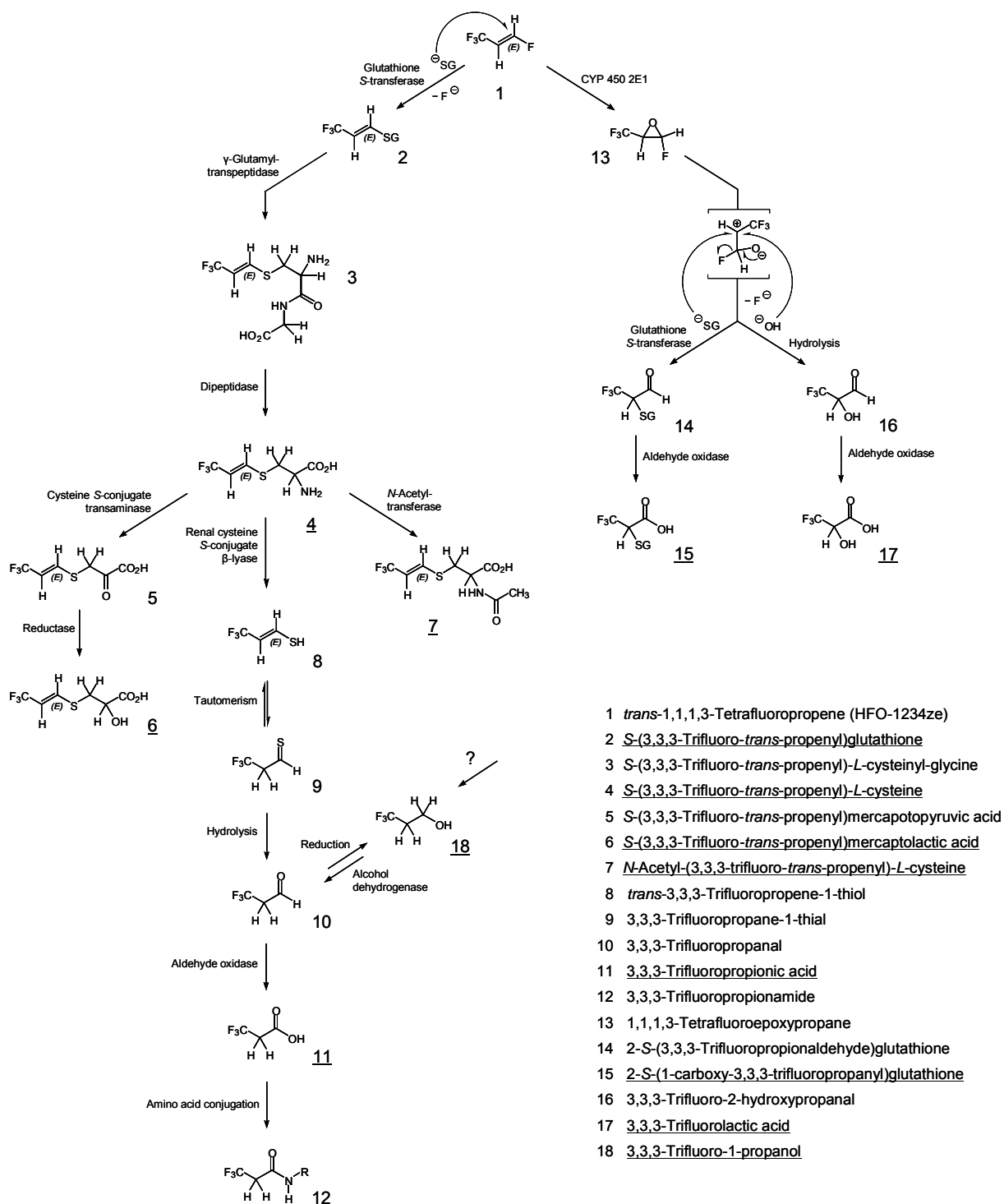
Figure 30: Comparison of extents of biotransformation of 10,000 ppm HFO-1234yf and HFO-1225yeZ and 20,000 ppm JDH (HFO-1234yf/HFO-1225yeZ, 1/1, v/v). The names of six common metabolites, accounting for approx. 85 % of total ^{19}F -related signal intensities in all urines, are listed above the diagram. Single metabolite percentages are listed next to the bars.

4 Discussion

4.1 Biotransformation of HFO-1234ze in rats and mice

Based on the structures of the metabolites in urine samples of rats exposed to HFO-1234ze, the biotransformation pathways as shown in Scheme 1 can be delineated. HFO-1234ze (**1**, Scheme 1) undergoes an addition-elimination reaction with glutathione resulting in the release of inorganic fluoride from the carbon atom in β -position to the CF_3 -moiety. The loss of inorganic fluoride is indicated by the absence of any ^{19}F - ^{19}F -coupling in ^1H -decoupled ^{19}F -NMR spectra from both rat and mouse urine. Addition-elimination reaction of HFO-1234ze (**1**, Scheme 1) with glutathione yields *S*-(3,3,3-trifluoro-*trans*-propenyl)glutathione (**2**, Scheme 1) which was tentatively identified by LC/MS-MS in incubations with rat liver microsomes and HFO-1234ze. Addition-elimination reaction of **1** (Scheme 1) with glutathione is likely catalyzed by glutathione *S*-transferases as observed with other fluoroalkenes [39] [73]. The glutathione *S*-conjugate **2** (Scheme 1) is cleaved by γ -glutamyltranspeptidase to the corresponding cysteinyl-glycine *S*-conjugate **3** (Scheme 1) which is further processed by dipeptidase to *S*-(3,3,3-trifluoro-*trans*-propenyl)-*L*-cysteine (**4**, Scheme 1), a minor metabolite of HFO-1234ze identified in urines of rats and mice. The cysteine *S*-conjugate **4** (Scheme 1) may be further metabolized in three different ways [16]. i) Transamination results in mercaptopyruvic acid *S*-conjugate **5** (Scheme 1) which is reduced to *S*-(3,3,3-trifluoro-*trans*-propenyl)mercaptolactic acid (**6**, Scheme 1), the major metabolite of HFO-1234ze present in rat urine. ii) *N*-Acetylation to the mercapturic acid *N*-acetyl-*S*-(3,3,3-trifluoro-*trans*-propenyl)-*L*-cysteine (**7**, Scheme 1) which is excreted as a minor metabolite of HFO-1234ze. iii) Cleavage by the renal cysteine *S*-conjugate β -lyase to *trans*-3,3,3-trifluoropropene-1-thiol (**8**, Scheme 1) which tautomerizes to 3,3,3-trifluoropropanethial (**9**, Scheme 1). Hydrolysis of **9** to 3,3,3-trifluoropropanal (**10**, Scheme 1) followed by oxidation may explain the formation of 3,3,3-trifluoropropionic acid (**11**, Scheme 1), a minor metabolite of HFO-1234ze, conclusively identified in urines from rats and mice by GC/MS. 3,3,3-Trifluoro-1-propanol (**18**, Scheme 1) has been tentatively identified as urinary metabolite of HFO-1234ze by ^{19}F -NMR and may be formed by reduction of **10** (Scheme 1). 3,3,3-Trifluoropropionic acid (**11**, Scheme 1) may be conjugated with an amino acid to give a 3,3,3-trifluoropropionamide (**12**,

Scheme 1) which is likely to be the major metabolite in urines of mice and also present as a minor metabolite in urine samples of rats. ^{19}F -NMR data of the presumed 3,3,3-trifluoropropionamide **12** (Scheme 1) are consistent with those of the metabolite present in rat urine after oral gavage of 3,3,3-trifluoropropionic acid [66]. Moreover, a metabolite with identical ^{19}F -NMR data as the presumed amino acid conjugate **12** (Scheme 1) was formed together with 3,3,3-trifluoropropionic acid (**11**, Scheme 1) from 3,3,3-trifluoro-1-propanol (**18**, Scheme 1) after oral gavage to a rat (Figure 8). In mice, the hypothesized amino acid conjugation of 3,3,3-trifluoropropionic acid (**11**, Scheme 1) seems to be quantitative, indicated by the absence of the resonance of **11** (Scheme 1) at $\delta = -63.5$ ppm in the ^{19}F -NMR spectrum (Figures 6 B and 7 B). Besides a reaction with glutathione, **1** (Scheme 1) might also undergo a CYP450-catalyzed oxidation to give 1,1,1,3-tetrafluoroepoxypropane (**13**, Scheme 1). Ring opening of epoxide **11** (Scheme 1) by glutathione conjugation results in the formation of glutathione S-conjugate **14** (Scheme 1) which may be oxidized to 2-S-(1-carboxy-3,3,3-trifluoropropanyl)-glutathione (**15**, Scheme 1). The latter was tentatively identified by LC/MS-MS in incubations of rat liver microsomes with HFO-1234ze (Figure 13). The identification of glutathione S-conjugate **15** (Scheme 1) may provide an indication for the identity of the uncharacterized metabolite present in ^{19}F -NMR spectra from rat and mouse urines at $\delta = -59.4$ ppm (Figures 6 and 7). This metabolite showed a singlet in ^1H -decoupled ^{19}F -NMR spectra, indicating the loss of inorganic fluoride from the carbon atom in β -position to the CF_3 -moiety. Moreover, this molecule shows a doublet in ^1H -coupled ^{19}F -NMR spectra, probably due to a single proton present at the carbon atom in α -position to the CF_3 -moiety. The second substituent of this carbon atom is likely to be neither a hydroxy group nor a second proton, since the first would give a resonance with a chemical shift of approx. -75 ppm and the latter is expected to yield a triplet in ^1H -coupled ^{19}F -NMR spectra. Furthermore, this uncharacterized metabolite may not contain a carbon atom with a proton in β -position to a vinylic CF_3 -moiety since this would split the ^1H -coupled resonance into a doublet of doublets. As shown in Scheme 1, 2-S-(1-carboxy-3,3,3-trifluoropropanyl)glutathione (**15**, Scheme 1) might be the metabolic precursor of the uncharacterized metabolite present at $\delta = -59.4$ ppm (d, $J_{\text{HF}} = 8.9$ Hz) in ^{19}F -NMR spectra of urine samples of rats and mice (Figures 6 and 7). Regarding these spectra, the hypothesized epoxidation of HFO-1234ze (**1**, Scheme 1) is further strengthened by the signal at $\delta = -75.3$ ppm



Scheme 1: Biotransformation of HFO-1234ze in rats and mice. Names and numbers of conclusively identified metabolites are underlined.

(d, $J_{\text{HF}} = 8.2$ Hz) which is attributable to 3,3,3-trifluorolactic acid (**17**, Scheme 1) the hydrolysis product of 1,1,1,3-tetrafluoroepoxypropane (**13**, Scheme 1).

None of the metabolites found *in vivo* could be confirmed conclusively by *in vitro* investigations. The absence of any signal in ^{19}F -NMR spectra of incubations with subcellular fractions is indicative of a very low biotransformation of HFO-1234ze *in vitro* and consistent with the observation of a very low extent of biotransformation of HFO-1234ze *in vivo*, even after exposures to high concentrations of up to 50,000 ppm. However, more sensitive MS-MS analysis of microsomal incubations showed small signals indicative of formation of 2-S-(1-carboxy-3,3,3-trifluoropropyl)-glutathione and S-(3,3,3-trifluoro-*trans*-propenyl)glutathione (Figure 13). However, the *in vitro* findings support the proposed pathway of biotransformation of HFO-1234ze in rats by both epoxidation and addition-elimination reaction with glutathione. Formation of ^{19}F -NMR signals indicative of S-conjugates derived from an addition reaction of glutathione to the C-C double bond in HFO-1234ze were not detected, since the reaction products of an addition reaction of HFO-1234ze and glutathione are expected to show characteristic ^{19}F - ^{19}F coupling constants. The low reactivity of HFO-1234ze with glutathione may be due to steric and electronic factors reducing the reactivity of HFO-1234ze with soft nucleophiles such as the thiolate ion of glutathione. In both rats and mice, the oxidation of HFO-1234ze was only a minor pathway based on the ^{19}F -related signal intensities which represent less than 15% of all metabolites.

4.2. Assessment of the toxicity potential of HFO-1234ze

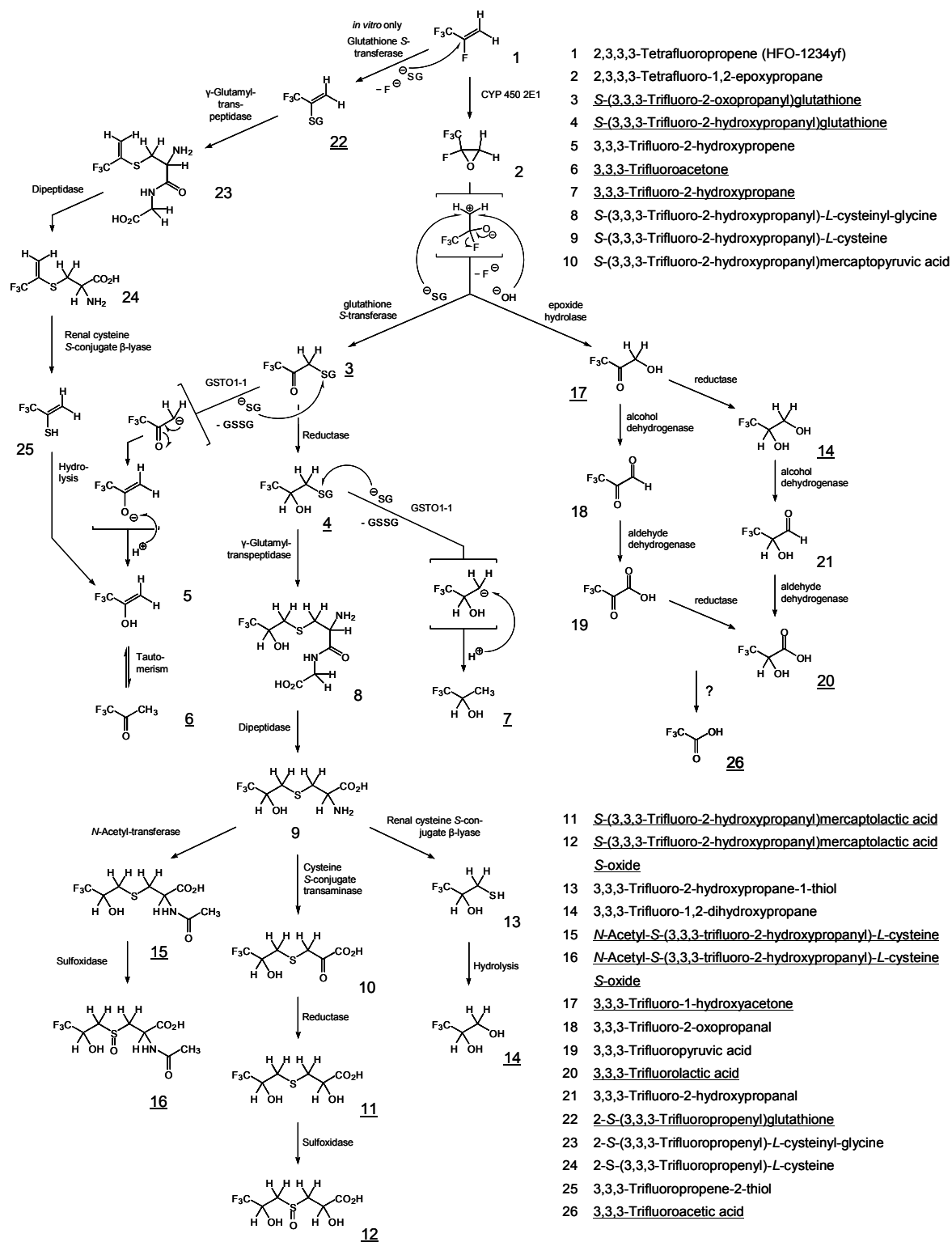
Despite the formation of a glutathione S-conjugate by an addition-elimination reaction, structural considerations on reactivity of such S-conjugates are consistent with the absence of overt nephrotoxicity in the 90-day inhalation study. Nephrotoxicity and genotoxicity were observed as the dominant adverse effects with other fluoroolefins, since the glutathione S-conjugates formed by a direct addition reaction of several polyhalogenated olefins cause renal damage following bioactivation by cysteine S-conjugate β -lyase to give thioketenes or thionoacyl fluorides [17, 74, 75]. However, the HFO-1234ze derived cysteine S-conjugate cannot be cleaved to an

electrophilic thioketene or thionoacyl fluoride due to the absence of a halogen atom on the olefinic carbon next to the sulfur. This circumstance, in combination with the low rate of biotransformation (0.007 and 0.08% of dose received in rats and mice, respectively), may explain the absence of toxic effects after inhalation exposure to HFO-1234ze. Most of the inhaled HFO-1234ze is expected to be rapidly exhaled due to its low boiling point. As shown in Table 8, metabolite recovery from mouse urine is lower than from rat urine, likely due to smaller activities of CYP450 2E1 in the mouse liver [76].

The intermediate formation of 1,1,1,3-tetrafluoroepoxypropane (**13**, Scheme 1) from HFO-1234ze **1** may indicate a potential of **1** for liver toxicity due to the formation of a reactive epoxide in this organ. However, as indicated by the very low extent of biotransformation of **1** after inhalation exposures to high concentrations, the rates of formation may only be low and covalent binding resulting in liver toxicity may be prevented by the efficient detoxication of the epoxide by glutathione conjugation. The efficient detoxication may explain the absence of pathologic changes in the liver as observed in the 90-day inhalation study with HFO-1234ze. Moreover, the very low rates of biotransformation of HFO-1234ze may further explain the absence of cardiotoxic effects known to be displayed by 3,3,3-trifluoropropionic acid (**11**, Scheme 1), a minor metabolite in urines from rats and mice after inhalation exposure to HFO-1234ze.

4.3. Biotransformation of HFO-1234yf in rabbits, rats and mice

Based on the structures of the metabolites in urine samples of rabbits, rats and mice exposed to HFO-1234yf, the biotransformation pathways as shown in scheme 2 can be delineated. HFO-1234yf (**1**, Scheme 2) undergoes a CYP450-catalyzed oxidation to 2,3,3,3-tetrafluoro-1,2-epoxypropane (**2**, Scheme 2). In rats and mice, CYP450 2E1 has been shown to be the major mediator for this reaction and thus may also contribute to the epoxidation of HFO-1234yf in rabbits [57]. In rabbits, rats and mice, **2** is further processed by a nucleophilic attack of the thiolate ion of glutathione to the carbon atom in β -position to the CF_3 -moiety to give S-(3,3,3-trifluoro-2-oxopropanyl)glutathione (**3**, Scheme 2). This reaction is paralleled by the loss of inorganic fluoride from the carbon atom in α -position to the CF_3 -group of **2** (Scheme 2). Inorganic fluoride has been identified as metabolite of HFO-1234yf in incubations with liver protein from rabbits and rats (Figures 23 and 24). The metabolic fate of **3** (Scheme 2) can be rationalized in two different ways. i) Reduction to S-(3,3,3-trifluoro-2-hydroxypropanyl)glutathione (**4**, Scheme 2) which is present in incubations of rabbit liver S9 fractions and HFO-1234yf. ii) GSTO1-1 catalyzed attack of the thiolate ion of glutathione to the sulfur of **3** (Scheme 2) yielding dimerized glutathione (GSSG) and an intermediary anion which is protonated to give 3,3,3-trifluoropropene-2-ol (**5**, Scheme 2). GSTO1-1 has been reported to catalyze the attack of a thiol on the sulfur atom of glutathione S-conjugates to yield a disulfide and a carbanion that is stabilized by enolization [77, 78]. **5** (Scheme 2) may tautomerize to 3,3,3-trifluoroacetone **6** (Scheme 2) which is an urinary metabolite of HFO-1234yf in rats and mice, and present among the minor metabolites in incubations with rabbit liver S9 fractions. 3,3,3-Trifluoroacetone **6** (Scheme 2) may be further reduced to 3,3,3-trifluoro-2-propanol (**7**, Scheme 2), a minor metabolite in urine samples of rabbits and the major derivate of HFO-1234yf in incubations of rabbit liver S9 fractions. As presumed for glutathione S-conjugate **3** (Scheme 2), S-(3,3,3-trifluoro-2-hydroxypropanyl)glutathione (**4**, Scheme 2) may also be subjected to a GSTO1-1 mediated nucleophilic attack of the thiolate ion of glutathione yielding GSSG and an intermediary anion which is protonated to give 3,3,3-trifluoro-2-propanol (**7**, Scheme 2). Enzymatic degradation of **4** (Scheme 2) by γ -glutamyltranspeptidase yields cysteinyl-glycine S-conjugate **8** (Scheme 2) which is further cleaved by dipeptidase to



Scheme 2: Biotransformation of HFO-1234yf in rabbits, rats and mice. Names and numbers of conclusively or tentatively identified metabolites in urines or incubations with liver microsomes or S9 fractions are underlined. Abbreviations: GSSG (glutathione disulfide); ^{-}SG (thiolate ion of glutathione); GSTO1-1 (glutathione S-transferase omega-class 1).

S-(3,3,3-trifluoro-2-hydroxypropyl)-L-cysteine (**9**, Scheme 2). The latter, however, could not be identified in urine samples of rabbits, rats and mice after exposure to HFO-1234yf. Cysteine S-conjugate **9** (Scheme 2) may be further processed in three different ways [16]. i) Transamination to the corresponding mercaptopyruvic acid S-conjugate **10** (Scheme 2) which is reduced to S-(3,3,3-trifluoro-2-hydroxypropyl)mercaptolactic acid (**11**, Scheme 2). The latter is one of the major metabolites present in rabbit urines after exposure to HFO-1234yf and possibly further sulfoxidated to S-(3,3,3-trifluoro-2-hydroxypropyl)mercapto-lactic acid S-oxide (**12**, Scheme 2), indicated by LC/MS-MS analyses of urine samples from rabbits (Figure 20). ii) Cleavage by renal cysteine S-conjugate β -lyase to 3,3,3-trifluoro-2-hydroxypropane-1-thiol (**13**, Scheme 2) which is hydrolysed to 3,3,3-trifluoro-1,2-dihydroxypropane (**14**, Scheme 2), a minor metabolite of HFO-1234yf identified in urines from rabbits, rats and mice by ^{19}F -NMR and GC/MS (Figures 15, 16 and 21). iii) *N*-Acetylation to the corresponding mercapturic acid *N*-acetyl-S-(3,3,3-trifluoro-2-hydroxypropyl)-L-cysteine (**15**, Scheme 2) which was the major metabolite of HFO-1234yf in urines from rabbits, rats and mice after the inhalation exposures. A metabolic successor of **15** (Scheme 2) may be *N*-acetyl-S-(3,3,3-trifluoro-2-hydroxypropyl)-L-cysteine S-oxide (**16**, Scheme 2) which was identified in urine samples from rabbits, rats and mice by LC/MS-MS (Figure 20).

A qualitative difference in biotransformation of HFO-1234yf (**1**, Scheme 2) in rabbits, rats and mice is obvious regarding the metabolic fate of 2,3,3,3-tetrafluoro-1,2-epoxypropane (**2**, Scheme 2). In rabbits, ring opening of **2** (Scheme 2) may occur exclusively by glutathione conjugation, whereas in rats and mice, **2** (Scheme 2) is also a substrate of epoxide hydrolase which mediates the formation of 3,3,3-trifluoro-1-hydroxyacetone (**17**, Scheme 2). 3,3,3-Trifluoro-1-hydroxyacetone has been tentatively identified by ^{19}F -NMR as minor metabolite of HFO-1234yf in urines from rats and mice (Figures 15 and 16) and in incubations with rat liver microsomes (Figure 23). Contrarily, 3,3,3-trifluoro-1-hydroxyacetone (**17**, Scheme 2) was absent in ^{19}F -NMR spectra of both rabbit urine samples (Figures 15 A and 16 A) and incubations with rabbit liver S9 fractions (Figure 24), indicated by the absence of the signal at $\delta = -83.4$ ppm. In rats and mice, 3,3,3-trifluoro-1-hydroxyacetone (**17**, Scheme 2) may be oxidized to 3,3,3-trifluoro-2-oxo-propanal (**18**, Scheme 2) which is further processed to 3,3,3-trifluoropyruvic acid (**19**, Scheme 2). Even though 3,3,3-trifluoropyruvic acid was not present in ^{19}F -NMR spectra of any incubation or urine

sample, it has been shown to be the metabolic precursor of 3,3,3-trifluorolactic acid (**20**, Scheme 2) after oral gavage of **19** (Scheme 2) to a rat (Figure 19). Additionally, 3,3,3-trifluoro-1-hydroxyacetone (**17**, Scheme 2) may be reduced to 3,3,3-trifluoro-1,2-dihydroxypropane (**14**, Scheme 2), identified as minor metabolite of HFO-1234yf in urines from rabbits, rats and mice. As outlined in Scheme 2, formation of **14** in rabbits may be rationalized by GSTO1-1 catalyzed attack of glutathione to S-(3,3,3-trifluoro-2-hydroxypropenyl)glutathione (**4**, Scheme 2), thus being independent from prior formation of 3,3,3-trifluoro-1-hydroxyacetone (**17**, Scheme 2). In rats and mice, 3,3,3-trifluoro-1,2-dihydroxypropane (**14**, Scheme 2) is oxidized to 3,3,3-trifluorolactic acid (**20**, Scheme 2), investigated by oral gavage of **14** (Scheme 2) to a rat (Figure 18). For the minor metabolite 3,3,3-trifluoroacetic acid (**26**, Scheme 2) in urines from rats and mice, mechanisms of formation consistent with the available knowledge on the biotransformation cannot be derived. Formation of trifluoroacetic acid (**26**, Scheme 2) requires cleavage of a C–C bond which may occur by pyruvate decarboxylase-catalyzed decarboxylation of trifluoropyruvic acid. However, previous studies were unable to observe formation of trifluoroacetic acid from trifluoropyruvic acid [66].

Beside CYP450 2E1-mediated epoxidation, HFO-1234yf (**1**, Scheme 2) undergoes an addition-elimination reaction with glutathione *in vitro* which is paralleled by the release of inorganic fluoride. Even though incubations of HFO-1234yf with rat liver microsomes and cytosol under conditions favouring direct glutathione conjugation did not yield any ¹⁹F-NMR signals, analysis of microsomal incubations of HFO-1234yf using the very sensitive MS-MS methods identified 2-S-(3,3,3-trifluoropropenyl)glutathione (**22**, Scheme 2) in low concentrations [57]. The low reactivity of HFO-1234yf with glutathione may be due to steric and electronic factors reducing the reactivity of HFO-1234yf with soft nucleophiles such as the thiolate ion of glutathione. Processing of glutathione S-conjugate **22** (Scheme 2) by γ -glutamyltranspeptidase and dipeptidase may yield cysteine S-conjugate **24** (Scheme 2) which is cleaved by renal cysteine S-conjugate β -lyase to 3,3,3-trifluoropropene-2-thiol (**25**, Scheme 2). Hydrolysis of **25** may explain the formation of 3,3,3-trifluoro-2-hydroxypropene (**5**, Scheme 2), the presumed metabolic precursor of 3,3,3-trifluoroacetone (**6**, Scheme 2) which has been conclusively identified by GC/MS in urines from rats and mice (Figure 21).

The structures of the metabolites identified *in vitro* suggest that HFO-1234yf predominantly undergoes a CYP450-mediated epoxidation, followed by glutathione conjugation and hydrolytic ring opening in rodents and exclusively by glutathione conjugation in rabbits. Formation of ^{19}F -NMR signals indicative of mercapturates derived from an addition or an addition-elimination reaction of glutathione to the C-C double bond in HFO-1234yf were not detected. A vinylic CF_3 -moiety expected in the reaction products of an addition-elimination reaction of HFO-1234yf and glutathione yields a ^{19}F -NMR resonance at approx. -60 ppm and products from an addition of glutathione are expected to show ^{19}F -NMR spectra with characteristic ^{19}F - ^{19}F -coupling constants. Such signals were not observed in any of the urine samples collected from the HFO-1234yf exposed animals. Moreover, incubations of HFO-1234yf with rabbit and rat liver S9 fractions under conditions favouring direct glutathione conjugation also did not yield any ^{19}F -NMR signals indicative of the formation of glutathione S-conjugates under conditions not resulting in oxidation of HFO-1234yf. However, analysis of microsomal incubations of HFO-1234yf using the very sensitive MS-MS methods identified 2-S-(3,3,3-trifluoropropenyl)glutathione in low concentrations, thus indicating a low susceptibility of HFO-1234yf for an addition-elimination reaction with glutathione. The low reactivity of HFO-1234yf with glutathione may be due to steric and electronic factors reducing the reactivity of HFO-1234yf with soft nucleophiles such as the thiolate ion of glutathione.

4.4 Assessment of the toxicity potential of HFO-1234yf

The very low rates of a direct glutathione conjugation reaction of HFO-1234yf (**1**, Scheme 2) is consistent with the absence of nephrotoxicity in the 90-day inhalation studies. Nephrotoxicity was observed as the dominant adverse effect in repeat dose studies with other fluoroolefins, since the glutathione conjugates formed by a direct reaction with glutathione are expected to cause renal proximal tubular damage due to bioactivation by cysteine conjugate β -lyase [17]. However, the HFO-1234yf derived cysteine S-conjugate (**9**, Scheme 2) cannot be cleaved to an electrophilic thioketene or thionoacyl fluoride due to the absence of a C-C double bond with a halogen atom next to the sulfur (Figure 3). Moreover, the alkylic mercapturic acid sulfoxide (**16**, Scheme 2) may not display cytotoxicity by reacting as a Michael Acceptor (Figure 3).

This circumstance, in combination with the low rate of biotransformation (0.05, 0.002 and 0.03% of dose received in rabbits, rats and mice, respectively), may explain the absence of toxic effects after inhalation exposure of rats to HFO-1234yf.

The metabolic formation of epoxide **2** (Scheme 2) from HFO-1234yf (**1**, Scheme 2) may indicate a potential of **1** for liver toxicity due to the formation of a reactive epoxide in this organ. However, as indicated by the very low extent (\ll 1% of dose received) of biotransformation of **1** (Scheme 2) after inhalation exposures to high concentrations, the rates of formation of **2** (Scheme 2) are very low and covalent binding to tissue nucleophiles resulting in liver toxicity likely is prevented by the efficient detoxication of **2** (Scheme 2) by glutathione conjugation to give glutathione S-conjugate **3** (Scheme 2). The efficient detoxication may explain the absence of pathologic changes in the liver as observed in the 90-day inhalation study with HFO-1234yf. Furtheron, the low rates of formation of epoxide **2** (Scheme 2) from HFO-1234yf are likely due to the high volatility of HFO-1234yf resulting in a very low retention of inhaled **1** (Scheme 2) in the mammalian organism.

4.5 Biotransformation of pure HFO-1225yeZ and JDH, a mixture containing equal volumes of HFO-1225yeZ and HFO-1234yf

Total ^{19}F -related signal intensities in rat urines were similar after inhalation exposures to HFO-1234yf and HFO-1225yeZ (10,000 ppm, both) and JDH (20,000 ppm). The finding, that the signal intensities in JDH urines do not represent the sum of signal intensities in the single compound urines indicates, that HFO-1234yf and HFO-1225yeZ display inhibitory effects on each other in the mixture. Regarding JDH urines, no additional or absent metabolites were present in ^{19}F -NMR spectra compared to HFO-1225yeZ urines. However, no conclusions can be drawn from this finding on the toxicity potential of JDH which may display similar adverse effects on the test animals as the single compound.

5 Summary

trans-1,1,1,3-Tetrafluoropropene (HFO-1234ze) and 2,3,3,3-tetrafluoropropene (HFO-1234yf) are non-ozone-depleting fluorocarbon replacements with low global warming potentials and short atmospheric lifetimes. They are developed as foam blowing agent and refrigerant, respectively. Investigations on biotransformation in different test species and *in vitro* systems are required to assess possible health risks of human exposure and needed for commercial development. The biotransformation of HFO-1234ze and HFO-1234yf was therefore investigated after inhalation exposure. Male Sprague-Dawley rats were exposed to air containing 2 000; 10,000; or 50,000 ppm ($n=5/\text{concentration}$) HFO-1234ze or HFO-1234yf. Male B6C3F1 mice were only exposed to 50,000 ppm HFO-1234ze or HFO-1234yf. Due to lethality observed in a developmental study with rabbits after exposure to high concentrations of HFO-1234yf, the metabolic fate of the compound was tested by whole body inhalation exposure of female New Zealand White rabbits to air containing 2 000; 10,000; or 50,000 ppm ($n=3/\text{concentration}$) HFO-1234yf. All inhalation exposures were conducted for 6 h in a dynamic exposure chamber. After the end of the exposures, animals were individually housed in metabolic cages and urines were collected at 6 or 12 h intervals for 48 h (rats and mice) or 60 h (rabbits). For metabolite identification, urine samples were analyzed by ^1H -coupled and ^1H -decoupled ^{19}F -NMR and by LC/MS-MS or GC/MS. Metabolites were identified by ^{19}F -NMR chemical shifts, signal multiplicity, ^1H - ^{19}F coupling constants and by comparison with synthetic reference compounds.

Biotransformation of HFO-1234ze in rats exposed to 50,000 ppm yielded *S*-(3,3,3-trifluoro-*trans*-propenyl)mercaptolactic acid as the predominant metabolite which accounted for 66% of all integrated ^{19}F -NMR signals in urines. No ^{19}F -NMR signals were found in spectra of rat urine samples collected after inhalation exposure to 2 000 or 10,000 ppm HFO-1234ze likely due to insufficient sensitivity. *S*-(3,3,3-Trifluoro-*trans*-propenyl)-*L*-cysteine, *N*-acetyl-*S*-(3,3,3-trifluoro-*trans*-propenyl)-*L*-cysteine, 3,3,3-trifluoropropionic acid and 3,3,3-trifluorolactic acid were also present as metabolites in urine samples of rats and mice at the 50,000 ppm level. A presumed amino acid conjugate of 3,3,3-trifluoropropionic acid was the major metabolite of HFO-1234ze in urine samples of mice exposed to 50,000 ppm and

related to 18% of total integrated ^{19}F -NMR signals. Quantitation of three metabolites in urines of rats and mice was performed, using LC/MS-MS or GC/MS. The quantified amounts of the metabolites excreted with urine in both mice and rats, suggest only a low extent ($\ll 1\%$ of dose received) of biotransformation of HFO-1234ze and 95% of all metabolites were excreted within 18 h after the end of the exposures ($t_{1/2}$ approx. 6 h). Due to its low boiling point of $-22\text{ }^\circ\text{C}$, most of the inhaled HFO-1234ze is expected to be readily exhaled. Moreover, steric and electronic factors may decrease the reactivity of the parent compound with soft nucleophiles such as glutathione. The obtained results suggest that HFO-1234ze is subjected to an addition-elimination reaction with glutathione and to a cytochrome P450-mediated epoxidation at low rates. The extent of a direct addition reaction of HFO-1234ze with glutathione is negligible, compared to that of the observed addition-elimination reaction. The results of *in vivo* testing of HFO-1234ze could not be supported by *in vitro* investigations, since HFO-1234ze was not metabolized in incubations with either liver microsomes or subcellular fractions from rat and human. Regarding the structures delineated in the biotransformation scheme of HFO-1234ze, 1,1,1,3-tetrafluoroepoxypropane and 3,3,3-trifluoropropionic acid are toxic intermediates which, however, are not supposed to display toxicity in the species after exposure to HFO-1234ze, due to the low extent of formation and an efficient detoxification of the epoxide by hydrolysis and glutathione conjugation. The findings of biotransformation of HFO-1234ze in rats and mice correlate with the absence of adverse effects in the toxicity testings and indicate their innocuousness to a human exposure.

Biotransformation of HFO-1234yf yielded *N*-acetyl-S-(3,3,3-trifluoro-2-hydroxypropyl)-L-cysteine as predominant metabolite which accounted for approx. 44, 90 and 32% (50,000 ppm) of total ^{19}F -NMR signal intensities in urine samples from rabbits, rats and mice, respectively. S-(3,3,3-Trifluoro-2-hydroxypropyl)mercaptolactic acid and the sulfoxides of mercapturic acid and mercaptolactic acid S-conjugate were identified as minor metabolites of HFO-1234yf in urine samples from rabbits, rats and mice, whereas trifluoroacetic acid, 3,3,3-trifluorolactic acid and 3,3,3-trifluoro-1-hydroxyacetone were present as minor metabolites only in urine samples from rats and mice. The absence of these metabolites in rabbit urine samples represents the major species difference in biotransformation of HFO-1234yf, observed in this work. Apparently, the initially

formed 2,3,3,3-tetrafluoro-1,2-epoxypropane is exclusively metabolized by rabbit glutathione S-transferase and is not a substrate of epoxide hydrolase in this species. Further minor metabolites of HFO-1234yf present in urines of rabbits, rats and mice were allocated to 3,3,3-trifluoro-1,2-dihydroxypropane, 3,3,3-trifluoro-2-propanol and 3,3,3-trifluoroacetone, possibly formed by GSTO1-1 mediated processing of the intermediary glutathione S-conjugates. Metabolites identified in incubations of HFO-1234yf with rat and human liver microsomes and with rabbit liver subcellular fractions support the metabolic pathways of HFO-1234yf revealed *in vivo*. The release of inorganic fluoride from HFO-1234yf *in vitro* was shown to depend on time, cofactors and protein concentration. The obtained results suggest that HFO-1234yf is subjected to a biotransformation reaction typical for haloolefins, likely by a cytochrome P450 2E1-catalyzed formation of 2,3,3,3-tetrafluoroepoxypropane at low rates, followed by glutathione conjugation or hydrolytic ring opening (the latter was not observed in rabbits). The extent of an addition-elimination reaction of HFO-1234yf with glutathione is negligible, compared to that of the CYP450-mediated epoxidation, and furthermore no evidence was given for a direct addition reaction of HFO-1234yf with glutathione. Quantitation of the major metabolite *N*-acetyl-S-(3,3,3-trifluoro-2-hydroxypropyl)-L-cysteine by LC/MS-MS showed that most of it (90%) was excreted within 18 h after the end of exposure ($t_{1/2}$ approx. 6 h) in rats and mice. In rabbits, 95% of the mercapturic acid was excreted within 12 h after the end of the exposures ($t_{1/2}$ approx. 9.5 h). The low boiling point of HFO-1234yf ($-22\text{ }^{\circ}\text{C}$) suggests an almost quantitative exhalation and steric and electronic factors may explain the inert nature of the parent compound. These circumstances may provide an explanation for the low extent of metabolism of HFO-1234yf ($\ll 1\%$ of dose received in rabbits, rats and mice). Potentially toxic metabolites, i.e. 2,3,3,3-tetrafluoroepoxypropane and 3,3,3-trifluoroacetic acid outlined in the Scheme 2 did not cause any damage in the test species, probably due to the low extent of formation and the efficient detoxification of the epoxide by glutathione conjugation. No explanation can be given for the causes of mortality and moribundity observed in a developmental toxicity testing with rabbits. Differences in urinary metabolite patterns between rabbits, rats and mice seen with HFO-1234yf are likely due to species-specific processing of glutathione S-conjugates but do not indicate differences in potential toxicity. However, the development of HFO-1234yf for use as refrigerant may be justifiable, since adverse effects in rabbits were only observed at

relatively high exposure levels after several days of inhalative administration, and comparable exposures of humans are unlikely to occur in household applications.

Quantitative comparisons of biotransformation HFO-1225yeZ and HFO-1234yf at the 10,000 ppm level and JDH, a mixture containing equal volumes of both compounds, at the 20,000 ppm level showed that similar quantities of metabolites were present in rat urines after exposure to HFO-1225yeZ and HFO-1234yf. However, lower amounts of metabolites have been detected in urines from JDH exposed animals compared to the sum of metabolites observed in urines collected from animals after inhalation exposure to HFO-1225yeZ or HFO-1234yf. This finding suggests, that HFO-1225yeZ and HFO-1234yf display inhibitory effects upon each other and are biotransformed to a lower extent in the JDH-mixture than as single compounds. Qualitative analyses of all urines showed the presence of identical major metabolites which, however, were formed to different extents. The percentages of the metabolites in JDH urine represented approximately the means built of the corresponding values from HFO-1225yeZ and HFO-1234yf urines, indicating the perpetuation of metabolite patterns of both gases in the mixture. Since HFO-1225yeZ exhibited toxicity in mice at exposure levels of approx. 10,000 pm, the lower extent of biotransformation of JDH at the 20,000 ppm level, may be associated with a decrease in toxicity.

6 Zusammenfassung

trans-1,1,1,3-Tetrafluorpropen (HFO-1234ze) und 2,3,3,3-Tetrafluorpropen (HFO-1234yf) sind FKW-Ersatzstoffe, die eine kurze atmosphärische Lebensdauer besitzen und weder die Ozonschicht beeinträchtigen noch wesentlich zur globalen Erwärmung beitragen. Sie werden derzeit als Treibmittel für Schäume beziehungsweise als Kühlmittel entwickelt. Untersuchungen der Biotransformation in verschiedenen Tierspezies und in *in vitro* Systemen tragen zur Risikobewertung einer Humanexposition bei und werden für die kommerzielle Entwicklung benötigt. In dieser Arbeit wurde die Biotransformation von HFO-1234ze und HFO-1234yf nach inhalativer Exposition untersucht. Männliche Sprague-Dawley Ratten wurden Luftkonzentrationen von 2.000, 10.000 und 50.000 ppm (n=5/Konzentration) ausgesetzt. Männliche B6C3F1 Mäuse wurden dagegen nur einer Konzentration von 50.000 ppm ausgesetzt. Aufgrund von Todesfällen in einer Entwicklungstoxizitätsstudie mit Kaninchen wurde in dieser Arbeit auch die Biotransformation von HFO-1234yf in weiblichen Kaninchen mit Konzentrationen von 2.000, 10.000 und 50.000 ppm untersucht. Alle Inhalationen dauerten 6 Stunden und fanden in einem dynamisch durchströmten Expositionssystem statt. Nach Ende der Inhalationen wurden die Versuchstiere individuell in Stoffwechsellkäfigen untergebracht und ihre Urine in 6 bzw. 12 h Intervallen gesammelt (insgesamt 48 h bei Ratten und Mäusen bzw. 60 h bei Kaninchen). Zur Identifizierung der Metabolite von HFO-1234ze und HFO-1234yf in den Urinen wurden ^1H -ge- und entkoppelte ^{19}F -NMR-Spektren aufgezeichnet und massenspektrometrische Untersuchungen mittels LC/MS-MS oder GC/MS durchgeführt. Die Metaboliten wurden anhand ihrer ^{19}F -NMR-Charakteristika (Chemische Verschiebung, Signalmultiplizität und ^1H - ^{19}F Kopplungskonstante) und durch Vergleich mit ihren synthetischen Referenzverbindungen identifiziert.

In Ratten, die einer Konzentration von 50.000 ppm HFO-1234ze ausgesetzt worden waren, konnte *S*-(3,3,3-Trifluor-*trans*-propenyl)merkaptolaktat als Hauptmetabolit nachgewiesen werden. Er machte 66% aller integrierten ^{19}F -NMR-Signale aus. In ^{19}F -NMR-Spektren von Rattenurinen der 2.000 und 10.000 ppm Expositionen konnten dagegen keine Signale detektiert werden, wahrscheinlich wegen unzureichender Empfindlichkeit der ^{19}F -NMR-Messungen. Als Nebenprodukte von

HFO-1234ze in Ratten- und Mäuseurinen wurden *S*-(3,3,3-Trifluor-*trans*-propenyl)-*L*-cystein, *N*-Acetyl-*S*-(3,3,3-trifluor-*trans*-propenyl)-*L*-cystein, 3,3,3-Trifluorpropionsäure und 3,3,3-Trifluorlaktat nachgewiesen. In Mäuseurinen war der Hauptmetabolit von HFO-1234ze ein vermutetes Aminosäurekonjugat von 3,3,3-Trifluorpropionsäure, auf das 18% aller integrierten ¹⁹F-NMR Signalintensitäten entfielen. In den Urinen von Ratten und Mäusen wurden 3 Metabolite mittels LC/MS-MS oder GC/MS quantifiziert. Die ermittelten Mengen weisen auf eine sehr niedrige Biotransformationsrate von HFO-1234ze hin (<<1% der verabreichten Dosis). 95% aller Metabolite wurden innerhalb von 18 h nach Ende der Inhalationen ausgeschieden ($t_{1/2}$ ca. 6 h). Aufgrund des niedrigen Siedepunkts von -22°C wird ein Großteil des aufgenommenen Gases möglicherweise rasch wieder exhaliiert, und sterische sowie elektronische Faktoren könnten die Reaktivität der Ausgangsverbindung mit schwachen Nucleophilen wie Glutathion senken. Die vorliegenden Ergebnisse legen nahe, dass HFO-1234ze in geringem Ausmaß durch Additions-Eliminations Reaktion mit Glutathion und einer CYP450-vermittelten Epoxidierung biotransformiert wird. Das Ausmaß einer direkten Additions Reaktion von HFO-1234ze mit Glutathion ist verglichen mit der vorherrschenden Additions-Eliminations Reaktion vernachlässigbar. Da kein Umsatz von HFO-1234ze in Inkubationen mit Rattenlebermikrosomen oder subzellulären Fraktionen von Human- und Rattenleber stattfand, konnten die *in vivo* Ergebnisse dieser Arbeit nicht mit *in vitro* Untersuchungen verglichen werden. Im Biotransformationsschema von HFO-1234ze sind 1,1,1,3-Tetrafluorepoxypropan und 3,3,3-Trifluorpropionsäure toxische Intermediate, die jedoch aufgrund der geringen gebildeten Mengen und einer effektiven Entgiftung des Epoxids durch Glutathionkonjugation keine toxischen Effekte in den verwendeten Tierspezies auslösten. Die Ergebnisse der Untersuchung der Biotransformation von HFO-1234ze in Ratten und Mäusen korrelieren mit der Abwesenheit nachteiliger Effekte in den Toxizitätsstudien und lassen eine Humanexposition gegenüber HFO-1234ze als unbedenklich erscheinen.

Bei der Biotransformation von HFO-1234yf entstand *N*-Acetyl-*S*-(3,3,3-trifluor-2-hydroxypropenyl)-*L*-cystein als Hauptmetabolit in allen Tierspezies. In den 50.000 ppm Studien machte die Mercaptursäure 44, 90 und 32% aller integrierten ¹⁹F-NMR-Signale in den Urinen von Kaninchen, Ratten beziehungsweise Mäusen aus. *S*-(3,3,3-Trifluor-2-hydroxypropenyl)mercaptolaktat und die Sulfoxide der

Merkaptursäure und des Merkaptolaktatkonjugats wurden als Nebenprodukte von HFO-1234yf in den Urinen der untersuchten Tierspezies identifiziert. Dagegen wurden geringen Mengen von 3,3,3-Trifluoressigsäure, 3,3,3-Trifluorlaktat und 3,3,3-Trifluor-1-hydroxyaceton nur in den Ratten- und Mäuseurinen, jedoch nicht in den Kaninchenurinen festgestellt. Die Abwesenheit dieser Metabolite in den Kaninchenurinen stellt den größten, qualitativen Unterschied der Biotransformation von HFO-1234yf dar. Offenbar wird das eingangs gebildete intermediäre Epoxid ausschließlich durch Glutathionkonjugation in Kaninchen umgesetzt, jedoch nicht hydrolytisch geöffnet wie in Ratten und Mäusen. Weitere Nebenprodukte von HFO-1234yf in den Urinen waren 3,3,3-Trifluor-1,2-dihydroxypropan, 3,3,3-Trifluor-2-propanol und 3,3,3-Trifluoraceton, die möglicherweise durch GSTO1-1 katalysierte Degradierung der intermediären Glutathionkonjugate entstanden. Die Metabolite von HFO-1234yf, die in Inkubationen mit Ratten- oder Humanlebermikrosomen nachgewiesen werden konnten, beziehungsweise in Inkubationen mit subzellulären Fraktionen der Rattenleber, bekräftigen das postulierte Biotransformationsschema von HFO-1234yf. Anhand der Abspaltung anorganischen Fluorids von HFO-1234yf in mikrosomalen Inkubationen wurde gezeigt, dass die Biotransformation des Gases in Abhängigkeit von Inkubationsdauer, Kofaktoren und Proteinkonzentration stattfand. Die im Rahmen dieser Arbeit gewonnenen Erkenntnisse legen nahe, dass HFO-1234yf einer für Haloolefine typischen Metabolisierung unterliegt, welche mit einer CYP450 2E1-katalysierten Epoxidierung beginnt. Das elektrophile Intermediat wird anschließend durch Glutathionkonjugation und hydrolytischer Ringöffnung weiter verstoffwechselt (letztere nicht in Kaninchen). Das Ausmaß einer Additions-Eliminations Reaktion von HFO-1234yf mit Glutathion ist im Vergleich zur vorherrschenden CYP450-vermittelten Epoxidierung gering und es wurde kein Hinweis für eine direkte Additionsreaktion von HFO-1234yf mit Glutathion gefunden. Quantifizierungen des Hauptmetaboliten *N*-Acetyl-S-(3,3,3-trifluor-2-hydroxypropanyl)-L-cystein mittels LC/MS-MS zeigten, dass ein Großteil (90%) innerhalb von 18 h nach Ende der Inhalationen von Ratten und Mäusen ausgeschieden wurde ($t_{1/2}$ ca. 6 h). Von Kaninchen wurden 95% der Merkaptursäure innerhalb der ersten 12 h nach Inhalationsende ausgeschieden ($t_{1/2}$ ca. 9,5 h). Der niedrige Siedepunkt von HFO-1234yf (-22 °C) ist wahrscheinlich ausschlaggebend für eine nahezu vollständige Abatmung, und sterische sowie elektronische Faktoren könnten für die Reaktionsträgheit der Ausgangsverbindung verantwortlich sein. Diese

Umstände erklären das geringe Ausmaß der Biotransformation von HFO-1234yf in allen verwendeten Tierspezies ($\ll 1\%$ der verabreichten Dosis). Die potentiell toxischen Metaboliten 2,3,3,3-Tetrafluorepoxypropan und 3,3,3-Trifluoressigsäure im Biotransformationsschema (**2** und **26**, Scheme 2) verursachten keine Schäden in den Versuchstieren, wahrscheinlich aufgrund der geringen gebildeten Mengen und der effizienten Entgiftung des Epoxids durch Glutathionkonjugation. Die Ergebnisse der Biotransformation von HFO-1234yf können nicht die Todesfälle der Kaninchen in der Entwicklungstoxizitätsstudie erklären. Die unterschiedlichen Metabolitenmuster von HFO-1234yf in den Urinen von Kaninchen, Ratten und Mäusen entstanden durch artspezifische Verstoffwechslung der Glutathionkonjugate, deuten jedoch nicht auf unterschiedliche Toxizitätspotentiale von HFO-1234yf in den verwendeten Tierspezies hin.

Quantitative Vergleiche der Biotransformation von 10.000 ppm HFO-1225yeZ und HFO-1234yf und 20.000 ppm JDH, einer Mischung aus gleichen Volumen HFO-1225yeZ und HFO-1234yf zeigten, dass in den Rattenurinen der Einzelsubstanzen vergleichbare Metabolitenmengen gebildet wurden. In den JDH-Urinen jedoch entsprach die ermittelte Metabolitenmenge nicht der Summe dessen, was bei den Einzelsubstanzen gefunden wurde, sondern lag knapp unter diesen Werten. Dies lässt schlussfolgern, dass HFO-1225yeZ und HFO-1234yf einen inhibitorischen Effekt aufeinander ausüben und zusammen in der JDH-Mischung in deutlich geringerem Ausmaß biotransformiert werden als die Einzelsubstanzen. Qualitative Analysen ergaben, dass in allen Urinen die gleichen Hauptmetabolite vorhanden waren, jedoch unterschiedlich stark gebildet wurden. Das prozentuale Verhältnis der Metaboliten in den JDH-Urinen entspricht dabei den Mittelwerten der korrespondierenden Werte von den HFO-1225yeZ- und HFO-1234yf-Urinen, was eine Beibehaltung der Metabolitenmuster beider Gase in der Mischung entspricht. Diese Beobachtung lässt vermuten, dass der inhibitorische Einfluss den HFO-1225yeZ und HFO-1234yf aufeinander ausüben, nicht die Bildung einzelner Metabolite verändert, sondern alle gleichermaßen betrifft. Da HFO-1225yeZ toxische Effekte in Mäusen bei Konzentrationen von ca. 10.000 ppm auslöste, könnte das verringerte Ausmaß der Biotransformation von 20.000 ppm JDH eine Verringerung der Toxizität bedeuten.

7. References

1. Molina, M., and Rowland, F.S. (1974). Stratospheric sink of chlorofluoromethanes: chlorine atom-catalysed destruction of the ozone. *Nature* **249**, 810-812.
2. Fisher, D.A., Hales, C.H., Wang, W.-C., Ko, M.K.W., and Sze, N.D. (1990). Model calculations of the relative effects of CFCs and their replacements on global warming. *Nature* **344**, 513-516.
3. Langbein, T., Sonntag, H., Trapp, D., Hoffmann, A., Malms, W., Roth, E.P., Mors, V., and Zellner, R. (1999). Volatile anaesthetics and the atmosphere: atmospheric lifetimes and atmospheric effects of halothane, enflurane, isoflurane, desflurane and sevoflurane. *Br J Anaesth* **82**, 66-73.
4. Rhoderick, G.C., and Dorko, W.D. (2004). Standards development of global warming gas species: methane, nitrous oxide, trichlorofluoromethane, and dichlorodifluoromethane. *Environ Sci Technol* **38**, 2685-2692.
5. Krupa, S.V., and Kickert, R.N. (1989). The Greenhouse effect: impacts of ultraviolet-B (UV-B) radiation, carbon dioxide (CO₂), and ozone (O₃) on vegetation. *Environ Pollut* **61**, 263-393.
6. Majumdar, D., Patel, J., Bhatt, N., and Desai, P. (2006). Emission of methane and carbon dioxide and earthworm survival during composting of pharmaceutical sludge and spent mycelia. *Bioresour Technol* **97**, 648-658.
7. Sinclair, J. (1991). Global warming: a vicious circle. *Our Planet* **3**, 4-7.
8. Velders, G.J., Andersen, S.O., Daniel, J.S., Fahey, D.W., and McFarland, M. (2007). The importance of the Montreal Protocol in protecting climate. *Proc Natl Acad Sci U S A* **104**, 4814-4819.
9. Trochimowicz, H.J. (1993). Industrial research on alternative fluorocarbons. *Toxicol Lett* **68**, 25-30.
10. Urban, G., and Dekant, W. (1994). Metabolism of 1,1-dichloro-2,2,2-trifluoroethane in rats. *Xenobiotica* **24**, 881-892.
11. Hinchman, C.A., and Ballatori, N. (1994). Glutathione conjugation and conversion to mercapturic acids can occur as an intrahepatic process. *J Toxicol Environ Health* **41**, 387-409.
12. Orrenius, S., Ormstad, K., Thor, H., and Jewell, S.A. (1983). Turnover and functions of glutathione studied with isolated hepatic and renal cells. *Fed Proc* **42**, 3177-3188.
13. Bakke, J.E., Rafter, J., Larsen, G.L., Gustafsson, J.A., and Gustafsson, B.E. (1981). Enterohepatic circulation of the mercapturic acid and cysteine conjugates of propachlor. *Drug Metab Dispos* **9**, 525-528.
14. Hinchman, C.A., and Ballatori, N. (1990). Glutathione-degrading capacities of liver and kidney in different species. *Biochem Pharmacol* **40**, 1131-1135.
15. James, S.P., and Needham, D. (1973). Some metabolites of S-pentyl-L-cysteine in the rabbit and other species. *Xenobiotica* **3**, 207-218.
16. Commandeur, J.N., Stijntjes, G.J., and Vermeulen, N.P. (1995). Enzymes and transport systems involved in the formation and disposition of glutathione S-conjugates. Role in bioactivation and detoxication mechanisms of xenobiotics. *Pharmacol Rev* **47**, 271-330.
17. Anders, M.W., and Dekant, W. (1998). Glutathione-dependent bioactivation of haloalkenes. *Annu Rev Pharmacol Toxicol* **38**, 501-537.
18. Birner, G., Werner, M., Ott, M.M., and Dekant, W. (1995). Sex differences in hexachlorobutadiene biotransformation and nephrotoxicity. *Toxicol Appl Pharmacol* **132**, 203-212.

19. Werner, M., Birner, G., and Dekant, W. (1995). The role of cytochrome P4503A1/2 in the sex-specific sulfoxidation of the hexachlorobutadiene metabolite, N-acetyl-S-(pentachlorobutadienyl)-L-cysteine in rats. *Drug Metab Dispos* 23, 861-868.
20. Werner, M., Guo, Z., Birner, G., Dekant, W., and Guengerich, F.P. (1995). The sulfoxidation of the hexachlorobutadiene metabolite N-acetyl-S-(1,2,3,4,4-pentachlorobutadienyl)-L-cysteine is catalyzed by human cytochrome P450 3A enzymes. *Chem Res Toxicol* 8, 917-923.
21. Baker, M.T., Bates, J.N., and Leff, S.V. (1987). Comparative defluorination and cytochrome P-450 loss by the microsomal metabolism of fluoro- and fluorochloroethenes. *Drug Metab Dispos* 15, 499-503.
22. Harris, J.W., and Anders, M.W. (1991). Metabolism of the hydrochlorofluorocarbon 1,2-dichloro-1,1-difluoroethane. *Chem Res Toxicol* 4, 180-186.
23. Olson, M.J., Reidy, C.A., and Johnson, J.T. (1990). Defluorination of 1,1,1,2-tetrafluoroethane (R-134a) by rat hepatocytes. *Biochem Biophys Res Commun* 166, 1390-1397.
24. Olson, M.J., and Surbrook, S.E., Jr. (1991). Defluorination of the CFC-substitute 1,1,1,2-tetrafluoroethane: comparison in human, rat and rabbit hepatic microsomes. *Toxicol Lett* 59, 89-99.
25. Kadlubar, F.F., and Hammonds, G.J. (1987). The role of cytochrome P450 in the metabolism of chemical carcinogens. *Mammalian cytochrome P-450* (F.P. Guengerich, ed.), Vol II, CRC Press, Boca Raton, Florida, pp. 81-130.
26. Macdonald, T.L. (1983). Chemical mechanisms of halocarbon metabolism. *Crit Rev Toxicol* 11, 85-120.
27. Liebler, D.C., and Guengerich, F.P. (1983). Olefin oxidation by cytochrome P-450: evidence for group migration in catalytic intermediates formed with vinylidene chloride and trans-1-phenyl-1-butene. *Biochemistry* 22, 5482-5489.
28. Miller, R.E., and Guengerich, F.P. (1982). Oxidation of trichloroethylene by liver microsomal cytochrome P-450: evidence for chlorine migration in a transition state not involving trichloroethylene oxide. *Biochemistry* 21, 1090-1097.
29. Wolf, C.R., Mansuy, D., Nastainczyk, W., Deutschmann, G., and Ullrich, V. (1977). The reduction of polyhalogenated methanes by liver microsomal cytochrome P450. *Mol Pharmacol* 13, 698-705.
30. Cai, H., and Guengerich, F.P. (2001). Reaction of trichloroethylene oxide with proteins and dna: instability of adducts and modulation of functions. *Chem Res Toxicol* 14, 54-61.
31. Cai, H., and Guengerich, F.P. (2001). Reaction of trichloroethylene and trichloroethylene oxide with cytochrome P450 enzymes: inactivation and sites of modification. *Chem Res Toxicol* 14, 451-458.
32. Lash, L.H., Fisher, J.W., Lipscomb, J.C., and Parker, J.C. (2000). Metabolism of trichloroethylene. *Environ Health Perspect* 108 Suppl 2, 177-200.
33. Lee, R.P., and Forkert, P.G. (1994). In vitro biotransformation of 1,1-dichloroethylene by hepatic cytochrome P-450 2E1 in mice. *J Pharmacol Exp Ther* 270, 371-376.
34. Yoshioka, T., Krauser, J.A., and Guengerich, F.P. (2002). Tetrachloroethylene oxide: hydrolytic products and reactions with phosphate and lysine. *Chem Res Toxicol* 15, 1096-1105.

35. Bull, R.J. (2000). Mode of action of liver tumor induction by trichloroethylene and its metabolites, trichloroacetate and dichloroacetate. *Environ Health Perspect* 108 Suppl 2, 241-259.
36. Bull, R.J., Templin, M., Larson, J.L., and Stevens, D.K. (1993). The role of dichloroacetate in the hepatocarcinogenicity of trichloroethylene. *Toxicol Lett* 68, 203-211.
37. Stauber, A.J., and Bull, R.J. (1997). Differences in phenotype and cell replicative behavior of hepatic tumors induced by dichloroacetate (DCA) and trichloroacetate (TCA). *Toxicol Appl Pharmacol* 144, 235-246.
38. Jin, L., Davis, M.R., Kharasch, E.D., Doss, G.A., and Baillie, T.A. (1996). Identification in rat bile of glutathione conjugates of fluoromethyl 2,2-difluoro-1-(trifluoromethyl)vinyl ether, a nephrotoxic degradate of the anesthetic agent sevoflurane. *Chem Res Toxicol* 9, 555-561.
39. Koob, M., and Dekant, W. (1990). Metabolism of hexafluoropropene. Evidence for bioactivation by glutathione conjugate formation in the kidney. *Drug Metab Dispos* 18, 911-916.
40. Tate, S. (1980). Enzymes of mercapturic acid pathway: biosynthesis, intermediary metabolism, and physiological disposition. In *Glutathione: Chemical, Biochemical and Medical Aspect*, ed. D Dolphin, R Poulson, O Avramovic, pp. 46-84. New York: Wiley.
41. Birner, G., Richling, C., Henschler, D., Anders, M.W., and Dekant, W. (1994). Metabolism of tetrachloroethene in rats: identification of N epsilon-(dichloroacetyl)-L-lysine and N epsilon-(trichloroacetyl)-L-lysine as protein adducts. *Chem Res Toxicol* 7, 724-732.
42. Chen, Q., Jones, T.W., Brown, P.C., and Stevens, J.L. (1990). The mechanism of cysteine conjugate cytotoxicity in renal epithelial cells. Covalent binding leads to thiol depletion and lipid peroxidation. *J Biol Chem* 265, 21603-21611.
43. Schaumann, E. (1988). The chemistry of thioketenes. *Tetrahedron* 44, 1827-1871.
44. Vamvakas, S., Dekant, W., Berthold, K., Schmidt, S., Wild, D., and Henschler, D. (1987). Enzymatic transformation of mercapturic acids derived from halogenated alkenes to reactive and mutagenic intermediates. *Biochem Pharmacol* 36, 2741-2748.
45. Finkelstein, M., Dekant, W., Kende, A., and Anders, M. (1995). α -Thiolactones as novel intermediates in the cysteine conjugate β -lyase-catalyzed bioactivation of bromine-containing cysteine S-conjugates. *J. Am. Chem. Soc.* 117, 9590-9591.
46. Lash, L.H., Sausen, P.J., Duescher, R.J., Cooley, A.J., and Elfarra, A.A. (1994). Roles of cysteine conjugate beta-lyase and S-oxidase in nephrotoxicity: studies with S-(1,2-dichlorovinyl)-L-cysteine and S-(1,2-dichlorovinyl)-L-cysteine sulfoxide. *J Pharmacol Exp Ther* 269, 374-383.
47. Ripp, S.L., Overby, L.H., Philpot, R.M., and Elfarra, A.A. (1997). Oxidation of cysteine S-conjugates by rabbit liver microsomes and cDNA-expressed flavin-containing mono-oxygenases: studies with S-(1,2-dichlorovinyl)-L-cysteine, S-(1,2,2-trichlorovinyl)-L-cysteine, S-allyl-L-cysteine, and S-benzyl-L-cysteine. *Mol Pharmacol* 51, 507-515.
48. Sausen, P.J., and Elfarra, A.A. (1991). Reactivity of cysteine S-conjugate sulfoxides: formation of S-[1-chloro-2-(S-glutathionyl)vinyl]-L-cysteine sulfoxide by the reaction of S-(1,2-dichlorovinyl)-L-cysteine sulfoxide with glutathione. *Chem Res Toxicol* 4, 655-660.

49. Bhattacharya, R.K., and Schultze, M.O. (1967). Enzymes from bovine and turkey kidneys which cleave S-(1,2-dichlorovinyl)-L-cysteine. *Chomp. Biochem. Physiol.* 22, 723-735.
50. Lash, L.H., Sausen, P.J., Duescher, R.J., Cooley, A.J., and A.A.Elfarra (1993). Roles of cysteine conjugate β -lyase and S-Oxidase in nephrotoxicity: Studies with S-(1,2-dichlorovinyl)-L-cysteine and S-(1,2-dichlorovinyl)-L-cysteine sulfoxide. *The journal of pharmacology and experimental therapeutics* 269, 374-383.
51. Van den Broek, L., Delbrissine, L., and Ottenheijm, H. (1990). In: *The chemistry of sulfenic acids and their derivatives*. Patai S (ed), John Wiley and Sons, New York, pp 701-721.
52. Honeywell (2007). Toxicogenomic assessment of the carcinogenic potential of 2,3,3,3-tetrafluoropropene, Report no. 06014, Hamner Institute for Health Sciences, Research Triangle Park, NC, pp 1-36, Honeywell international, Morristown.
53. Honeywell (2008). An inhalation range-finding prenatal developmental toxicity study of HFO-1234yf (2,3,3,3-tetrafluoropropene) in rabbits, Report no. WIL-447021, WIL Research Laboratories, LLC, 1407 George Road, Ashland, OH 44805-8946.
54. Honeywell (2007). Toxicogenomic assessment of the carcinogenic potential of t-1,1,1,3-tetrafluoropropene (HFO-1234ze), pp. 1– 36. Report no. 06014, Hamner Institute for Health Sciences, Research Triangle Park, NC. Honeywell international, Morristown.
55. Schuster, P., Bertermann, R., Rusch, G.M., and Dekant, W. (2009). Biotransformation of trans-1,1,1,3-tetrafluoropropene (HFO-1234ze). *Toxicol Appl Pharmacol* 239, 215-223.
56. Procopio, A., Alcaro, S., Cundari, S., De Nino, A., Ortuso, F., Sacchetta, P., Pennelli, A., and Sindona, G. (2005). Molecular modeling, synthesis, and preliminary biological evaluation of glutathione-S-transferase inhibitors as potential therapeutic agents. *J Med Chem* 48, 6084-6089.
57. Schuster, P., Bertermann, R., Snow, T.A., Han, X., Rusch, G.M., Jepson, G.W., and Dekant, W. (2008). Biotransformation of 2,3,3,3-tetrafluoropropene (HFO-1234yf). *Toxicol Appl Pharmacol* 233, 323-332.
58. Ramachandran, P., Gong, B.Q., and Brown, H.C. (1995). Chiral Synthesis Via Organoboranes .40. Selective Reductions .55. A Simple One-Pot Synthesis of the Enantiomers of (Trifluoromethyl)Oxirane - a General-Synthesis in High Optical Purities of Alpha-Trifluoromethyl Secondary Alcohols Via the Ring-Cleavage R. *J. Org. Chem.* 60, 41-46.
59. Herbst, J., Koster, U., Kerssebaum, R., and Dekant, W. (1994). Role of P4502E1 in the metabolism of 1,1,2,2-tetrafluoro-1-(2,2,2-trifluoroethoxy)-ethane. *Xenobiotica* 24, 507-516.
60. Koster, U., Speerschneider, P., Kerssebaum, R., Wittmann, H., and Dekant, W. (1994). Role of cytochrome P450 2E1 in the metabolism of 1,1,2,3,3,3-hexafluoropropyl methyl ether. *Drug Metab Dispos* 22, 667-672.
61. Urban, G., Speerschneider, P., and Dekant, W. (1994). Metabolism of the chlorofluorocarbon substitute 1,1-dichloro-2,2,2-trifluoroethane by rat and human liver microsomes: the role of cytochrome P450 2E1. *Chem Res Toxicol* 7, 170-176.
62. Siekevitz, P. (1962). Preparation of microsomes and submicrosomal fractions: mammalian. *Methods in Enzymology* 5, 61-68.

63. Guengerich, F.P., Kim, D.H., and Iwasaki, M. (1991). Role of human cytochrome P-450 IIE1 in the oxidation of many low molecular weight cancer suspects. *Chem Res Toxicol* *4*, 168-179.
64. Koop, D.R. (1986). Hydroxylation of p-nitrophenol by rabbit ethanol-inducible cytochrome P-450 isozyme 3a. *Mol Pharmacol* *29*, 399-404.
65. Harris, J.W., Pohl, L.R., Martin, J.L., and Anders, M.W. (1991). Tissue acylation by the chlorofluorocarbon substitute 2,2-dichloro-1,1,1-trifluoroethane. *Proc Natl Acad Sci U S A* *88*, 1407-1410.
66. Bayer, T., Amberg, A., Bertermann, R., Rusch, G.M., Anders, M.W., and Dekant, W. (2002). Biotransformation of 1,1,1,3,3-Pentafluoropropane (HFC-245fa). *Chem Res Toxicol* *15*, 723-733.
67. Foris, A. (2004). ¹⁹F and ¹H NMR spectra of halocarbons. *Magn Reson Chem* *42*, 534-555.
68. Knights, K.M., Sykes, M.J., and Miners, J.O. (2007). Amino acid conjugation: contribution to the metabolism and toxicity of xenobiotic carboxylic acids. *Expert Opin Drug Metab Toxicol* *3*, 159-168.
69. Yin, H., Jones, J.P., and Anders, M.W. (1995). Metabolism of 1-fluoro-1,1,2-trichloroethane, 1,2-dichloro-1,1-difluoroethane, and 1,1,1-trifluoro-2-chloroethane. *Chem Res Toxicol* *8*, 262-268.
70. Phalen, R.F. (2009). Inhalation studies: foundations and techniques. Informa Healthcare USA, Inc., 195-208.
71. Farkas, M., Berry, J.O., and Aga, D.S. (2007). Determination of enzyme kinetics and glutathione conjugates of chlortetracycline and chloroacetanilides using liquid chromatography-mass spectrometry. *Analyst* *132*, 664-671.
72. Dekant, W. (1996). Toxicology of chlorofluorocarbon replacements. *Environ Health Perspect* *104 Suppl 1*, 75-83.
73. Hargus, S.J., Fitzsimmons, M.E., Aniya, Y., and Anders, M.W. (1991). Stereochemistry of the microsomal glutathione S-transferase catalyzed addition of glutathione to chlorotrifluoroethene. *Biochemistry* *30*, 717-721.
74. Dekant, W., Berthold, K., Vamvakas, S., Henschler, D., and Anders, M.W. (1988). Thioacylating intermediates as metabolites of S-(1,2-dichlorovinyl)-L-cysteine and S-(1,2,2-trichlorovinyl)-L-cysteine formed by cysteine conjugate beta-lyase. *Chem Res Toxicol* *1*, 175-178.
75. Vamvakas, S., Kochling, A., Berthold, K., and Dekant, W. (1989). Cytotoxicity of cysteine S-conjugates: structure-activity relationships. *Chem Biol Interact* *71*, 79-90.
76. Green, T., and Prout, M.S. (1985). Species differences in response to trichloroethylene. II. Biotransformation in rats and mice. *Toxicol Appl Pharmacol* *79*, 401-411.
77. Board, P.G., and Anders, M.W. (2007). Glutathione transferase omega 1 catalyzes the reduction of S-(phenacyl)glutathiones to acetophenones. *Chem Res Toxicol* *20*, 149-154.
78. Whitbread, A.K., Masoumi, A., Tetlow, N., Schmuck, E., Coggan, M., and Board, P.G. (2005). Characterization of the omega class of glutathione transferases. *Methods Enzymol* *401*, 78-99.

Veröffentlichungen

Schuster, P., Bertermann, R., Snow, T.A., Han, X., Rusch, G.M., Jepson, G.W., and Dekant, W. (2008). Biotransformation of 2,3,3,3-tetrafluoropropene (HFO-1234yf). *Toxicol Appl Pharmacol* 233, 323-332.

Schuster, P., Bertermann, R., Rusch, G.M., and Dekant, W. (2009). Biotransformation of *trans*-1,1,1,3-tetrafluoropropene (HFO-1234ze). *Toxicol Appl Pharmacol* 239, 215-223.

Schuster, P., Bertermann, R., Rusch, G.M., and Dekant, W. (2009). Biotransformation of 2,3,3,3-tetrafluoropropene (HFO-1234yf) in rabbits. Eingereicht bei *Toxicol Appl Pharmacol* am 28.10.2009.

Poster

Schuster, P., Bertermann, R., Rusch, G.M., and Dekant, W. Biotransformation of 2,3,3,3-tetrafluoropropene (HFO-1234yf). März 2008. SOT Annual Meeting & ToxExpoTM, Seattle, USA.

Danksagung

Besonders bedanken möchte ich mich bei Herrn Prof. Dr. Dekant, für die Themenstellung und seine tatkräftige Unterstützung während der gesamten Promotionszeit. Seine konstruktiven Anregungen sowie die permanente Gesprächsbereitschaft waren mir eine große Hilfe. Gleichzeitig lies er mir stets genug Freiraum meine Arbeiten selbständig durchzuführen. Weiterhin möchte ich mich herzlich für die Möglichkeit bedanken am SOT-Meeting teilzunehmen und verschiedene Fortbildungskurse zu besuchen.

Herrn Prof. Dr. Benz danke ich herzlich für sein Engagement als Zweitgutachter meiner Arbeit.

Frau Dr. Schauer danke ich für die netten Gespräche, die freundliche Atmosphäre im Büro 311 und ihre tatkräftige Unterstützung meiner Arbeiten, vor allem bei der Planung und Durchführung der ersten Inhalationsversuche.

Heike Keim-Heusler danke ich für ihre Unterstützung bei der Laborarbeit, vor allem am GC, und die zahlreichen Tipps und Hilfestellungen. Vor allem aber bedanke ich mich für Ihren beherzten Sprung in den Main, mit dem sie mich vor dem Ertrinken rettete.

Nataly Bittner gilt mein besonderer Dank für die wirklich zahlreichen Hilfestellungen bei den Messungen am LC.

Ein großes Dankeschön möchte ich Miriam Kraal, Elisabeth Rüb-Spiegel und Carolin Kröcher aussprechen, die mir stets bei meinen Arbeiten im institutseigenen Tierstall behilflich waren.

Bei Carolin Hamberger und Gabriella Wehr bedanke ich mich für die gründliche Korrektur meines ersten Dissertationsentwurfs.

Herrn Dr. Bertermann und Marie-Luise Schäfer sei für die zahlreichen ^{19}F -NMR Messungen gedankt.

Uwe Weinberger und den anderen Mitarbeitern vom Zentralen Tierhaus danke ich herzlich für die freundliche Unterstützung bei den Experimenten mit Kaninchen.

Herrn Hopf danke ich für den Bau der Kaninchenstoffwechselkäfige.

Vielen weiteren, hier nicht namentlich genannten Mitarbeitern des Instituts für Toxikologie danke ich herzlich für die kollegiale Arbeitsatmosphäre, die netten Gespräche, die vielen Tipps im Laboralltag und für Bonbons und Kuchen als Nervennahrung.

Lebenslauf

Persönliches

Name: Paul Xaver Schuster
Geburtsdatum: 25/07/1978
Geburtsort: München
Familienstand: ledig

Schul- und Hochschulausbildung

04/2006 - 09/2009 Anfertigung der Dissertation am Institut für Pharmakologie und Toxikologie der Universität Würzburg. Thema: "Biotransformation of *trans*-1,1,1,3-tetrafluorpropene, 2,3,3,3-tetrafluorpropene and 1,2,3,3,3-pentafluorpropene".

04/2005 - 02/2006 Wissenschaftliche Mitarbeit am Institut für Zell- und Entwicklungsbiologie der Universität Würzburg.

10/1999 - 02/2005 Studium der Biologie an der Bayerischen Julius-Maximilians-Universität Würzburg.

04/2004 - 12/2004 Diplomarbeit am Institut für Hygiene- und Mikrobiologie der Universität Würzburg, Arbeitskreis von Prof. Dr. Joachim Reidl
Thema: "Etablierung eines DNA-Microarrays für *Haemophilus influenzae* und Analysen zu Genomik und Transkriptomik".

11/1998 - 08/1999 Grundwehrdienst

09/1990 - 07/1999 Ignaz-Kögler-Gymnasium Landsberg am Lech; Abitur.

Erklärung

Hiermit erkläre ich ehrenwörtlich, dass ich die Dissertation "Biotransformation of *trans*-1,1,1,3-tetrafluorpropene, 2,3,3,3-tetrafluorpropene and 1,2,3,3,3-pentafluorpropene" selbständig angefertigt und keine anderen als die von mir angegebenen Hilfsmittel und Quellen verwendet habe.

Ich erkläre außerdem, dass diese Dissertation weder in gleicher noch anderer Form bereits in einem anderen Prüfungsverfahren vorlag.

Ich habe außer den mit dem Zulassungsgesuch urkundlich vorgelegten Graden keine weiteren akademischen Grade erworben oder zu erwerben versucht.

Würzburg, 04.11.2009